March 2019

SEDIMENT TRANSPORT AND CHANNEL MORPHOLOGY OF A NATURAL AND A LEVEED ALLUVIAL RIVER

BO WANG
Louisiana State University and Agricultural and Mechanical College

SEDIMENT TRANSPORT AND CHANNEL MORPHOLOGY OF A NATURAL AND A LEVEED ALLUVIAL RIVER

A Thesis

Submitted to the Graduate Faculty of the
Louisiana State University and
Agricultural and Mechanical College
in partial fulfillment of the
requirements for the degree of
Master of Science

in

School of Renewable Natural Resources

by
Bo Wang
B.S., China University of Geosciences, 2008
M.S., China University of Geosciences, 2011
Ph.D., Louisiana State University, 2017
May 2019

ACKNOWLEDGMENTS

I am grateful to my major professor, Dr. Yi-jun Xu. I will forever be indebted to him for his insightful guidance, knowledge, and inspiration through every stage of this project and for the trust he put on me to complete this work.

I would like to thank my committee members, Dr. Sam Bentley and Dr. Christopher Swarzenski for their support and enthusiasm for my research. They offered their help and insightful advice without reservation.

I would like to thank the Louisiana Coastal Protection and Restoration Authority for the financial support that allowed me to complete this research. This project was also supported by grants from the National Science Foundation and the Louisiana Department of Wildlife and Fisheries.

Above all, I am deeply grateful to my wife, Yan. Her sacrifice for supporting me to complete this project was much more than fair. To my children, Rocky and Andy: I love you, thanks for bringing endless happiness to this family and helping me get through the tough time.

TABLE OF CONTENTS

ABSTRACT

Alluvial rivers are shaped by interactions of flow and sediment transport. Their lower reaches to the world's oceans are highly dynamic, often presenting engineering and management challenges. This thesis research aimed to investigate channel dynamics and sediment transport in a natural river and a highly engineered river in South Louisiana, in order to gain much-needed science information for helping develop sustainable practices in river engineering, sediment management, and coastal restoration and protection. Especially, the thesis research examined (1) riverbed deformation from bank to bank in the final 500-km reach of the Mississippi River, (2) bed material transport at the Mississippi-Atchafalaya River diversion, and (3) long-term and short-term flood effects on the morphological changes of the Amite-Comite River confluence. The research employed morphological, hydrodynamic, and geospatial modeling and analysis. The research found that from 1992 to 2013 the lowermost Mississippi River channel trapped 337×10^6 m^3 sediment, equal to about 70% of riverine sand input from the upstream channel. The finding rejects the initial hypothesis that the highly engineered Mississippi River acts as a conduit for sediment transport. Sediment deposition mainly occurred in the immediate channel downstream of the Mississippi-Atchafalaya River diversion and the reach between RK 386 and RK 163, reflecting flow reduction and backwater influences. The bed material transport assessment revealed that in the recent decade the engineering-controlled Mississippi-Atchafalaya River diversion showed a slight disproportional transport of bed material loads. On average 24% of the Mississippi River was diverted into the Atchafalaya, but only 22% of bed material loads moved into the diversion outflow channel (i.e. 47 MT out of 215 MT). The confluence of Amite and Comite River continuously migrated about 55 m downstream between 2002 and 2017. Sediment deposition on the main channel side of the confluence mouth bar is the major driver for the confluence migration.

Regression analysis shows that the increase rate of the vegetated area of the bar is highly related to the days of moderate floods. Short-term Laser scanning measurements reveal that a single flood with the intensity close to a moderate flood could double the projected surface area of the mouth bar and increased its volume by 68%. Overall, the thesis research shows the complexity of sediment transport in the lower reach of a large alluvial river, in that distinctive bed deformation can occur in different reaches because of flow deduction and backwater effects. Our study is the first try of estimating bed material load at a largely controlled bifurcation based on a simple, well-established bed material transport model. The study also highlights the importance of episodic floods on the evolution and migration of a river confluence.

CHAPTER 1. INTRODUCTION

Alluvial rivers carry sediments in suspension and bedload shaping their downstream channel morphology, dynamics, and ecosystems. In general, the natural alluvial channels can be grouped into four basic patterns including straight, meandering, braided, or anastomosing. The patterns result from different sediment supply, discharge, gradient, bank material, vegetation on stream forms, and geology of watershed (Lane, 1957). Natural alluvial channels are usually unstable because their bed and banks are erodible. Some channel changes can be expected in alluvial rivers, such as bar shift, neck cutoff, meander shift, and avulsion (Schumm, 1985).

Sediment transport and sedimentation directly determine channel geometry and morphology. In terms of the sediment transport mechanism, sediments can be divided into suspended sediment, bedload, and saltation. For considering effects of sediment transport on channel morphology, sediments are more appropriately divided into wash material and bed material (Church, 2006). The former is fine material that is usually transported a long distance and has little contact with the bed. The latter is relatively coarse material that may move either as bedload or as intermittently suspended load. Many studies have tried to quantitatively estimate the relationship between sediment transport and channel forms. Lane (1955) developed a simple relationship QS - Q_sD in the 1950s, in which Q is discharge, S is bed gradient, Q_s is sediment flux, and D is grain size. He argued that discharge is the most obvious factor in determining stream form. Schumm (1963) published a river classification based on the dominant mode of sediment transport. He pointed out three types of channel forms which are mainly determined by suspended sediment, bedload, and mixed load. Overall, there are two ways to study the relationship between sediment transport and channel morphology (Church, 2006). This first one is a forward approach, in which known physics of sediment transport is applied to deduce fluvial sedimentation. Numerous

equations were developed for studying sediment transport which can be used in this approach (Ackers and White, 1973; Einstein, 1950; Engelund and Hansen, 1967; Toffaleti, 1977; Yang, 1973; Yang, 1979). The second one is an inverse approach, in which observed morphologic changes of the channel are used to estimate sediment transport process (Redolfi et al., 2017; Wheaton et al., 2013; Williams et al., 2015). This approach is more convenient because river morphology is much easier to observe (Church, 2006).

In the past century, the natural fluvial processes of many alluvial rivers have been altered by human interventions, including levee construction and other engineering practices, i.e., channel cutoffs, dredging, dam and reservoir, revetment, and water diversion construction. This is especially true in the lower reach of large alluvial rivers where navigation and flood control play ultimate roles for regional and national industrial and economic development. While the human intervention effects are widely recognized, comprehensive quantitative studies detailing the decadal dynamics of sediment deposition in the lower reach of alluvial rivers are limited. Such quantitative assessments are critical for understanding sediment transport and channel morphology in the backwater zones of large alluvial rivers. In addition, they can be also relevant for coastal protection and restoration as many river deltas in the world are rapidly losing land because of one or a combination of factors, including reduced riverine sediment supply (Walling and Fang, 2003), subsidence (i.e. Syvitski et al. (2009), Higgins (2016)), coastal land erosion (Chen and Zong, 1998; Pranzini et al., 2015; Silva et al., 2014), and sea level rise (Gornitz, 1995; Zhang et al., 2004).

As one of the largest alluvial rivers in the world, the Mississippi River (MR) avulsed and created a new course every 1,000-1,500 years before the construction of artificial levees (Coleman et al., 1998; Fisk, 1944; Fisk, 1952). The river in the present time has two distributary outlets, the Mississippi main channel and the Atchafalaya River (AR) (i.e., the oldest course of the MR several

thousand years ago) which, respectively, carry 70% and 30% of the combined flow. This flow ratio is artificially maintained through a controlled diversion after it was realized that the MR had begun changing its course back to the AR (Fisk, 1952). The diversion structure, also known as the Old River Control Structure (ORCS), was completed in 1963, including an overbank structure and a Lowsill structure. Meanwhile, the Lower Old River was closed to form a navigable channel. Although the flow was controlled by the ORCS, the large flood in 1973 almost destroyed the Lowsill structure and almost caused the course of the MR change. In 1987, an Auxiliary structure with a new inflow channel was built to relieve the stress of the Lowsill and Overbank structures. The Sidney A. Murray, Jr. Hydroelectric Plant was completed in 1991 which created another bifurcation in the channel. The average flow diversion in the past three decades was about 23% of the Mississippi flow upstream of the ORCS (Wang and Xu, 2016).

Bifurcations are important nodal points in river systems that redistribute flow and sediment in braided and anastomosing channels on fluvial plains and deltas. Bifurcations can cause downstream aggradation in the original channels and enlargement of the newly bifurcated channels (Kleinhans et al., 2008). Such processes usually make the bifurcations unstable, resulting in final avulsions. Long-term development of bifurcations in large or small alluvial rivers depends on flow and sediment transport, especially fluxes and variations of bed material loads (Church, 2006). While the water and suspended sediment discharges into downstream channels can be normally quantified with a satisfactory degree, determining the fluxes of riverbed material load at bifurcations is rather difficult. It is even more challenging to quantify bedload fluxes at engineered and controlled bifurcations because of irregular flow regulations and unknown numeric solutions. Yet such information can be crucial for alluvial rivers in assessing the long-term stability of bifurcations as well as the downstream channel dynamics, flood risk, and navigation safety.

The Mississippi-Atchafalaya River diversion is a prime example in case. Several studies have looked into sediment transport near the ORCS. Located about 10 km downstream of the ORCS, Tarbert Landing (TBL) gauging station operated by the U.S. Army Corps of Engineers (USACE) supplied long-term suspended sediment concentration data. Utilizing these data, Rosen and Xu (2014) quantified total suspended sediment and Joshi and Xu (2015) estimated suspended sand load for the last four decades at TBL. Knox and Latrubesse (2016) estimated bed-load transport using time-elapsed bathymetric method immediately downstream of TBL. At the ORCS, a similar method was used to calculate bed-load transport at several locations up- and downstream of the ORCS in the Mississippi mainstem and the diversion outflow channel (Heath et al., 2015). In a modeling study on the stability of the diversion under natural conditions, Edmonds (2012) concluded that it would take about 300 years to see a final avulsion of the MR into the AR. However, as a controlled river diversion, Wang and Xu (2018a) argued that the ORCS may be unstable based on the results from a model developed by Pittaluga et al. (2015). Although they pointed out that the diverted sediment may be lower than the transport capacity of the diversion outflow channel, it is still unknown how much sediment was actually diverted via the outflow channel to the Atchafalaya River.

Except for the Mississippi River, there are many natural alluvial rivers in Louisiana, such as the Amite River, Tickfaw River, Tangipahoa River, Pearl River, etc. These rivers are important in material transport, flood protection, and recreation. The 2016 catastrophic flood in south Louisiana is the worst natural disaster to strike the United States since Hurricane Sandy four years ago. The Lower Amite River-Lake Maurepas Basin to the Northern Gulf of Mexico suffered severe inundation due to intense precipitation and quick backwater flooding. The massive flood submerged an estimated 146,000 homes, forced over 40,000 people to relocate, and damaged

thousands of businesses, tremendously devastating the state's economy and regional development. Except for severe precipitation, reduced flow capacity in the Amite River channel may be another main reason for the 2016 flood. This is because that the floodplain of the Amite River had been intensively mined for sand and gravel since the early 1970s (Hood et al., 2007; Mossa and McLean, 1997) and the Amite River normally carries abundant sediment downstream during floods.

River confluences are important zones for water and sediment routing, which can significantly influence channel morphology, migration, and avulsion (Best, 1986; Mosley, 1976). Over the past several decades, flow structure, sediment dynamics, and bed morphology at the river confluences have been extensively studied in laboratory experiments, theoretical analyses, and modeling simulations (Ashmore and Parker, 1983; Best, 1986; Best, 1988; Biron et al., 1993; Booker et al., 2001; Boyer et al., 2006; Bradbrook et al., 2000; Sukhodolov et al., 2017). In a recent study on the planform morphodynamics of large river confluences over decadal timescales, Dixon et al. (2018) found that confluence migrations would be much higher and more common than previously assumed. For example, in the Ganges-Brahmaputra-Meghna basin, more than 80% of large confluences were mobile over the past 40 years.

A river confluence is typically composed of a confluence mouth bar, a separation zone bar, a downstream scour zone, and a mid-channel bar in the post-confluence channel (Best, 1986; Mosley, 1976). As a critical element for confluence migration, morphologic changes of confluence mouth bars have not been thoroughly studied. Investigation of confluence mouth bars can not only improve the scientific understanding of confluence migration under different flow conditions but also can have practical relevance for assessing hazard risk for downstream engineering structures such as bridges and roads. In South Louisiana of the United States, for instance, a 70-m long bridge crosses the Amite River downstream near the confluence of its confluence with the Comite River.

The two rivers are both alluvial rivers on the Mississippi Valley Loess Plain, carrying high sand loads during floods. There is a concern over the migration of the confluence bar, which could possess a direct threat to the safety of the bridge. Understanding flood effects on and predicting confluence bar migration can help develop engineering solutions to mitigate potential hazards to the bridge and save human lives.

The goal of this thesis research was to determine quantitative relationship between sediment transport and channel morphology in engineered and natural alluvial rivers. To achieve this goal, three interrelated studies were conducted in the Lower Mississippi River and the Amite-Comite River confluence. This thesis attempts to introduce the studies in three separate chapters. Following this Introduction, the second chapter presents a study assessing patterns and mechanisms of riverbed deformation in the last 500-km channel of the Mississippi River to test the hypothesis that the lower reach of a large alluvial river can function as a conduit for sediment transport under the current engineering focus of navigation safety and flood control. The third chapter focuses on bed material load transport at the engineered Mississippi-Atchafalaya River diversion. The fourth chapter describes a study on how long-term and short-term floods affect the confluence bar migration and morphology of two alluvial rivers. Chapters two, three, and four are written as stand-alone manuscripts. Chapter two was recently published in *Journal of Geophysical Research: Earth Surface*.

CHAPTER 2. DECADAL-SCALE RIVERBED DEFORMATION AND SAND BUDGET OF THE LAST 500 KM OF THE MISSISSIPPI RIVER: INSIGHTS INTO NATURAL AND RIVER ENGINEERING EFFECTS ON A LARGE ALLUVIAL RIVER

2.1. INTRODUCTION

Alluvial rivers are shaped by interactions of river flow, sediment transport, and bed deformation. Under natural conditions, avulsion of alluvial rivers is common in low-lying coastal areas, as a result of channel bed aggradation. The old channel is suddenly abandoned and a new channel is formed, e.g., the Rhine River in the Netherlands (Stouthamer et al., 2011; Tornqvist, 1994), the Yellow River in China (Qian, 1990; Xue, 1993), and the Mississippi River in the United States (Aslan and Autin, 1999; Frazier, 1967). Following an avulsion, new in-channel sedimentation continues until the next avulsion occurs (Lamb et al., 2012).

As one of the largest alluvial rivers in the world, the Mississippi River (MR) avulsed and created a new course every 1,000-1,500 years before the construction of artificial levees (Coleman et al., 1998; Fisk, 1944; Fisk, 1952). The river in the present time has two distributary outlets, the Mississippi main channel and the Atchafalaya River (AR) (i.e., the oldest course of the MR several thousand years ago) which, respectively, carry 70% and 30% of the combined flow. This flow ratio is artificially maintained through a control structure built in 1963 after it was realized that the MR had begun changing its course back to the AR (Fisk, 1952). Human alterations to the AR channel in the late 19th century (e.g., removal of a large number of wood log jams) caused the AR to carry an increasing quantity of the Mississippi flow, which often has been attributed to the avulsion tendency of the MR. However, little attention has been paid to the importance of possible riverbed changes downstream of the avulsion node on the MR course. From a fluvial geomorphology point of view, avulsion of all alluvial rivers has one fundamental requirement: in-channel aggradation

which makes the river poised for an avulsion (Mohrig et al., 2000). It is not clear how the riverbed of the MR downstream of the avulsion node developed at that time, but we propose that a close look at the recent-decadal bathymetric development of the river reach will offer crucial insights not only into the past but also into future development.

In the past century, the natural fluvial processes of many alluvial rivers have been altered by human interventions, including levee construction and other engineering practices, i.e., channel cutoffs, dredging, dam, and water diversion construction. This is especially true in the lower reach of large alluvial rivers where navigation and flood control play ultimate roles for regional and national industrial and economic development, such as the Lower Mississippi River. While the human intervention effects are widely recognized, comprehensive quantitative studies detailing the decadal dynamics of sediment deposition in the lower reach of alluvial rivers are limited. Such quantitative assessments can be relevant for coastal protection and restoration as many river deltas in the world are rapidly losing land because of one or a combination of factors, including reduced riverine sediment supply (Walling and Fang, 2003), subsidence (i.e. Syvitski et al. (2009), Higgins (2016)), coastal land erosion (Chen and Zong, 1998; Pranzini et al., 2015; Silva et al., 2014), and sea level rise (Gornitz, 1995; Zhang et al., 2004).

The last 500-km reach of the Mississippi River below the avulsion node often referred to as the lowermost Mississippi River (LmMR), is the lifeline that supplies sediment to the river's delta. In the past century, this river reach has undergone extensive river engineering, while the Mississippi River Delta (MRD) kept losing coastal land at a high rate: since 1932, the MRD has lost approximately 4,877 km^2 land (Couvillion et al., 2011). While annual sediment yields of the Lower Mississippi River reduced from *ca* 400 million metric tons (MT) a century ago to less than 200 MT in the recent two decades (Rosen and Xu, 2013; Rosen and Xu, 2014), channelization and

levee constructions prohibited the supply of the sediment to the previous deltaic floodplains. The MRD and all other low-lying river deltas in the world face tremendous challenges in the future, as climate change and sea level rise continue. Large sediment diversions have been proposed at several locations of the LmMR to deliver riverine sediment into the coastal wetland (CPRA, 2012). In the context of sediment transport and availability in the LmMR, understanding long-term riverbed deformation in this river reach is crucial to the success of the coastal wetland restoration.

In this study, we used hydrographic survey data of the LmMR collected in 1992, 2004 and 2013 to analyze long-term changes in riverbed elevation, erosion, and deposition. The primary goal of our study was to identify the patterns and mechanisms of riverbed deformation in the last 500-km channel of the Mississippi River and to test the hypothesis that the lower reach of a large alluvial river can function as a conduit for sediment transport under the current engineering focus of navigation safety and flood control. We have focused on three critical questions including 1) How has the riverbed changed in its first 100-km reach downstream the Mississippi-Atchafalaya avulsion node over the past two decades? 2) Where has the river experienced continuous bed aggradation and erosion? 3) Has the river channel been managed as an effective conduit for sediment transport? If not, how much sediment (i.e., sand) has been trapped in the river channel and how much has been delivered to the Gulf of Mexico in the past two decades? Answers to these questions will provide crucial insights into channel deformation and sediment dynamics in the backwater zone of one of the world's largest and most engineered alluvial rivers. Knowing the importance of the Mississippi River Delta in the U.S. economy, human-related activities, and the environmental pressures, there is a high interest in updated information on the river channel development. Such information will also have relevant implications for management of the world's other alluvial rivers entering the oceans as global sea level continues to rise.

2.2. MATERIALS AND METHODS

2.2.1. The Lowermost Mississippi River

Draining approximately 3.2 million square kilometers of land, the Mississippi River is the largest river in North America. The river's last 500-km reach starts at the Mississippi-Atchafalaya River avulsion node, where a diversion control structure was built (also known as the Old River Control Structure, ORCS), and ends at Head of the Passes, where the river breaches off into various channels entering the Gulf of Mexico (Figure 2.1). Riverbed of the first 130-km reach below the ORCS can be described as an alluvial channel. Below this reach to Head of the Passes, the river has been found to be a mixed bedrock-alluvial channel, comprising discontinuous alluvial sediment cover and exposed channel-bottom and sidewall substratum (Nittrouer et al., 2011). Nine large channel bars lie between ORCS and Baton Rouge (RK 370) and only two mid-channel bars existed downstream of Baton Rouge (Table 2.1). Major river engineering in the lowermost Mississippi River after the Great Mississippi Flood of 1927 is shown in Table 2.1. In this 500-km river reach, dredging has been mainly conducted on the crossings between Baton Rouge (RK 368) and New Orleans (RK 165) to keep the channel navigable. The annual dredging volume during 1988-2011 has been reported to be approximately 13×10^6 m^3 (Little and Biedenharn, 2014).

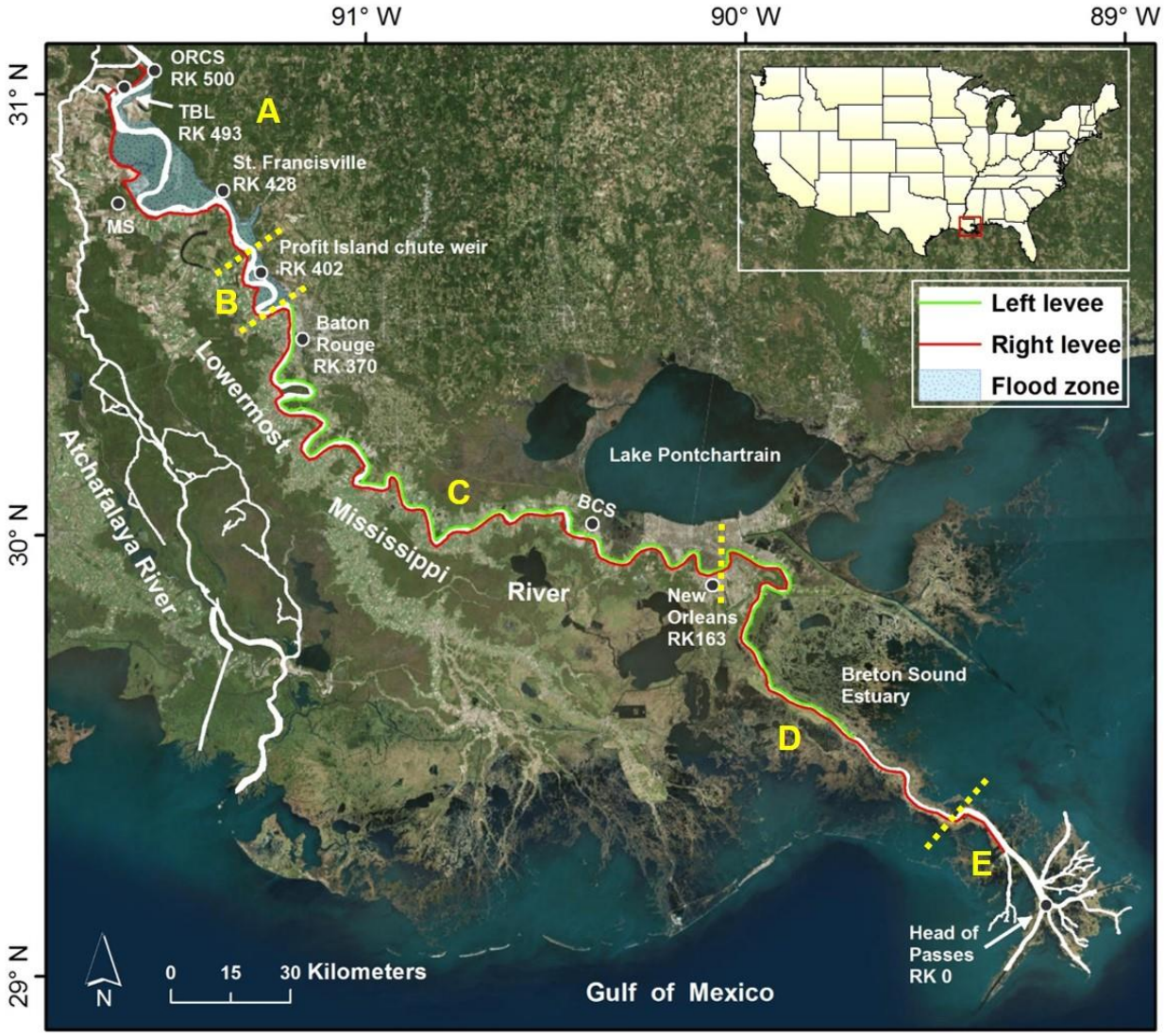

Figure 2.1. Geographical location of the lowermost Mississippi River beginning at the Mississippi – Atchafalaya River diversion, also known as the Old River Control Structure (ORCS) at RK 500 and ending at the river's Gulf outlet, also known as Head of the Passes at RK 0. Artificial levees exist along the entire channel except for the left bank between ORCS and Baton Rouge and downstream of RK 72. Overbank flooding mainly occurs between Tarbert Landing (TBL) and St. Francisville. Two flood spillways, the Morganza Spillway (MS) and Bonnet Carré Spillway (BCS), were designed for protecting the levee system by diverting excess flood water into the Atchafalaya River with wide floodplains and Lake Pontchartrain north of New Orleans, respectively. Reaches A-E are divided by the authors based on the different riverbed deformation from 1992 to 2013 (see Table 2.2 in the Results section).

Table 2.1. Information of major channel bars in the lowermost Mississippi River below its diversion to the Atchafalaya River at the Old River Control Structure, river kilometer (RK) 504.

Number	Name	Location	Type	Vegetation cover
1	Shreves Bar	RK 489	mid-channel bar	bar tail
2	Angola Landing	RK 481	point bar	bar tail
3	Miles Bar	RK 481	mid-channel bar	full
4	Brandon Bend	RK 470	point bar	middle
5	Tunica Island	RK 460	side bar	bar tail
6	Cat Island Bend	RK 450	point bar	none
7	St. Maurice Towhead	RK 438	mid-channel bar	bar tail
8	Fancy Point Towhead	RK 415	mid-channel bar	full
9	Profit Island	RK 402	mid-channel bar	full
10	Unnamed	RK 340	mid-channel bar	bar tail
11	Bayou Goula Towhead	RK 315	mid-channel bar	full

During the period of 1985-2015, daily discharge at Tarbert Landing (USACE station ID# 01100, RK 493), shortly below the ORCS, averaged 14,968 cubic meters per second (cms), varying from 3143 cms in the dry year of 1988 to 45,845 cms in the wet year of 2011. Average annual discharge of suspended sediment at Tarbert Landing has been estimated to be 127 million metric tons (MT) for the period 1980 – 2010 [*Rosen and Xu*, 2014] and 145 MT for the period 1987 - 2006 (Meade and Moody, 2010), while an average annual bedload at this location has been estimated to be 6.9 MT for the period 2004 – 2015 (Joshi and Xu, 2017) and downstream near New Orleans to be 2.2 MT for the period 2003 – 2006 (Nittrouer et al., 2008). Saltwater would intrude into the lowermost Mississippi River when the river discharge drops below 8500 cms [*Soileau, 1989*] and could migrate up to RK 116, where an earthen structure was placed to prevent the further intrusion (Allison and Meselhe, 2010).

2.2.2. Channel Survey and Bathymetric Data

The main datasets used in this study consisted of three hydrographic surveys of the lowermost Mississippi River conducted by the U.S. Army Corps of Engineers (USACE) in 1992, 2004, and 2013. The data provided bathymetry measurements using single beam fathometer

covering the 500-km long river channel starting at immediately downstream of the ORCS and ending at Head of Passes (Figure 1). Each dataset contains approximately 2000 cross sections with a distance of about 30-400 m to each other depending on channel morphology (i.e., denser measurements in bends) (Figure 2.2). The distance between two elevation measurements within a cross section was about 30 m. Considering the data coverage, the spatial resolution of measured elevation data is considerably high (Harmar et al., 2005). Most importantly, the survey datasets from the three years are comparable because the locations of all survey points were held consistent during these surveys. All the elevation data were used in the analysis except the data covering a 5-km long chute at Profit Island (RK 402). The elevations from 2004 and 2013 were given with reference to the North American Vertical Datum of 1988 (NAVD 88), while the elevation data in 1992 were based on the National Geodetic Vertical Datum of 1929 (NGVD 29). For consistency, the 1992 survey data were converted to NAVD 88. In addition to the hydrographic survey data, daily river discharge and suspended sediment concentrations recorded at Tarbert Landing were obtained from the USACE and the U.S. Geological Survey (USGS) to characterize sediment transport in the past 20 years.

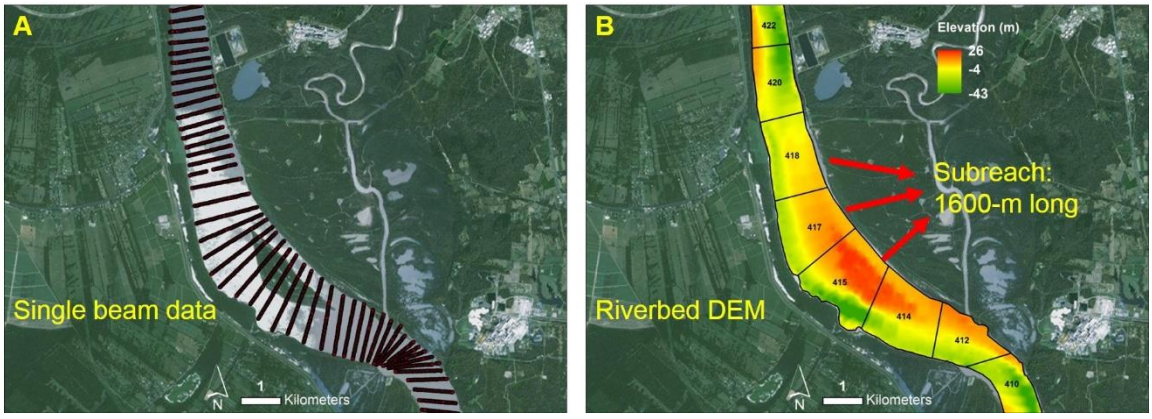

Figure 2.2. (A) Raw single beam survey data used to develop riverbed digital elevation model (DEM). Denser cross-sectional measurements were made in river bends. (B) A total of 311 continuous DEM maps were generated by IDW interpolation for the entire 500-km lowermost

Mississippi River from the Old River Control Structure to Head of the Passes at the Gulf of Mexico. Each DEM map represents a 1,600-m (1-mile) long reach in bankfull width.

2.2.3. Assessment of Longitudinal Riverbed Profiles and Channel Bed Deformation

A spatial interpolation technology, Inverse Distance Weighted (IDW) interpolation, was applied to the hydrographic survey data to create Digital Elevation Models (DEMs) of 10 x 10 m resolution. To obtain a detailed estimation for channel elevations, the entire channel of the lowermost Mississippi River was divided into 311 sub-reaches, each representing a 1,600-m (1-mile) long reach in bankfull width. Complete riverbed profiles were created by averaging the DEMs in each sub-reach using ArcGIS 10.3 (ESRI, Redlands, CA, USA).

With multi-year elevation data, changes in riverbed elevation and sediment volume were calculated to assess riverbed deformation of the LmMR over time. The volume change was estimated in ArcGIS using an add-in software - Geomorphic Change Detection (Wheaton et al., 2010a; Wheaton et al., 2010b). In the model, DEMs from every two years were used as elevation input to produce DEMs of difference by subtracting the elevations in one DEM from the other on a cell-by-cell basis. Net volume change in every sub-reach was then estimated by summing the product of calculated elevation change and the surface area of each cell (i.e., 100 m^2). Deposition and erosion of the riverbed in each of the 311 sub-reaches were then calculated.

2.2.4. Bifurcation Modeling for Avulsion Risk Assessment

The Old River Control Structure is maintained by the United States Army Corps of Engineers and built to prevent possible course changing from the Mississippi River to the Atchafalaya River. During the 1973 large Mississippi flood, the ORCS Low Sill Control Structure built in 1963 almost failed because of severe scour developed underneath the structure (Figure 2.3). In 1986, the Auxiliary structure was built to alleviate the pressure on the main control structure during large floods. In 1990, the Sidney Murray Hydroelectric Plant was completed to benefit from

the resource as well as to decrease the pressure of other ORCS structures (Mossa, 2016). From 1985 to 2013, the ORCS diverts approximately 23% Mississippi River flow into the Atchafalaya River (AR) (Wang and Xu, 2016), leaving the majority of flow to the main channel.

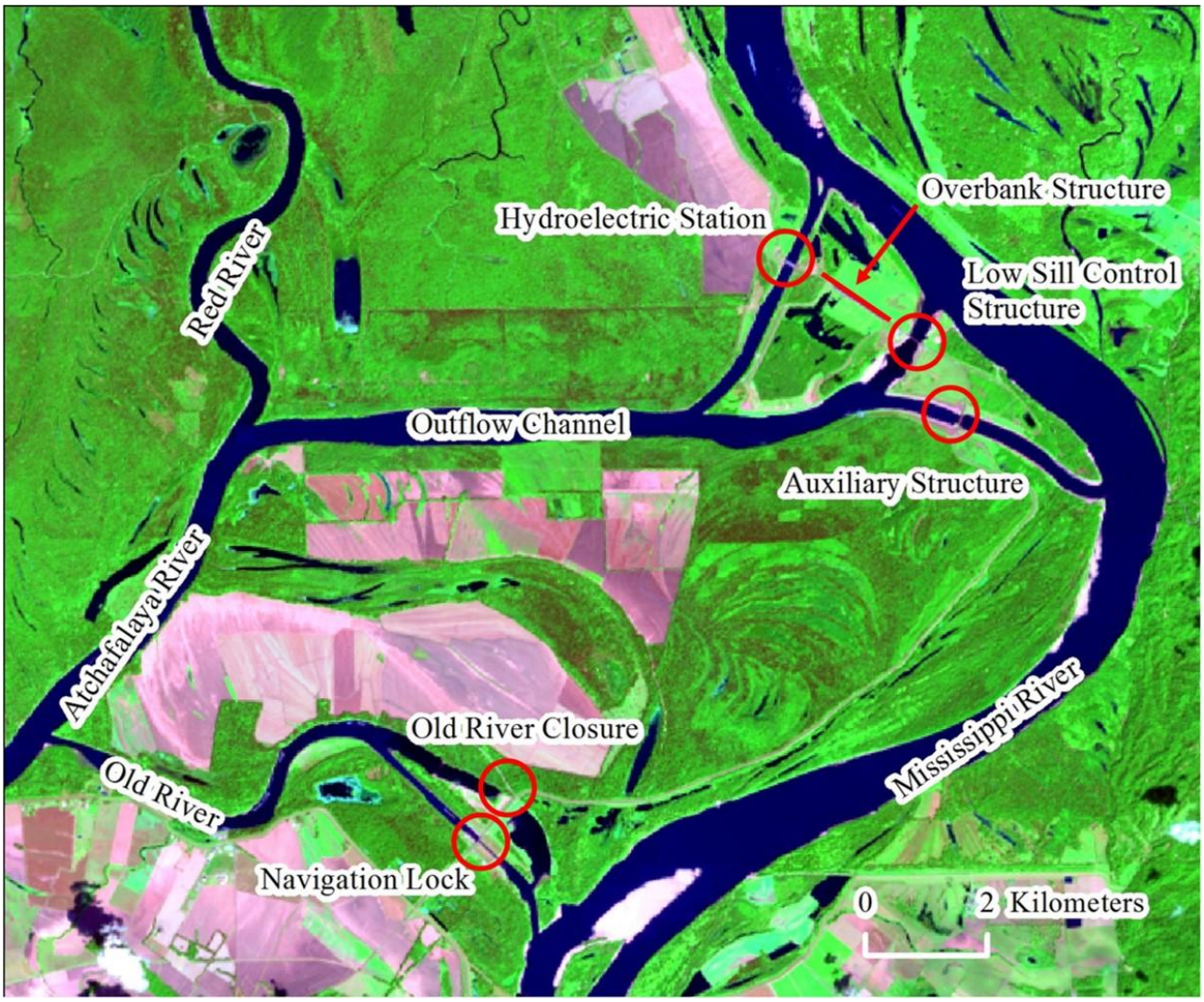

Figure 2.3. Old River Control Structure. The Low Sill Control Structure was completed in 1963 at the Old River channel (hence known as the Old River Control Structure, or ORCS) to regulate Mississippi River's inflow to the Atchafalaya River. An auxiliary structure was constructed in 1986 after the Low Sill Control Structure was damaged during the Mississippi River Flood of 1973.

Sediment transport and channel morphology of a natural and a leveed alluvial river

The diversion can be considered as a bifurcating branch. Previous studies found that a bifurcating branch may cause avulsion (Kleinhans et al., 2010; Slingerland and Smith, 1998) when sediment flow into the branch is much less than the branch's sediment transport capacity. Pittaluga

et al. (2015) recently developed a model to predict bifurcation stability for both sand bed rivers and gravel bed rivers, which is based on a comparison between sediment inflow and sediment transport capacity of a bifurcating branch. In this study, we applied this model to assess the potential risk of the Mississippi River avulsion into the Atchafalaya River at the Old River Control Structure. The model is given as below:

$$\left(\frac{3}{2}+\frac{2.5}{C_a}\right)+\frac{8\alpha\gamma}{\beta_a\sqrt{\vartheta_a}}=m\frac{\vartheta_a}{\vartheta a-\vartheta_{cr}}+\frac{1}{n}\frac{dn}{dD}\Big|_{\varepsilon=0}D_a \qquad (2.1)$$

where ϑ_a and β_a are the Shields stress and aspect ratio of the upstream channel, respectively, C_a is the dimensionless Chézy coefficient, ϑ_{cr} is the critical Shields value for sediment mobilization, the coefficients m and n depend on the sediment transport closure relation, D_a is the upstream flow depth, α is the dimensionless length of the final reach of the upstream channel, and γ is the empirical constant for transverse slope effect (Pittaluga et al., 2003).

The entire left side of the equation represents sediment inflow into a branch, while the entire right side represents sediment transport capacity. Based on this model, sediment transport capacity in a branch will increase when an initial perturbation occurs in one of the two downstream branches, e.g., a slight increase of water depth. The bifurcation remains stable if sediment inflow to the branch is greater than the increased sediment transport capacity of the branch. The stability is because the initial perturbation is diminished owing to the excess sediment input.

In this study, we first examined channel geometry immediately upstream of the ORCS to acquire the aspect ratio used in Equation 1. We then computed sediment inflow to the diversion channel and sediment transport capacity and compared the two terms to assess bifurcation stability of the ORCS. Additionally, using the same hydrographic survey data described in section 2.2.2,

we analyzed riverbed changes of the three outflow channels at the ORCS from 1992 to 2013 to validate the modeling result.

2.3. RESULTS

2.3.1. Longitudinal Trend of Riverbed Profiles

The longitudinal riverbed profiles of the lowermost Mississippi River in 1992, 2004 and 2013 are similar (Figure 2.4). Starting at river kilometer 500, the riverbed profile first rises about 10 meters within the first 20 kilometers downstream of the Mississippi-Atchafalaya River diversion. Then, it shows an overall declining trend for the next 300 km till RK 150. In the following 100 km, the riverbed shows a flat trend but with over a dozen deep channel cuts. The last 37-km reach of the LmMR to the Gulf of Mexico rises sharply for about 20 meters (Figure 2.4). The regular oscillations in the space of the profile are mainly controlled by the sequences of pools and crossings of the meandering pattern of the river. The emerged channel bars in the upper LmMR also contribute peaks in the riverbed profiles.

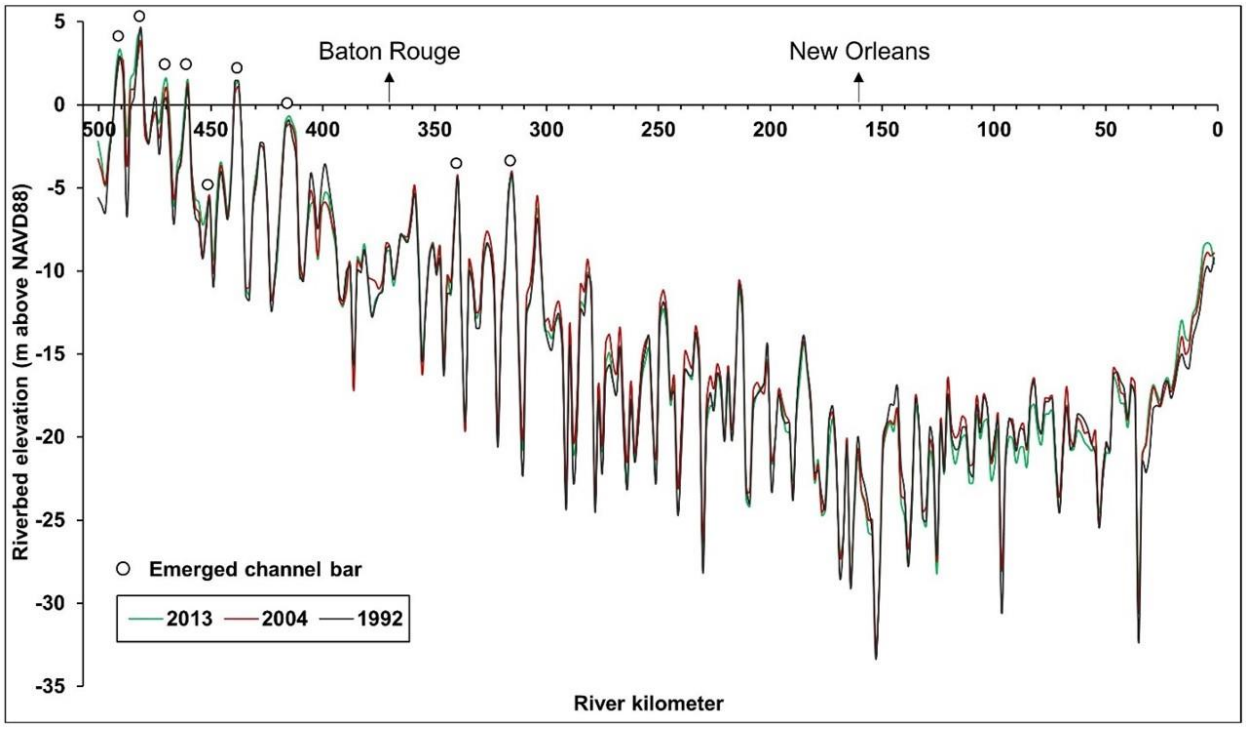

Figure 2.4. Riverbed profiles downstream of the lowermost Mississippi River in 1992, 2004 and 2013. The x-axis is river kilometer converted from river mile upstream of the river outlet at Head of Passes (RK 0). Y-axis is the riverbed elevation relative to the NAVD 88. Circles indicate the locations of emerged channel bars.

2.3.2. Riverbed Elevation Changes of the Lowermost Mississippi River

Based on changing characteristics of the riverbed elevation from 1992 to 2013, we divided the 500-km lowermost Mississippi River into five reaches (Figure 2.5). Over the 22-year period, the lowest reach of the LmMR, Reach E, experienced the largest channel aggradation (+1.3 m), followed by the uppermost reach A (+0.8 m). Reach C showed little channel aggregation (+0.1 m), whereas reaches B and D had the highest degradation, 0.7 and 0.6 m, respectively (Figure 2.5b, Table 2.2). During the two periods of 1992-2004 and 2004-2013, the changing trend of riverbed elevation was consistent in reaches A, B, and E, but was opposite in reaches C and D (i.e., from aggradation to degradation) (Figure 2.5 a). As a whole, the channel bed of the LmMR increased slightly (0.1 m) from 1992 to 2013, resulting from a 0.4 m aggradation during the first 12 years and a subsequent 0.3 m degradation in the last ten years.

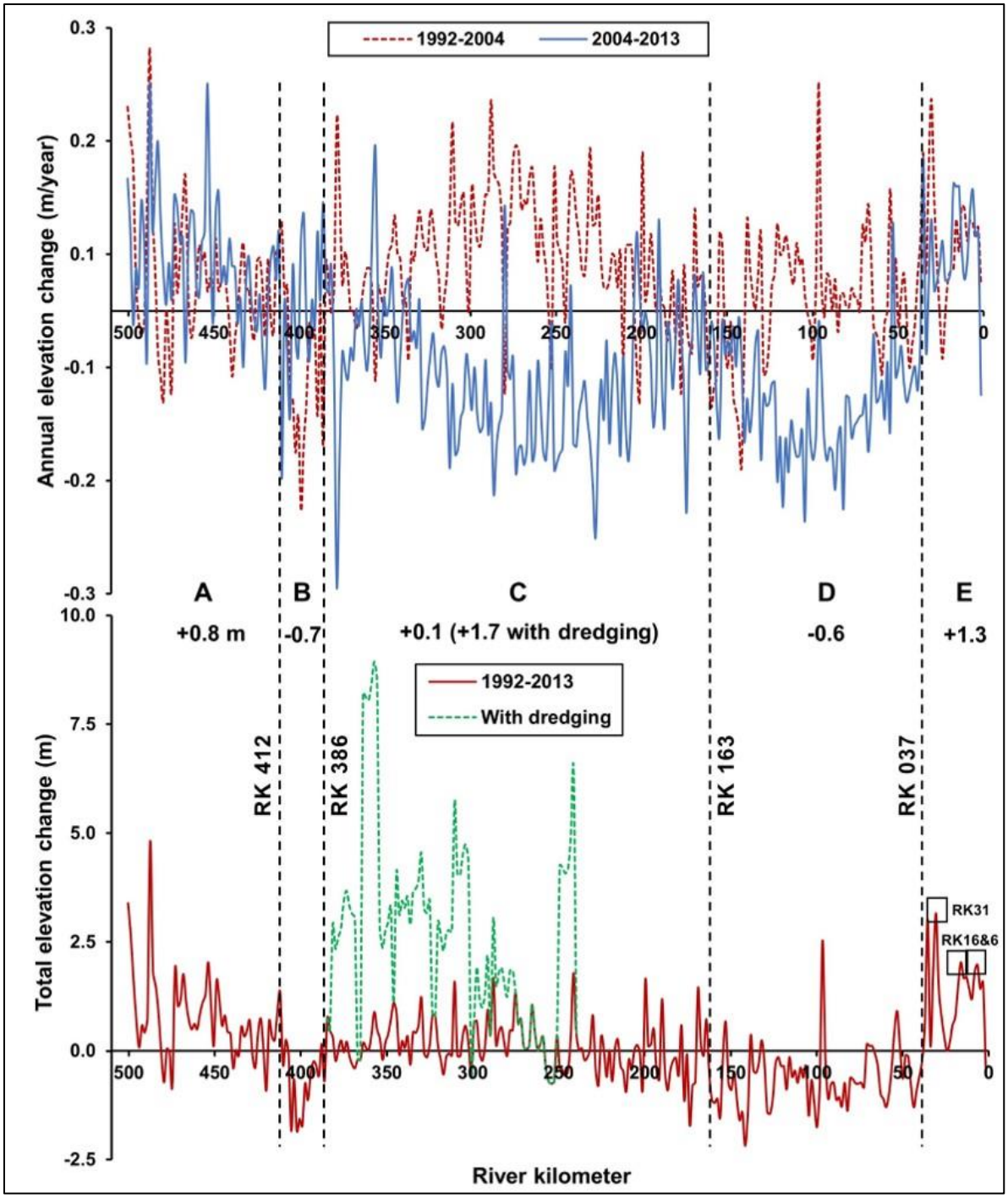

Figure 2.5. Top: Annual riverbed elevation changes (m/year) during the periods 1992-2004 and 2004-2013 in the lowermost Mississippi River. Bottom: Total riverbed elevation change (m) during 1992-2013. The dashed green line shows estimated actual bed elevation change from 1992 to 2013 when annually dredged sediment in reach C is added back to the observed values. The large riverbed aggradation in reach E occurred immediately downstream of the natural crevasses (e.g., RK 32) or flow passes (e.g., RK 19, 18, 6).

Table 2.2. Average changes of riverbed elevation in the lowermost Mississippi River from 1992 to 2013. Sub-reaches were divided based on the changing trends and degrees (see Figure 4). Reaches C and D showed a reversing trend during 1992-2004 and 2004-2013, while the other reaches kept the same changing trends. Values in the parentheses are estimated bed elevation changes when annually dredged sediment in reach C was added back to the observed values.

Reach	RK	Elevation change (m)			Change rate (m yr^{-1})		
		1992-2004	2004-2013	1992-2013	1992-2004	2004-2013	1992-2013
A	500-412	0.4	0.4	0.8	0.03	0.05	0.04
B	412-386	-0.7	0	-0.7	-0.06	0	-0.03
C	386-163	0.6 (1.6)	-0.5 (0.2)	0.1 (1.7)	0.05 (0.12)	-0.06 (0.02)	0.01 (0.09)
D	163-37	0.1	-0.7	-0.6	0.01	-0.08	-0.03
E	37-0	0.8	0.4	1.3	0.06	0.05	0.06
Total	500-0	0.4 (0.8)	-0.3 (0.0)	0.1 (0.8)	0.03 (0.06)	-0.03 (0.00)	0 (0.04)

2.3.3. Sediment Volume Change of Riverbed Surface

Over the past two decades, the volume changes of riverbed surface sediment in the lowermost Mississippi River showed a similar trend as the riverbed elevation change (Figure 2.6). From 1992 to 2013, reach A trapped the largest amount of sediment (62×10^6 m^3), followed by reaches E (46×10^6 m^3) and C (14×10^6 m^3) (Table 2.3). Reaches D and B lost a total of 58×10^6 and 13×10^6 m^3 sediment, respectively. With respect to the average rate of aggradation (i.e., $\times 10^6$ m^3 km^{-1} yr^{-1}), reach E had twice as high rate as reach A (i.e., 0.06 versus 0.03), reach B showed a similar rate as reach D (-0.02), and reach C was in a state of dynamic equilibrium (0.00). For the entire LmMR, there was 51×10^6 m^3 net sediment deposition over the 22-year period, including a net gain of 156×10^6 m^3 during 1992-2004 and a net loss of 105×10^6 m^3 from 2004 to 2013. The net gain during 1992-2004 occurred in the entire LmMR except for reach B (Figure 2.6). On the contrary, within the 150-km reach from RK 350 to RK 200, the net loss during 2004-2013 was found over a much longer reach, namely from RK 350 to RK 37 (Figure 2.6).

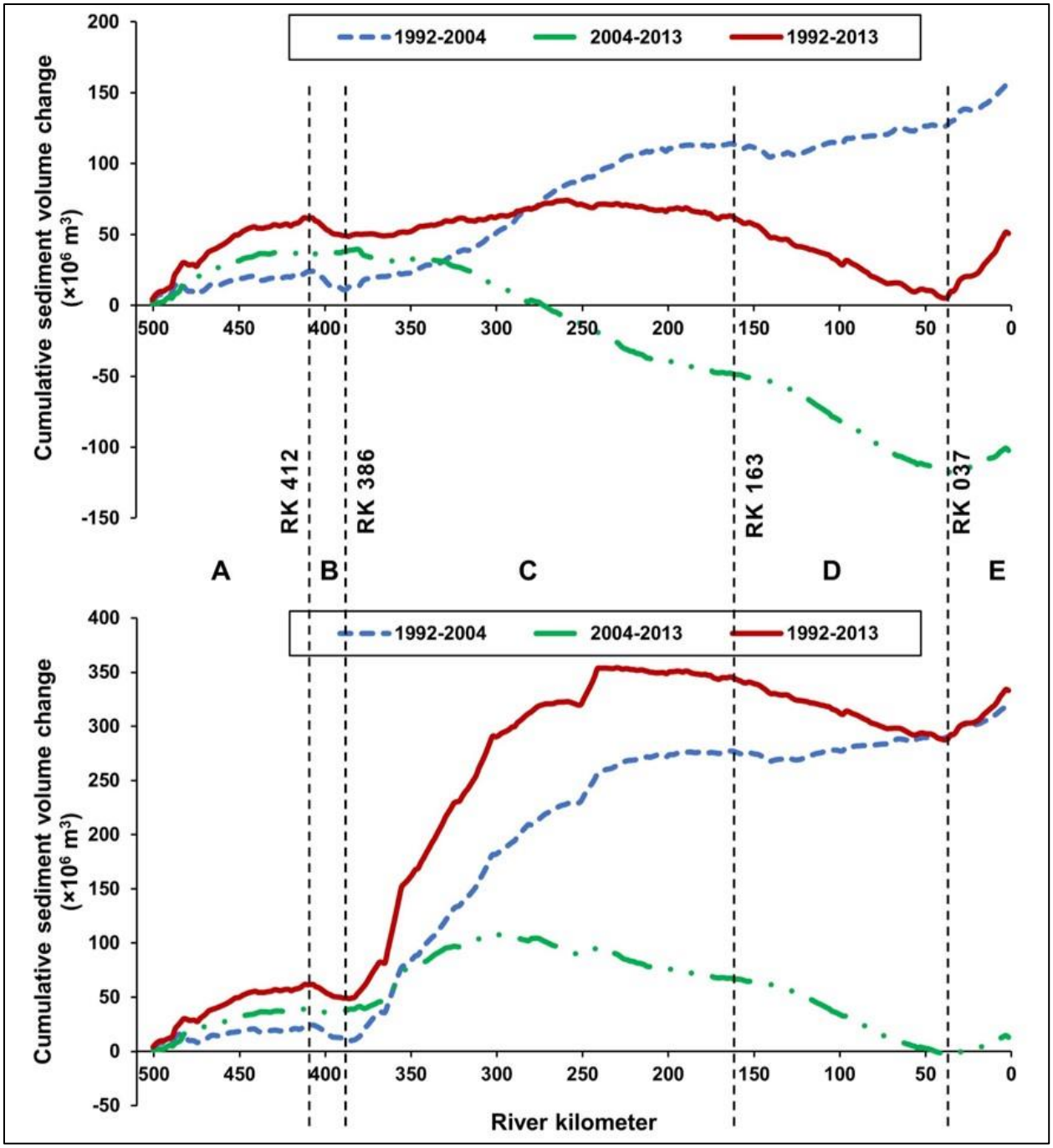

Figure 2.6. Top: Cumulative sediment volume changes in the riverbed of the lowermost Mississippi River from 1992 to 2013. The time series were created by summing the sediment volume from each sub reach in the downstream direction. A positive trend indicates sediment deposited on the riverbed, while a negative trend indicates sediment loss from the riverbed. Bottom: Cumulative sediment volume changes in the riverbed when annually dredged sediment in reach C was added back to the observed values.

Table 2.3. Cumulative sediment volume in the riverbed and corresponding change rate in reaches A - E of the lowermost Mississippi River from1992 to 2013. The reach divisions are the same as given in Table 2.1. Values in the parentheses are estimated actual volume changes when annually dredged sediment in reach C was added back to the observed values.

Reach	RK	Volume change ($\times 10^6$ m^3)			Change rate ($\times 10^6$ m^3 km^{-1} yr^{-1})		
		1992-2004	2004-2013	1992-2013	1992-2004	2004-2013	1992-2013
A	500-412	23	39	62	0.02	0.05	0.03
B	412-386	-10	-3	-13	-0.03	-0.01	-0.02
C	386-163	101 (270)	-87 (30)	14 (300)	0.03 (0.09)	-0.04 (0.01)	0.00 (0.06)
D	163-37	12	-70	-58	0.01	-0.06	-0.02
E	37-0	30	16	46	0.06	0.05	0.06
Total	500-0	156 (325)	-105 (12)	51 (337)	0.02 (0.05)	-0.02 (0.00)	0.00 (0.03)

2.3.4. LmMR Avulsion Risk Assessment

In sand bed rivers, the Engelund and Hansen relation should be applied in equation (1) (n = $0.05C^2$, m = 2.5, and ϑ_{cr} = 0) (Pittaluga et al., 2015). In the Lower Mississippi River, the dimensionless Chezy coefficient (C_a) is equal to 14.55 based on measured value from the previous studies (Nittrouer et al., 2012). Estimated channel aspect ratio immediately upstream of the Mississippi – Atchafalaya River diversion (RK 511) is ~35 (β_a). Shields stress ϑ_a is calculated between 0.96 and 15 under different flow velocity (i.e. from 1 m/s to 4 m/s). The value of $\alpha\gamma$ is given to 2 according to Pittaluga et al. (2015).

With estimated aspect ratio immediately upstream of the Old River Control Structure and derived various channel parameters from the previous studies, the left-hand side of the Equation 2.1 (representing sediment input) ranges from 1.78 to 2.14, while the right-hand side (representing sediment carrying capacity) is equal to 2.53. When the sediment supply is less than the sediment carrying capacity, more sediment would leave the Mississippi-Atchafalaya outflow channel, and the channel consequently tends to be scoured. Under such condition, the bifurcation would be unstable according to the model by Pittaluga et al. (2015). Erosion of the outflow channel was

confirmed by the analysis of bathymetric data measured in 1992 and 2013 (Figure 2.7). Bed deposition mainly occurred downstream of the Low Sill and Auxiliary Structures, while bed erosion was clearly shown downstream of the Hydroelectric Station. Overall, the outflow channel at the ORCS was scoured 1.31 m on average over the past two decades.

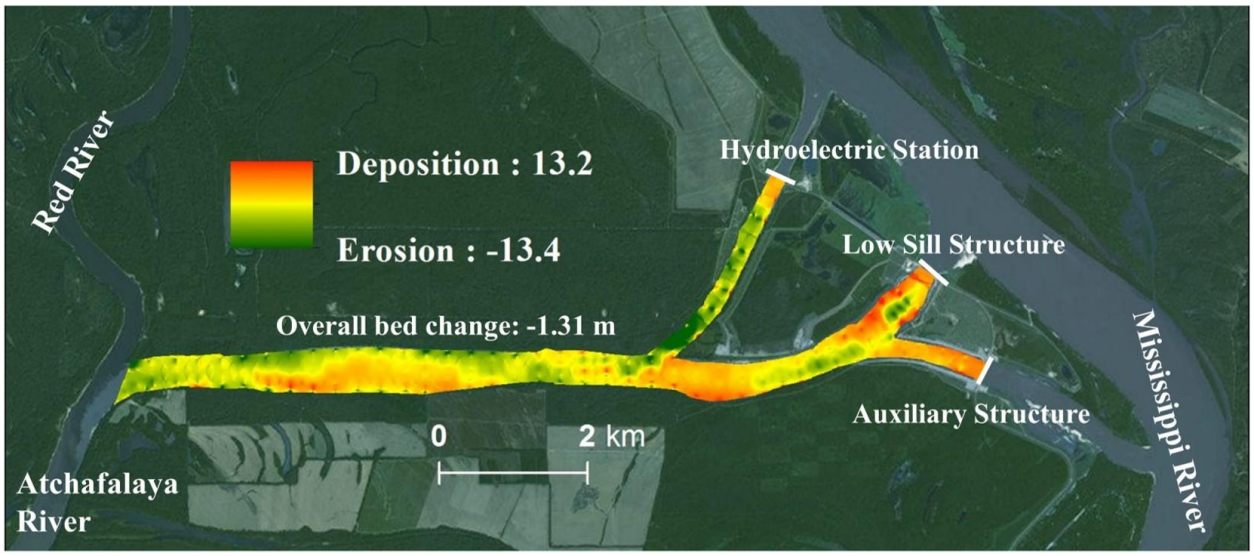

Figure 2.7. Riverbed deformation in the outflow channel of the Mississippi-Atchafalaya River diversion from 1992 to 2013. Overall, the outflow channel was scoured 1.31 m on average.

2.4. DISCUSSION

2.4.1. Riverbed deformation and hydrologic effects

Over the past 22 years, the 500-km lowermost Mississippi River showed a clear aggradation trend in its uppermost 88 km (reach A) and its last 37 km (reach E), and a degrading trend in the 26-km reach B. The reach from RK 386 to RK 37 had an opposing trend (i.e. reaches C and D) showing first an aggradation from 1992 to 2004 and then a degradation from 2004 to 2013. During the entire studied period, reach C shows little bed change, while reach D had a significant bed erosion. Overall, considering the long distance of the river reach assessed and the change in total volume observed over time, the bed deformation (i.e., approximately 4,636 m^3 km^{-1} yr^{-1}) in the LmMR is relatively marginal (largely caused by the continuous river dredging, see

more below). However, spatially, the extent of riverbed deformation varied largely from reach A to reach E over time.

The continuous riverbed aggradation in reach A over the past two decades is consistent with the long-term (i.e., 10^2-10^3 yr) depositional feature of the LmMR. Located downstream of the Mississippi-Atchafalaya River diversion, which is the latest avulsion node in the Late Holocene (Aslan et al., 2006), reach A may have experienced in-channel aggradation since the 16th century when the switch of the Mississippi to the Atchafalaya was already underway (Fisk, 1944; Fisk, 1952). A recent analysis of sedimentary deposits of the Mississippi, constructed over the Late Holocene, revealed that lateral migration rate of channel belts decreased from ~60 m/yr to less than 5 m/yr between RK 500 and RK 300 and remained very low downstream of RK 300 (Fernandes et al., 2016), indicating that reach A is a site of sediment trapping over millennial time scales because sedimentation rates are known to be higher in the meander belt (Allen, 1965; Bridge and Leeder, 1979; Bryant et al., 1995). The result from a one-dimension hydrologic model also demonstrates that the riverbed of the LmMR between RK 600 and RK 150 has a tendency to aggrade and reach A has the highest aggradation rate (Nittrouer et al., 2012). Based on these findings, we believe that the observed bed aggradation in reach A in the past two decades is mainly a long-term and slowly occurring natural process.

However, the Mississippi-Atchafalaya River diversion at the Old River Control Structures may have accelerated the in-channel aggradation in reach A. By diverting ~23% of the Mississippi flow into the Atchafalaya River during 1985-2013, the ORCS could largely reduce the downstream flow velocity, which may have increased downstream sediment settling. Assessment of the hydrographic surveys conducted in 1963 and 1975, which followed the operation of the ORCS in 1963, found significant downstream bed aggradation (i.e., 30×10^6 m^3) between RK 507 (i.e., the

ORCS Low Sill Structure) and RK 490. In a recent study, we also found a considerable sediment accumulation (i.e., 30×10^6 m^3) on the three large channel bars downstream of the ORCS between RK 491 and RK481 from 1985 to 2013 (Wang and Xu, 2016). In the current study, the uppermost 19-km channel in reach A amassed approximately 48% (i.e., 30 of 62×10^6 m^3) of the total sediment deposited in the reach (Figure 2.6). These findings indicate the effect of the ORCS on downstream channel siltation may exist after it was built in 1963. In the future, a detailed modeling study on sediment dynamics in reach A may help to understand the effects of the ORCS.

Several factors may have played a role in the highest deposition rate in the last 37 kilometers of the LmMR (i.e., reach E). A high rate of deltaic sedimentation can be a response to the accelerated sea level rise in the recent decades as found in the history of the LmMR (Saucier, 1994). However, the average annual deposition rate of 0.06 m or 60 mm in reach E over the past 22 years is much higher than both the 20th century average annual rate of sea-level rise [1.7 ± 0.3 mm (Church and White, 2006) and the estimate of a relative sea level rise for the area [10-18 mm yr^{-1} (Penland and Ramsey, 1990). Also, the intrusion of the saltwater wedge during low discharge can also produce seasonal sediment deposition in this area (Galler and Allison, 2008), but such impact should be low owing to the micro-tidal environment of the Gulf of Mexico. Checking the locations with a high deposition rate, we found that most of the deposition has occurred immediately downstream of the natural crevasses (e.g., RK 32) and river passes (e.g., RK 19, 18, and 6) (Figure 2.5 & 2.8). This finding strongly suggests that the reduction in flow velocity is one of the dominating factors for various high sedimentation rates in the LmMR over the past two decades. However, this widely-known effect of flow reduction on deposition has not been taken into careful consideration in the current planning (CPRA, 2007; CPRA, 2012) for future river diversions.

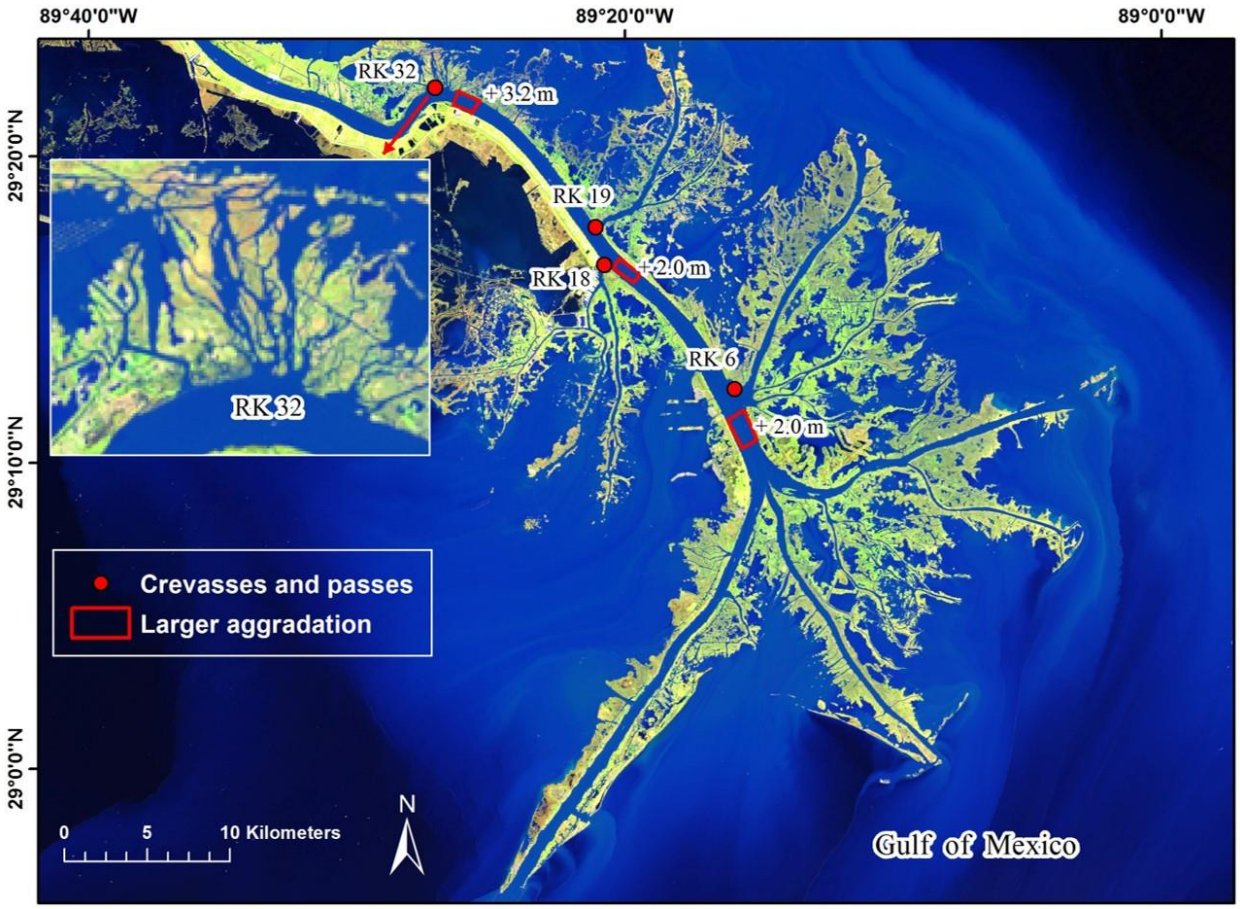

Figure 2.8. Substantial bed deposition occurred in reach E, generally immediately downstream of a natural crevasse (e.g., RK 32) or flow pass (e.g., RK 19, 18, 6). The increased bed elevation in the three subreaches was derived from Figure 2.5.

For reach B, it is noted that there is a chute located on the east side of the Profit Island (RK 402, Figure 2.1). However, we only estimated riverbed deformation in the main channel of this reach. The strong bed erosion during 1992-2004 may have resulted from the chute closure (Figure 2.1). One chute weir was constructed in 1986 to control the flow of water into the chute and maintain flow and navigation in the main channel. Discharge readings show flow through the chute ranging from 6% to 26% of the total flow of the river. Thus, the river flow in the main channel was accelerated and likely expended the extra energy by scouring the channel bed. The little further erosion found during 2004-2013 indicates that reach B became equilibrium.

Over the entire 22 years from 1992 to 2013, reach C showed a reverse trend and a significant difference in riverbed volume change (i.e., +101 vs. -87 × 10^6 m^3, Table 2.3). However, in the LmMR, dredging is mainly operated in the 11 reaches in reach C between RK 381 and RK 241 (detailed dredging information shown in Table 2.4). Considering the amount of annually dredged sediment in this reach (i.e., ~13 × 10^6 m^3, Little and Biedenharn (2014)), the riverbed of reach C has actually gained 270 x 10^6 m^3 sediment during 1992-2004 and 30 x 10^6 m^3 during 2004-2013. The estimated changes in bed elevation and cumulative sediment volume in consideration of dredging activities are shown in Figure 4 and 5 when the average annual dredging amount in each reach was added back to reach C. Different from reach C, reverse trends were observed in reach D (i.e., +12 vs. -70 × 10^6 m^3, Table 2.3). Overall, it is interesting to explore the reasons causing such large differences in riverbed sedimentation during the two sub-periods in these two reaches.

Table 2.4. Dredged reaches and amount (MCY= million cubic yard; CM=cubic meter) in the lowermost Mississippi River below its diversion to the Atchafalaya River at the Old River Control Structure, river kilometer (RK) 504.

Reach	Name	RK	Average annual dredging amount (MCY)	Average annual dredging amount (CM)	Dredging amount per mile (m^3/mile)	Bed surface area of each reach (m^2)	Annual dredging elevation per reach (m/yr)
1	Wilkerson Point	377-381	0.7	535,188	133,797	4,764,177	0.11
2	Baton Rouge Front	369-377	1.5	1,146,832	191,139	7,613,246	0.15
3	Redeye	356-364	4	3,058,220	509,703	8,753,808	0.35
4	Sardine Point	348-356	1	764,555	127,426	6,840,870	0.11
5	Medora	335-344	1.6	1,223,288	174,755	9,837,897	0.12
6	Granada	325-333	1.5	1,146,832	191,139	7,946,067	0.14
7	Bayou Goula	312-320	1.5	1,146,832	191,139	9,280,137	0.12
8	Alhambra	303-311	2	1,529,110	254,852	8,450,871	0.18
9	Philadelphia Point	291-298	0.4	305,822	61,164	5,723,346	0.05
10	Smoke Bend	277-288	0.8	611,644	76,455	10,284,149	0.06
11	Belmont	241-249	2	1,529,110	254,852	7,562,379	0.20

There was no significant difference in the dredging volume during the two periods (Little and Biedenharn, 2014). The annual sediment and sand load at Tarbert Landing (RK 493) had no significant trend either (Joshi and Xu, 2015; Rosen and Xu, 2014). The oscillations of riverbed profiles are mainly caused by the crossings and pools of the river (Figure 2.4). However, the examination of effects of the profile oscillations on bed deformation shows little correlations between the bed changes and the appearance of the crossings and pools (Figure 2.9). Therefore, the dredging, sediment input, and distribution of crossings and pools cannot explain the different trends during the two sub-periods, 1992-2004 and 2004-2013. By examining previous theories and studies (Chatanantavet et al., 2012; Lamb et al., 2012; Nittrouer et al., 2012), we found that the observed bed deformation in the LmMR can be well explained by backwater effects.

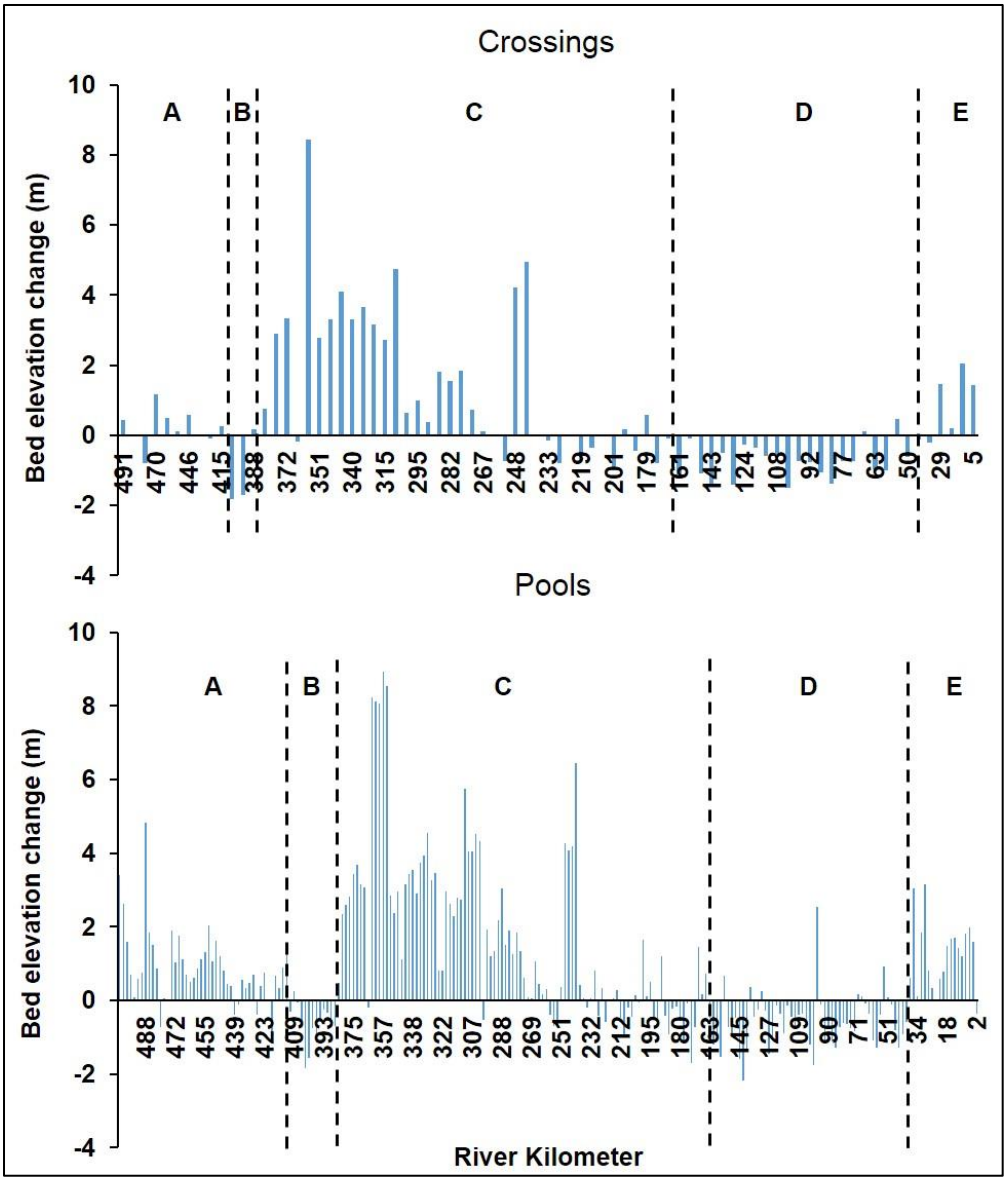

Figure 2.9. Riverbed deformation at the crossings and pools of the lowermost Mississippi River from 1992 to 2013 The consistent trends of bed deformation indicate that the sequences of crossings and pools could not decide the scour and deposition patterns of the riverbed.

Backwater effects occur when a river approaches its receiving basin where the flow is decelerated because of channel deepening and spreading of the offshore plume (Chow, 1959; Lane, 1957). Recent modeling and experiment analysis found that the riverbed of backwater zones of alluvial rivers tends to aggrade during low flow, but degrades during high flow because the water surface is drawn down near the river mouth to match that of the offshore plume and generates

accelerated flow (Chatanantavet et al., 2012; Ganti et al., 2016; Lamb et al., 2012). For the Mississippi River, the length of the backwater zone was estimated about 650 km upstream of the Head of Passes (Nittrouer et al., 2012). Both 1-D and quasi 2-D modeling results showed that the riverbed of the LmMR tends to aggrade in its upper reach, while degrades in the lower half of the backwater zone (Chatanantavet et al., 2012), especially in the last 150-km reach (Lamb et al., 2012; Nittrouer et al., 2012).

Neglecting reach B where the bed elevation was affected by the river engineering and reach E where flow reduction largely contributed to the bed aggradation, the channel bed deformation in the LmMR during the 22-year period followed the backwater theory well: the upper reach (i.e., reaches A and C showed substantial bed aggradation, while the lower 163-km reach was eroded (Table 2.3 & Figure 2.6). In terms of different periods, the observed large differences of the bed deformation in reaches C and D were caused by the major floods occurred during 1992-2013. Modeling results showed that the bed erosion in the backwater segment of LMR is triggered when water discharge is over ~26,000 m^3 and the bed erosion rate has exponential increase with the increased discharge above this threshold value (Chatanantavet et al., 2012; Lamb et al., 2012). For example, the maximum bed erosion rate at the discharge of 3.9×10^4 m^3/s is more than two and 30 times the rates of relatively low discharge (i.e., 3.2×10^4 and 2.6×10^4 m^3/s), respectively (Chatanantavet et al., 2012). The large floods in 2005, 2008, 2009, and 2011 with high peak discharge were, therefore, reasonable to remove more sediment in reaches C and D than the previous decade when only the 1993 and 1997 floods had the similar peak discharge (Figure 2.10). It should be noted that we consider these three floods had the similar drawdown effects downstream of RK 205 because the Bonnet Carré Spillway at the location (RK 205, Figure 2.1) was operated in 1997, 2008 and 2011 to divert the flood water into Lake Pontchartrain for ensuring

the downstream discharge flowing by New Orleans was less than ~35,000 m^3/s. However, the 2011 Mississippi flood, the largest flood occurred in the LmMR in terms of the peak discharge (i.e., ~4.6×10^4 m^3/s) after the Great Mississippi Flood of 1927 (i.e., peak discharge 4.8×10^4 m^3/s), may have scoured the riverbed up to RK 328. This is supported by the modeling analysis that the estimated length of the eroded bed during the Great Mississippi Flood of 1927 was 340 km from the Head of Passes (Lamb et al., 2012). The bed erosion during 2004-2013 in reaches C and D started at RK 328 (Figure 2.6), which is close to the modeling result and therefore it was very likely caused by the 2011 flood.

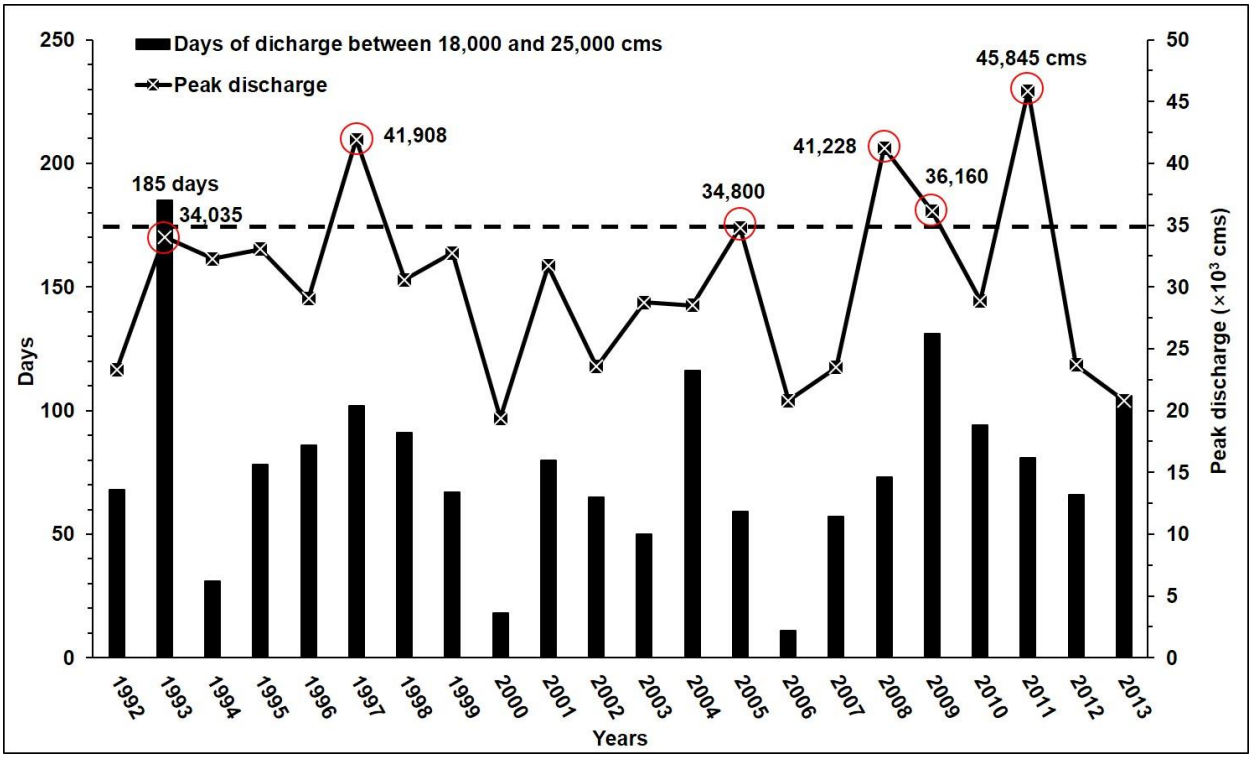

Figure 2.10. The annual peak discharge of the lowermost Mississippi River (at Tarbert Landing) from 1992 to 2013. The higher frequency of large floods during 2004-2013, e.g., the floods in 2005, 2008, 2009, and 2011 may have removed large amounts of riverbed sediment from reaches C and D because of the drawdown effect in the lower segment of the backwater zone. On the contrary, the longest days of discharge between 18,000 and 25,000 cms during the 1993 Great Mississippi Flood may have most likely caused sediment deposition on the channel bed of reaches C and D, which weakened the drawdown effect of the 1993 flood.

It should be noted that the drawdown effect of the Great Mississippi Flood of 1993 may have been largely weakened. The 1993 flood was the largest flood in terms of duration and inundated area after the 1927 flood. During the 1993 flood, the days of discharge between 1.8×10^4 m^3/s and 2.5×10^4 m^3/s at Tarbert Landing was 185 days which was much longer than the average number of days (i.e., 78 days) in the other years from 1992 to 2013 (Figure 2.10). The discharge in this range typically results in the maximum suspended sand concentration (Rosen and Xu, 2014) and extensive channel bed aggradation over the entire LmMR bed (Chatanantavet et al., 2012; Nittrouer et al., 2012). Hence, the 1993 flood may have contributed to the sediment deposition in reach C and D rather than the bed scour.

Backwater hydrodynamics associated with a river entering the ocean were widely studied recently by hydrodynamic models (Chatanantavet et al., 2012; Lamb et al., 2012; Nittrouer et al., 2012; Viparelli et al., 2015). However, these models had difficulties in simulating bed erosion in the lower segments of the backwater zones when long-term discharge-frequency data derived from a hydrograph was applied (Chatanantavet et al., 2012; Viparelli et al., 2015). This is apparently inconsistent with the observed bed erosion in the last 160-km reach of the Mississippi River since the 1920s (Galler et al., 2003). It indicates that the neglected factors in the current modeling studies, e.g., emerged channel bars, channel meandering pattern, and channel sinuosity may have largely contributed to the long-term riverbed deformation. The detailed riverbed deformation study in the current study could be very useful in the future modeling study, especially for simulating the long-term bed erosion in the lower segment of the backwater zones.

2.4.2. Channel Geomorphological Classification and Management Implications

In terms of mass of the trapped sediment in the LmMR over the entire 22-year study period, the total volume of 337 x 10^6 m^3 riverbed deposition (i.e., sum of 51 x 10^6 m^3 net deposition and

286 x 10^6 m^3 dredged sediment) is equivalent to 404.4 million metric tons (MT) of sediment, assuming a dry bulk density of 1.2 metric ton per cubic meter for the riverbed sediment. Because much of the riverine fine particles (i.e., clay and silt, < 0.0625 mm) cannot settle because of the high flow, this essentially represents an average annual of 18.4 MT sand deposition, which accounts for 68% of the annual 27 MT suspended sand (>0.0625 mm) load estimated by Joshi and Xu (2015) that entered the LmMR during 1973-2013 (Figure 2.11). This result indicates that the highly trained LmMR has a strong capacity to trap sand, and does not behave as an effective conduit for sediment to reach the coast (Kesel, 2003). Dredging removed 13 x 10^6 m^3 sand annually, or 15.6 MT in mass, representing 85% (or 15.6 of 18.4 MT) of deposited sand out of the river system (Figure 2.11). Thus, there was only about 62 MT (or 51×10^6 m^3) net sand gain during 1992-2013. Such amount of sand only accounts for 10% of annual average suspended sand load in the LmMR. Although it is successful for keeping the deep draft navigation channel in the LmMR (i.e., 0.00×10^6 m^3 km^{-1} yr^{-1} bed aggradation), dredging seems to have conflicted with the current coastal protection and restoration plan, especially when all the dredged materials from the river are put into the open water instead of beneficially used for creating marshes. Because the LmMR is regulated by artificial levees and the amount of sand entering the river would have no significant decrease over the next several centuries (Nittrouer and Viparelli, 2014), we believe that sand will continue to deposit in reach C in the future. As the most important material for the growth of subaerial delta (Roberts et al., 2003), sand sources should be well managed. If all trapped sediment in reach C (i.e., 13×10^6 m^3) could be mobilized and delivered downstream during large floods and efficiently captured by the proposed sediment diversions, 130 km^2 new coastal land (i.e., with 10-cm thick sand) could be created every year, helping sustain and restore the sinking Mississippi River Delta.

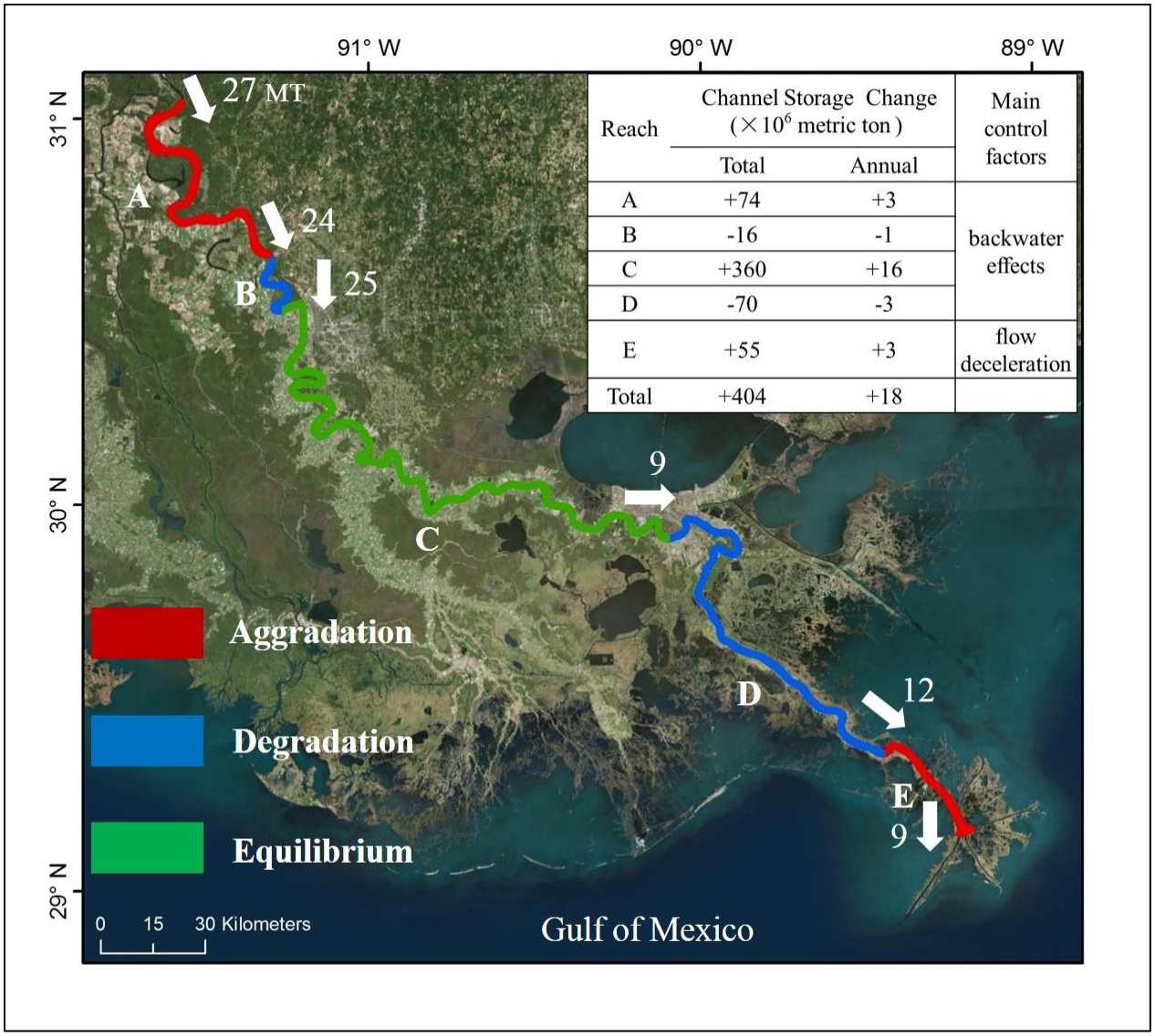

Reach	Channel Storage Change ($\times 10^6$ metric ton)		Main control factors
	Total	Annual	
A	+74	+3	backwater effects
B	-16	-1	
C	+360	+16	
D	-70	-3	
E	+55	+3	flow deceleration
Total	+404	+18	

Figure 2.11. Patterns of riverbed deformation and sand budget variation in the 500-km lowermost Mississippi River during 1992-2013. Reaches A and E experienced continuous bed aggradation, while reaches B had continuous degradation in the past two decades. Reaches C and D had a reversed trend of deformation and was also heavily dredged, resulting in a riverbed elevation equilibrium under the current channel management. Overall, the riverbed deformation in reaches B and E are mainly controlled by reduced flow velocity, while reaches A, C and D are highly affected by backwater effects. Also shown are channel sand storage change (total and annual) in reach A-E. The numbers next to the arrows show the sand discharge into the reaches.

Continuous riverbed aggradation in reach A will cause increased water surface elevation of this reach below the ORCS. This has been shown by Wang and Xu (2016) that the river stage at a specific discharge at Tarbert Landing has increased about 1.5 meters in the past 30 years.

During the same period, the river channel has also narrowed about 800 meters on average. The condition contributes to one of the critical factors for a river avulsion: in-channel deposition in the main channel.

Another factor that can cause a sudden change of a river course is a triggering flood. Historical and current observed trends suggest that the riverbed aggradation in reach A may continue, which may further reduce the flow gradient in the Mississippi River. With more sediment falls to the bottom and flattens the bed of the MR, the water flowing into the Atchafalaya River (AR) may contain less sediment. As a result, the AR would continue to scour its bed to balance the input water which makes its channel larger and draws more water from the MR. In the long term, this process increases the risk of the MR changing its course to the AR when a historic flood occurs. It is, therefore, pertinent to develop management strategies to mobilize the sediment in the reach, especially in the uppermost 19-km channel.

2.4.3. Implications for other large river systems

Many of the world's large rivers have been dammed upstream in the past century (Blum and Roberts, 2009; Cochrane et al., 2014; Yang et al., 2011). This engineering practice has been found to significantly reduce downstream sediment transport (Vorosmarty et al., 2003; Walling, 2006; Walling and Fang, 2003), which has led to channel erosions downstream of the dams in the upper and middle river reaches. For example, the riverbed of the middle Yangtze River has been found to be eroded after the closure of the Three Gorges Dam (TGD) (Yang et al., 2011; Yang et al., 2007). Similar riverbed erosion has also been found in the middle Yellow River after the closure of the Xiaolangdi Dam in 2002 (Wang et al., 2017). While these studies offer insights into channel erosion immediately downstream of dams, we found very few studies investigating riverbed deformation in the backwater zones of large alluvial rivers, owing to the lack of long-

term bathymetric data and often frequent channel engineering for river-sea cargo shipping. Our study shows the complexity of sediment transport in the lower reach of a large alluvial river, in that distinctive bed deformation can occur in different reaches because of flow deduction and backwater effects. The findings offer insights into potential bed deformation trends for lower reaches of other large river systems with no or limited bathymetry, discharge, and sediment data. Such information could also be applicable for other rivers to develop sustainable river engineering strategies and plans.

The observed bed deposition found downstream of the Mississippi-Atchafalaya River diversion in this study suggests that large-scale water diversions could cause downstream siltation. This insight can be utilized in river engineering to mitigate downstream channel infilling for other large river diversion projects, e.g., the South-to-North Water Diversion project of the Yangtze River in China. Although the present study could not separate flow reduction and backwater effects on channel siltation, the findings gained from the study indicate that future sea-level rise due to climate change may likely increase upstream siltation in the Mississippi and the other alluvial rivers in the world. Further studies are needed to elucidate individual effects of river flow reduction and tides on riverbed deformation of large alluvial rivers in their backwater zones.

2.5. CONCLUSIONS

Alluvial rivers under natural conditions are subject to river flow and sediment discharge. Channel confinement and other engineering practices in such rivers can alter flow and sediment transport, leading to different bed deformation dynamics and equilibrium. This study found that in the 500-km lowermost Mississippi River, significant sediment deposition occurred in the uppermost 88 kilometers immediately below the Mississippi-Atchafalaya River diversion and the last 37 kilometers where the river starts to breach off into the Gulf of Mexico, causing flow

reduction and downstream sedimentation. Continuous bed aggradation downstream of the Mississippi-Atchafalaya diversion may largely increase the risk of avulsion if unprecedented floods occur. The observed trends in the reach between RK 386 and RK 163 suggest that it has substantial potential for trapping sediment. From 1992 to 2013, although marginal sediment deposition was found in the lowermost Mississippi River (i.e., 51×10^6 m^3), the river trapped approximately 337×10^6 m^3 sediment (mainly sand) considering the dredged volume of riverbed sediment. This rejects the initial hypothesis that the lower reach of this highly engineered large alluvial river functions as a conduit for sediment transport. The total volume of trapped sediment over the past 22 years is equivalent in mass to 68% (i.e., 404 MT) of the total suspended sand discharged into the LmMR (i.e., 598 MT), assuming a bulk density of 1.2 metric ton per cubic meter for the riverbed material. On an annual mass budget, only about 9 MT sand is discharged from the river into the Gulf of Mexico. Backwater effects have mainly controlled in-channel deposition and erosion in the lowermost Mississippi River, while flow reduction may have also contributed to channel aggradation in the uppermost and lowermost reaches. The finding may suggest that lower reaches of the world's other alluvial rivers entering the sea would experience greater channel deformation in the future as global sea level continues to rise. In the past, river engineering has focused on flow regulation for navigation and flood control. Future river engineering and management also need to develop strategies and solutions that will improve sediment transport and utilize the dredged material for coastal restoration to counter deltaic land loss. The revealed trends of the bed deformation in this large low-lying river could further help understanding the bed morphodynamics of the other lowland river systems, and ultimately help river management and delta protection.

CHAPTER 3. ESTIMATION OF BEDLOAD SEDIMENT FLUXES UPSTREAM AND DOWNSTREAM OF A CONTROLLED BIFURCATION NODE - THE MISSISSIPPI-ATCHAFALAYA RIVER DIVERSION

3.1. INTRODUCTION

Bifurcations are important nodal points in river systems that redistribute flow and sediment downstream in braided and anastomosing channels on fluvial plains and deltas. Bifurcations can cause downstream aggradation in the original channels and enlargement of the newly bifurcated channels (Kleinhans, Jagers, Mosselman, & Sloff, 2008). Such processes usually make the bifurcations unstable, resulting in final avulsions. A number of studies have developed numerical models to assess bifurcation stability for both gravel-bed and sand-bed rivers (Edmonds & Slingerland, 2008; Kleinhans et al., 2008; Miori, Repetto, & Tubino, 2006; Pittaluga, Coco, & Kleinhans, 2015; Pittaluga, Repetto, & Tubino, 2003; Slingerland & Smith, 1998; Wang, Fokkink, DeVries, & Langerak, 1995). These studies have identified a number of factors that can, under natural conditions, influence the bifurcation symmetry and stability including bed slope, bend structure, sediment sorting, and width-depth ratio upstream of the bifurcation. While the findings are fundamental for understanding bifurcation processes, our knowledge about bed material load transport at bifurcations is rather limited.

The Mississippi-Atchafalaya River diversion is a prime example. The Atchafalaya River used to be one of the ancient channels of the Mississippi River (Fisk, 1952), and the current diversion is located about 500 km upstream of the Mississippi River mainstem's outlet to the Gulf of Mexico (Figure 3.1). In the 15th century, the Mississippi River made a large meander at the location, often known as the Old River. The meander's west side eventually intercepted the north-to-south flowing Red River, making the Red River a tributary and the downstream channel, Atchafalaya River, a distributary of the Mississippi River. The entrance to the Atchafalaya River

was much blocked by logs before the 18th century. In 1831, Captain Henry M. Shreve cut the meandering bend to shorten the travel path. Afterward, the Upper Old River was abandoned, while the Lower Old River connected the RR, AR, and the MR. Between the 1830s and 1870s, logjams in the RR and AR were removed causing the flow from the MR into the AR to gradually increase (Mossa, 2013). The largest flood occurred in 1927 in the Lower Mississippi River further increased the flow into the AR. The flow in the MR and AR across the latitude at Red River Landing (30° 56' 20.4") is also known as "Latitude Flow" in the Mississippi-Atchafalaya River diversion management. The flow in the AR increased from less than 10 percent of the Latitude Flow in 1850 to 30 percent in 1950. To prevent the AR from completely capturing the MR flow, the United States Congress mandated the U.S. Army Corps of Engineers (USACE) to build a control structural complex at river mile 315 (or river kilometer 507) upstream from the river's mouth to the Gulf of Mexico (Figure 3.1), in order to regulate the flow of the Mississippi River water into the Atchafalaya River.

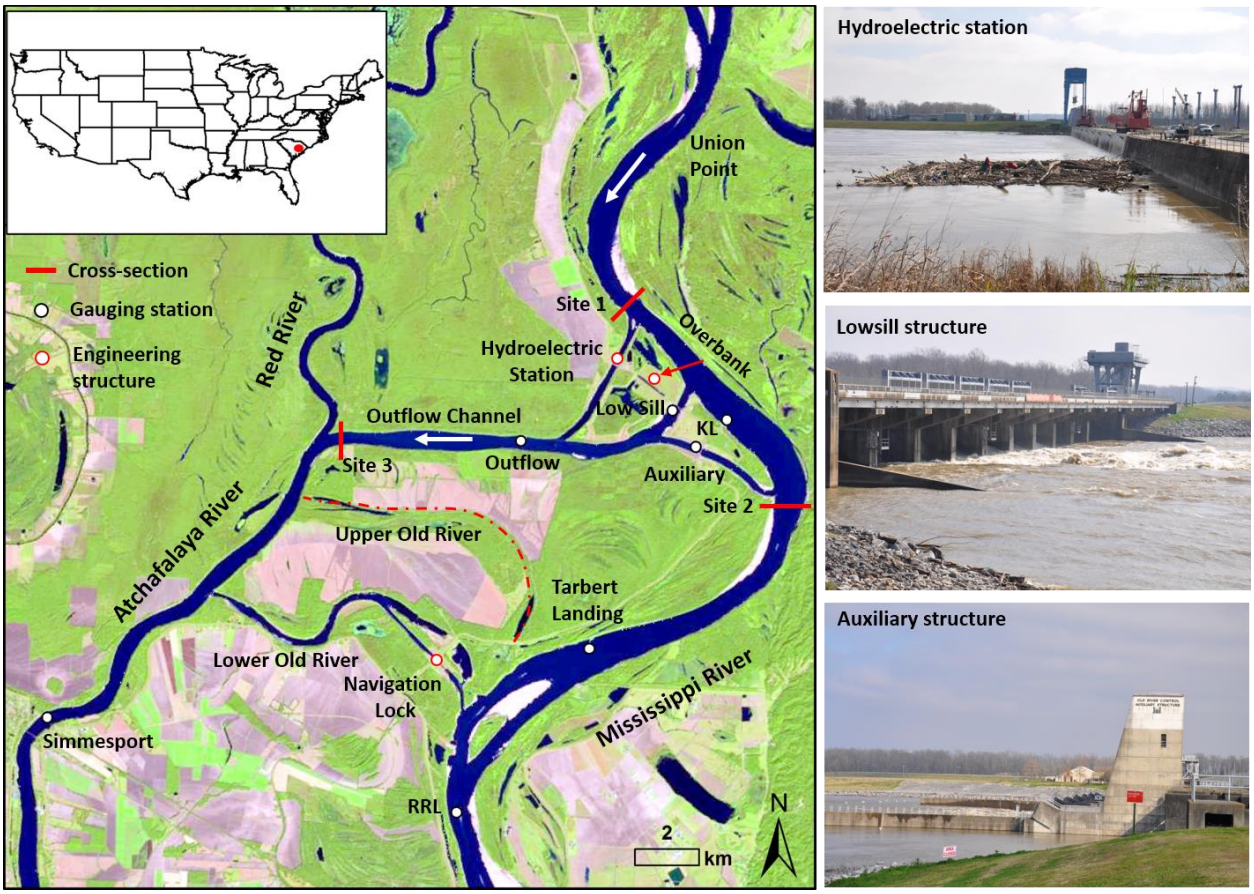

Figure 3.1. The Mississippi-Atchafalaya River diversion which is also called Old River Control Structures (ORCS) includes Hydroelectric station, Overbank Structure, Low Sill Structure, Auxiliary Structure, Old River Closure, and Navigation Lock. The bed material load was calculated at the three cross-sections located at immediately upstream (Site 1) and downstream (Site 2) of the ORCS and at the end of the Outflow Channel (Site 3). Daily river discharge is recorded at Tarbert Landing (TBL) and Outflow Channel gauging stations; Daily river stage is recorded at these two and additional three gauging stations: Knox Landing (KL), Lowsill outflow, and Auxiliary outflow.

This diversion complex, also known as the Old River Control Structure (ORCS), was completed in 1963, consisting of an overbank structure and a Low Sill Structure (Figure 3.1). Since then, water diverted into the AR from the MR has been regulated by the ORCS under a scheme of 30% in the AR and 70% in the MR at the Latitude Flow. The large flood in 1973 almost destroyed the Low Sill Structure and caused the course changing of the MR. In end 1986, an Auxiliary Structure with a new inflow channel was added to relieve the stress on the Low Sill and Overbank

structures. The Sidney A. Murray, Jr. Hydroelectric Plant was completed in 1991 which created another bifurcation in the channel. The average flow diversion in the past three decades has been about 23% of the Mississippi flow upstream of the ORCS (Wang & Xu, 2016).

Several studies have looked into sediment transport near the ORCS. Located about 10 km downstream of the ORCS, Tarbert Landing (TBL) gauging station operated by the USACE has long-term suspended sediment concentration data. Utilizing these data, Rosen and Xu (2014) quantified total suspended sediment and Joshi and Xu (2015) estimated suspended sand load for the last four decades at TBL. Knox and Latrubesse (2016) estimated bedload transport using a time-elapsed bathymetric method immediately downstream of TBL. At the ORCS, a similar method was used to calculate bed-load transport at several locations up- and downstream of the ORCS in the Mississippi mainstem and the diversion Outflow Channel (Heath et al., 2015). In a modeling study on the stability of the diversion, Edmonds (2012) concluded that it would take about 300 years to see a final avulsion of the MR into the AR under natural conditions. However, as a controlled diversion in a large alluvial river, Wang and Xu (2018a) argued that the ORCS may be unstable based on the results from a model developed by Pittaluga et al. (2015). Although they pointed out that the diverted sediment may be lower than the transport capacity of the diversion Outflow Channel, it is largely unknown how much sediment, especially riverbed material, is actually diverted via the Outflow Channel to the Atchafalaya River. The information is critical because studies have found considerable channel aggradation immediately downstream the ORCS (Mossa, 2013; Wang & Xu, 2018a).

Long-term development of bifurcations in large or small alluvial rivers depends on flow and sediment transport, especially fluxes and variations of bed material loads (Church, 2006). While the water and suspended sediment discharges into downstream channels can be normally

quantified with a satisfactory degree, determining the fluxes of riverbed material load at bifurcations is rather difficult. It is even more challenging to quantify bedload fluxes at engineered and controlled bifurcations because of irregular flow regulations and unknown numeric solutions. Yet such information can be crucial for alluvial rivers in assessing the long-term stability of bifurcations as well as the downstream channel dynamics, flood risk, and navigation safety. In general, little is known about sediment transport and long-term channel morphological development downstream of engineering-controlled bifurcations. Such knowledge can be crucial for planning and managing river diversion projects, especially for large alluvial rivers.

The goal of this study aimed to provide first-time information on bed material transport and channel morphodynamics at the river diversion control complex of the Mississippi-Atchafalaya Rivers, one of the world's largest engineered river bifurcation. Specifically, the study specifically was to (1) estimate 10-year long (2004-2013) riverbed material fluxes upstream and downstream of the diversion complex, (2) develop discharge – riverbed material load rating curves for the diversion locations for future management, and (3) quantify channel deformation in and around the diversion complex to discern long-term stability.

3.2. METHODS

3.2.1. Study site

This study selected two river reaches near the ORCS: from Union Point (UP) to Tarbert Landing (TBL) on the Mississippi River mainstem and the entire Outflow Channel (Figure 3.1). The UP location is approximately 10 km upstream and the TBL location is about 13 km downstream of the ORCS, making a 23-km long reach on the river mainstem. The east side of the river reach is natural floodplain and the west side of the reach is protected by levee structures. The

Outflow Channel is approximately 10 km long, both sides of the reach are revetted with limestone rocks.

Using single beam channel survey data collected by USACE in 2004 and 2013, we developed DEM from bank to bank for the river reach from Union Point to Tarbert Landing and for the Outflow Channel. We then determined changes in riverbeds of these two reaches for the 10 years and quantified sediment deposition and/or erosion rates. We calculated the daily bed material load at Site 1 (upstream), Site 2 (downstream), and Site 3 (the end of Outflow Channel) for the 10 years and assessed their transport rates under varying flow conditions.

3.2.2. Data collection

Data used in this study mainly included daily river discharge, daily river stage, and river bathymetric survey records. Discharge and stage data were utilized for bed material load calculation, and bathymetric data were used to determine spatially-referenced riverbed volumetric changes. River flow data were collected from several gauging stations near the ORCS and at the Natchez, Mississippi. All the stations were operated by the USACE. In specific, river stage data were collected at Natchez (#15155), Knox Landing (# 01080), Old River Lowsill Outflow Channel (#02100), Old River Auxiliary Outflow Channel (#02210), Red River Landing (#01120), and Simmesport (#03045). Water discharge data were collected at Old River Outflow Channel (#02600) and Tarbert Landing (#01100) (Figure 3.1).

Two sets of hydrographic survey data in 2004 and 2013 were collected from the U.S. Army Corps of Engineers (USACE). The data were single beam bathymetric measurements covering the mainstem of the Mississippi and outflow channel of the ORCS. The measurements also cover part of the floodplain. The distance between two neighbor cross-sections of the single beam measurements is between 30 and 400 m. Within a cross-section, the distance between two

elevation points was about 30 m. The elevation reference for the survey data is the North American Vertical Datum of 1988 (NAVD 88).

3.2.3. Calculation of bed material loads

There are a number of formulas developed for estimating bed material load (BML) for sand bed rivers; for instance, those by Ackers and White (1973); Einstein (1950); Engelund and Hansen (1967); Toffaleti (1977); Chih Ted Yang (1973); C. T. Yang (1979). There have been also a number of studies that have applied these equations for bed material load estimation for various rivers. In an evaluation of different equations using 40 sets of field data and 165 sets of flume data, the American Society of Civil Engineers (ASCE, 1982) ranked Yang's formula in the first place among eight classic equations. Yang's formula was further tested using 463 sets of laboratory data on flow and sediment parameters associated with the discharge of bed materials consisting of sand that has a median sieve diameter ranging from 0.015 to 1.71 mm. It was suggested that Yang's 1973 equation be used for sand transport in natural rivers if measured sediment loads for comparison is absent. In another study, 13 sediment transport formulas were tested using 3391 sets of laboratory and river data under varied flow and sediment conditions (Chih Ted Yang & Huang, 2001). Comparison results indicated that Yang's 1973 and 1979 formulas are most robust because their accuracies are least sensitive to the fluctuation of relative water depth, dimensionless shear velocity, dimensionless unit stream power, Froude number, and sediment concentration. However, Yang's 1979 formula is more appropriate when the sand concentration is higher than 100 ppm which is not the case in the Lower Mississippi River (Joshi & Xu, 2015). The U.S. Army Corps of Engineers recently conducted field measurements on bed-load and bed material load at several sites near the ORCS (Heath et al., 2015; Jones, Abraham, McAlpin, & Ganesh, 2018). This supplies us an excellent opportunity to study BML using the classic sediment transport formulas.

In this study, we used Yang's sand formula (Yang, 1973) to estimate bed material loads at three channel cross section near the Mississippi-Atchafalaya River diversion after testing several equations with apparently unreasonable results. The Yang's formula is given as follows:

$$\log C = 5.435 - 0.286 \log \frac{\omega D_{50}}{\vartheta} - 0.457 \log \frac{V_*}{\omega} + \left(1.799 - 0.409 \log \frac{\omega D_{50}}{\vartheta} - 0.314 \log \frac{V_*}{\omega}\right) \log\left(\frac{V S}{\omega} - \frac{V_{cr}}{\omega}\right) \quad (3.1)$$

in which the dimensionless critical velocity at incipient motion can be expressed as:

$$\frac{V_{cr}}{\omega} = \frac{2.5}{\log \frac{V_* D_{50}}{\vartheta} - 0.06} + 0.66 \text{ for } 1.2 < \frac{V_* D_{50}}{\vartheta} < 70$$

and $\frac{V_{cr}}{\omega} = 2.05$ for $70 \leq \frac{V_* D_{50}}{\vartheta}$

where C = the concentration of bed-material discharge, in parts per million by weight;

S = the channel bed slope;

D_{50} = the diameter of the sediment that 50% of sediment mass is smaller than;

ω = the average fall velocity, in m/s, of sediment particles of diameter D_{50};

ϑ = the kinematic viscosity, in m^2/s;

V_* = the shear velocity, in m/s;

V_{cr} = the average flow velocity, in m/s, at incipient motion.

$$q_s = C \times G_w \quad (3.2)$$

$$Q_s = 86.4 \times q_s \quad (3.3)$$

where G_w = the water discharge by weight (kg/s);

q_s = the bed-material discharge (kg/s);

Q_s = daily bed-material discharge (metric ton/day).

In this study, we used the median grain size (D_{50}) of 0.3 mm for the Mississippi River. The value was obtained from the 1989 Thalweg survey on bed material composition of the Lower

Mississippi River (Nordin and Queen, 1992). For the outflow channel, D_{50} of 0.4 mm was chosen based on the field measurements conducted by USACE in 2016 (Jones et al., 2018).

3.2.4. Cross-sectional geometry

Cross-sectional profiles at three sites were derived from the single-beam bathymetric measurements in 2004 and 2013 including (1) one site on the Mississippi main channel 320 kilometers upstream of (site 1, RK 320.2), (2) one site 14 kilometers downstream of three diversion channels (site 2, RK 306.3), and (3) one site in the outflow channel 7 kilometers from the confluence of the three diversion channels (site 3, Figure 3.2). Riverbed was eroded at site 1 and 3, while the bed aggraded at site 2. The varied bed elevations were over 1 meter at site 2 and 3 (i.e., +1.25 m vs. -1.21 m), while site 1 experienced slight erosion (i.e., from -2.22 m to -2.53 m). Riverbed elevation was determined from the profiles.

In the Mississippi mainstem, the nearest gauging station upstream and downstream of the ORCS is located at Natchez (RM 363.3), Know Landing (RM 313.7), and Red River Landing (RM 302.4), respectively. Herein we used interpolation method to estimate the river stage at site 1 and 2. For site 3, the average stage at the Lowsill and Auxiliary gauging stations was used. With the river stage data, river depth was estimated by subtracting average cross-sectional bed elevation from the river stage at each cross-section.

For any given river stage, cross-sectional area and channel width were calculated in MATLAB R2014b (Natick, MA, USA). Figure 3.2 shows that the bankfull stage had little change for all the three cross-sections from 2004 to 2013. With the river stage below the bankfull stage, river width varies with the stage. With the river stage above the bankfull stage, bankfull width was used as river width.

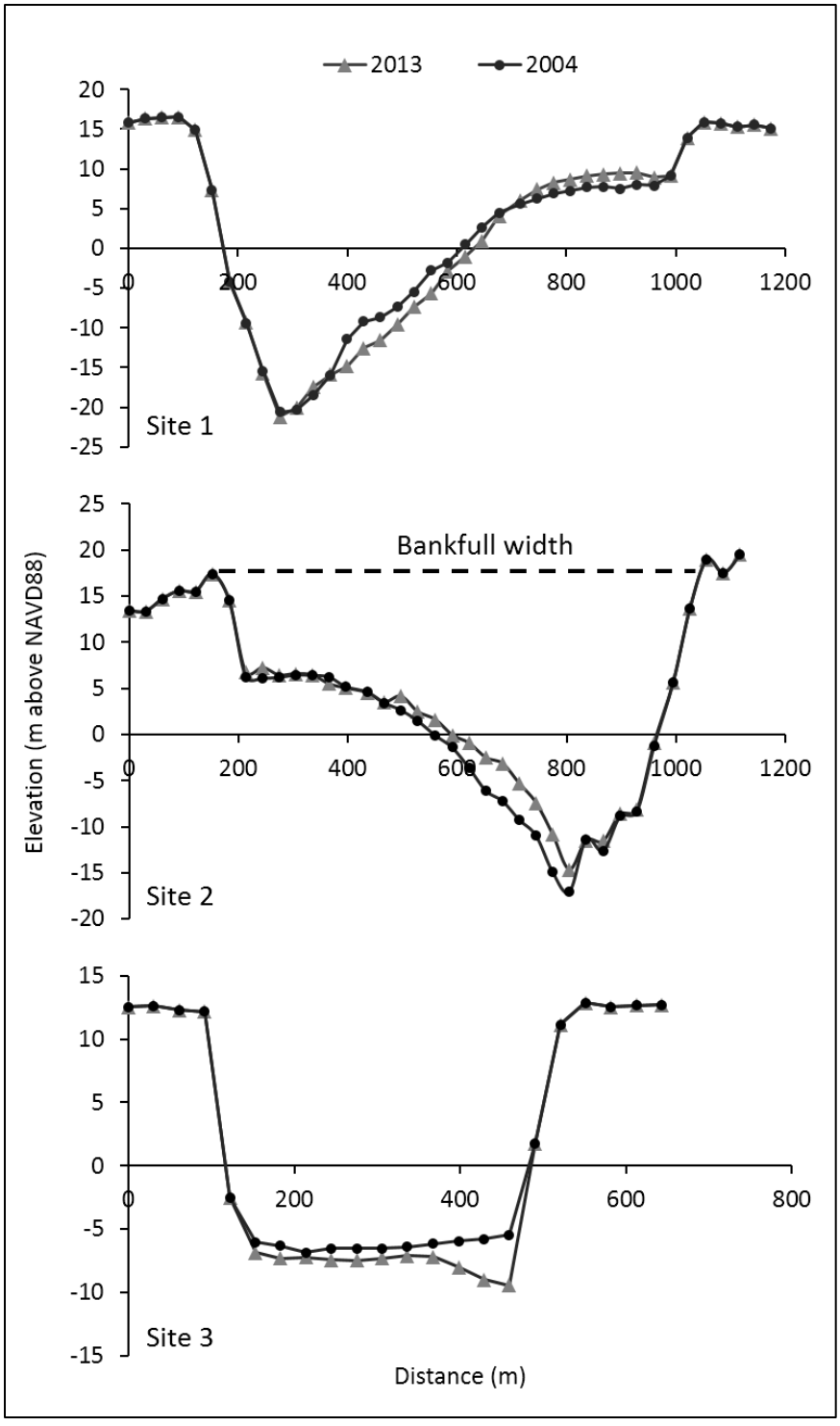

Figure 3.2. Cross-sectional profiles at site 1 (upstream), 2 (downstream), and 3 (outflow channel) in 2004 and 2013. The profiles were derived from single-beam hydrographic survey data collected by the U.S. Army Corps of Engineers. The measurements cover not only the channel bank to bank but also the nearby floodplains.

Table 3.1. Channel geometric characters of three cross-sections used in this study at upstream (Site 1), downstream (Site 2) of the ORCS and the end of the ORCS outflow channel (Site 3).

Location	River Kilometer	Middle point Coordinates	Bankfull stage (m)	Bankfull width (m)	Bankfull area (m^2)		Bed elevation (m)	
					2004	2013	2004	2013
Site 1	320.2	-91.595°, 31.089°	15.90	950	15,736	16,003	-2.22	-2.53
Site 2	306.3	-91.563°, 31.043°	17.41	894	15,805	14,808	-2.01	-0.76
Site 3	none	-91.704°, 31.065°	14.27	450	7007	7491	-5.35	-6.56

Bed slope is a critical parameter in the estimation of BML. Previous modeling studies for different river reaches of the Lower Mississippi River applied a bed slope between 1.9×10^{-5} (Viparelli et al., 2015) and 7×10^{-5} (Nittrouer and Viparelli, 2014). The numbers were normally determined by the Thalweg elevation over an arbitrary distance. However, for bedload transport estimation in the bifurcations of lowland alluvial rivers, Kleinhans et al. (2013) pointed out that the slope should be determined by energy gradient rather than bed surface gradient because the flow division is largely controlled by backwater effects. Our study site is in the backwater zone of the Lower Mississippi River. Therefore, we used the water surface slope in the calculation instead of bed slope. The daily river stage at Natchez, Knox Landing, Red River Landing were used to estimate the water surface slope in the mainstem. The daily river stage at the outflow channel and Simmesport were used to estimate the water surface slope in the diversion outflow channel. The calculated water surface slope ranges from 4.2×10^{-5} to 5.0×10^{-5} and 5.3×10^{-5} to 7.9×10^{-5} for the main steam and outflow channel during different flow conditions, respectively. The average water surface in the outflow channel is about 1.5 times steeper than that in the mainstem.

3.2.5. Riverbed deformation analysis

Digital Elevation Models (DEM) of the channel bed in 2004 and 2013 were created by interpolating of the hydrographic survey data near the ORCS. An inverse distance weighted

technique was used in the interpolation and the spatial resolution of the DEM is 10 × 10 m. With the two years of DEM, the difference of DEM (DOD) data was obtained by subtracting the 2004 DEM from the 2013 DEM. Volume changes of the sediment on channel bed were calculated based on pixels, which is equal to the value of multiplying the DOD data by the area of each pixel (i.e., 100 m^2). The riverbed changes including sediment deposition and erosion in each river mile of the Mississippi mainstem were also estimated.

3.3. RESULTS

3.3.1. River flow conditions

The average daily discharge at Tarbert Landing (TBL) and outflow channel (OC) during 2004-2013 were 14,652 and 4657 cubic meter per second (cms), respectively (Figure 3.2). Therefore, the average daily discharge upstream of the ORCS (UP) was 19,310 cms, i.e. the sum of discharge at TBL and OC. The ratio of discharge between the OC and the total discharge upstream of the ORCS varied from 6% to 38% with the average value of 24%. The ratio varied largely during low flow (i.e., 6% - 38%) (Figure 3.3). However, the ratio variation gradually decreased with the increasing discharge upstream of the diversion. The ratio varied between 20% and 30% when the upstream discharge was 35,000 cms.

Extremely dry and wet years occurred during 2004-2013. For example, the year of 2006 and 2012 were dry years with a peak discharge of 20,813 and 23,701 cms, respectively, i.e. only marginally above the average discharge of 19,310 cms. On the contrary, the year of 2008 and 2011 were wet years with peak discharge at 41,228 and 45,845 cms, respectively. The appearance of extremely dry and wet years during the period allows us to better understand bed material load during different flow conditions.

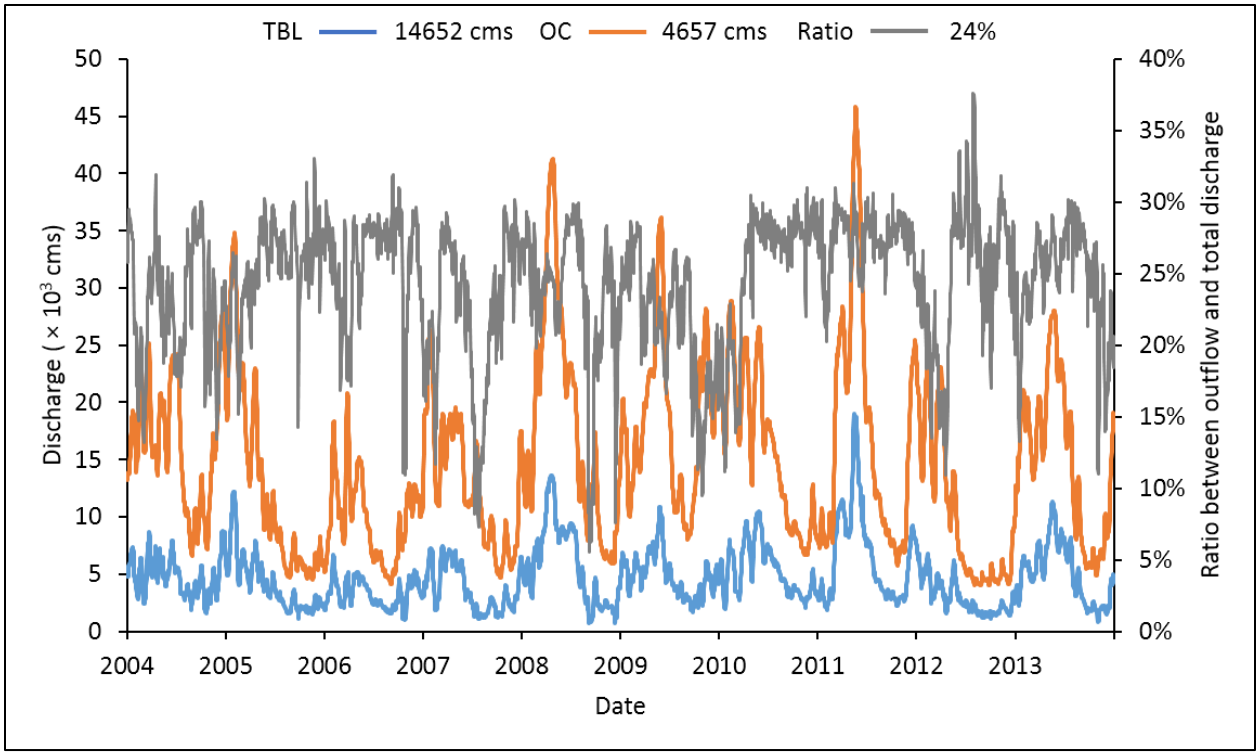

Figure 3.2. Water discharge at the outflow channel and Tarbert Landing during 2004-2013. The total discharge upstream of the ORCS was calculated by summing the discharge at these two stations. The ratio is the discharge at outflow channel divided by the total upstream discharge. The average discharge at TBL and outflow channel was 14,652 and 4657 cubic meter per second. The average water diversion rate was 24%.

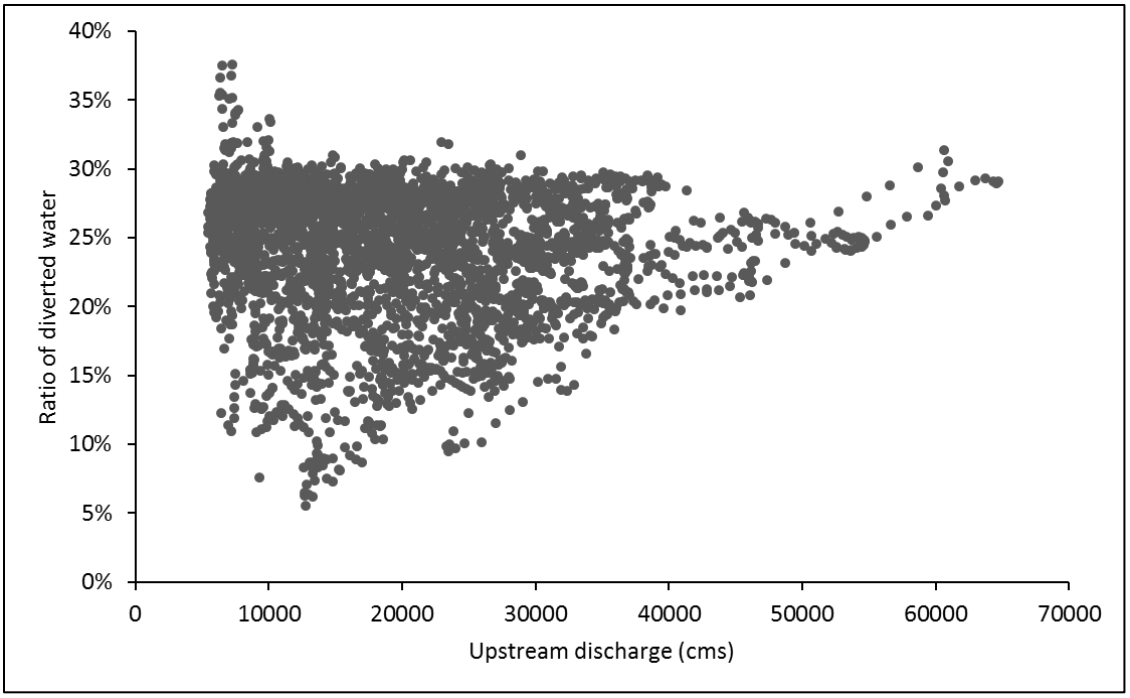

Figure 3.3. The correlation between total discharge upstream of the Mississippi-Atchafalaya River diversion and the diverted water ratio by the Old River Control Structure during 2004-2013.

3.3.2. Bed material loads upstream of the diversion

Daily bed material load (BML) ranged from less than 100 metric tons to over 500,000 metric tons per day at the cross-section upstream of diversion. The average daily BML at Site 1 was 55,239 during 2004-2013. Annual BML also varied largely at Site 1 (Figure 3.4). The maximum bed material load occurred in 2011 when 32.3 MT bed material transported across the cross-section of Site 1. However, only 10.3 MT bed material transported across the cross section in 2006. The total and annual average BML at Site 1 was 201 and 20.1 MT during 2004-2013.

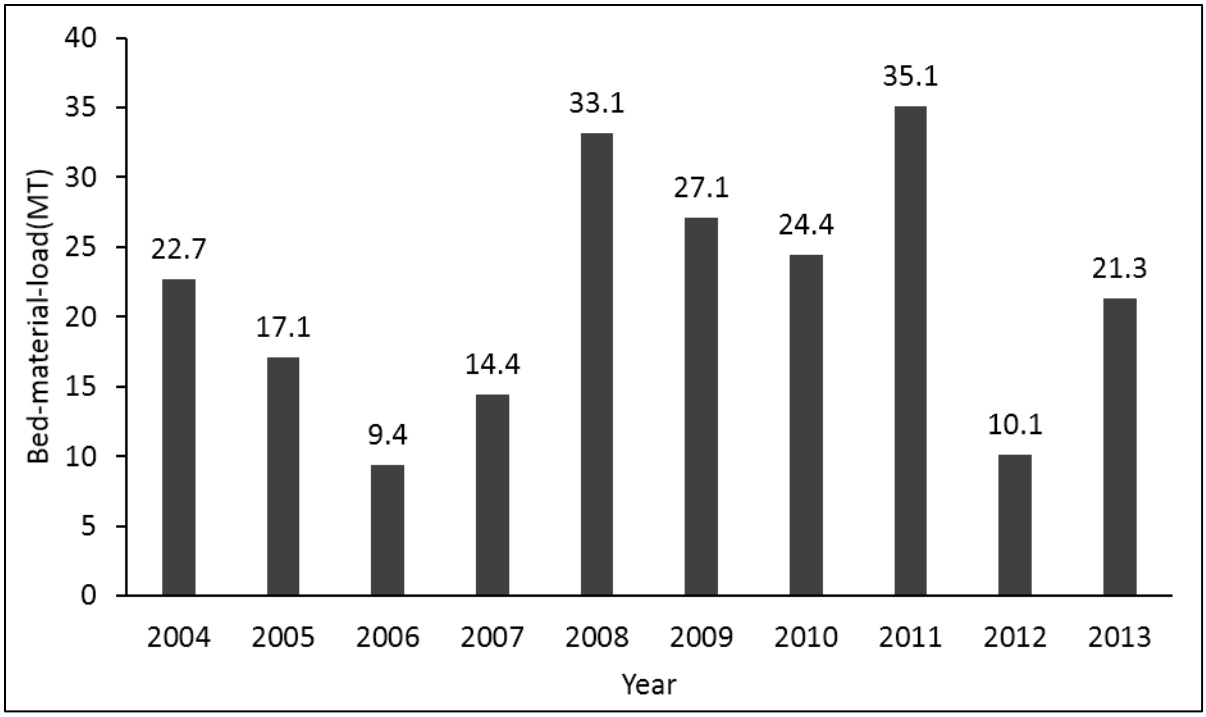

Figure 3.4. Estimated annual bed material loads in million metric tons (MT) upstream of the Mississippi-Atchafalaya River diversion (Site 1) between 2004 and 2013, with an average of 21.5 MT.

3.3.3. Bed material loads in the diversion channels

The maximum daily BML at Sites 2 and 3 were 280,000 and 181,553 metric tons, respectively. The average daily BML at Sites 2 and 3 were 40,193 and 11,882 metric tons, respectively. The annual BML downstream of the diversion at Site 2 averaged 14.1 MT, ranging between 7.5 and 21.7 MT during 2004-2013 (Figure 3.5). The minimum and maximum annual BML occurred in 2006 and 2011, corresponding with the annual discharge. For the diversion Outflow Channel (i.e., Site 3), the annual BML showed a fluctuation from 1.1 (2007) to 10.4 (2011) MT. The total BML transported across Sites 2 and 3 were 141 and 42 MT, respectively.

In terms of BML ratio between two outlets and the upstream channel, about 64% and 24% of BML exported from site 2 and 3 on average, respectively. However, the BML ratio at site 3 had significantly greater fluctuation (i.e., 10% - 40%) than that at site 2 (i.e., 54% - 70%) (Figure 3.5).

In 2011, the BML across Site 3 accounted for 40% of the BML at site 1.

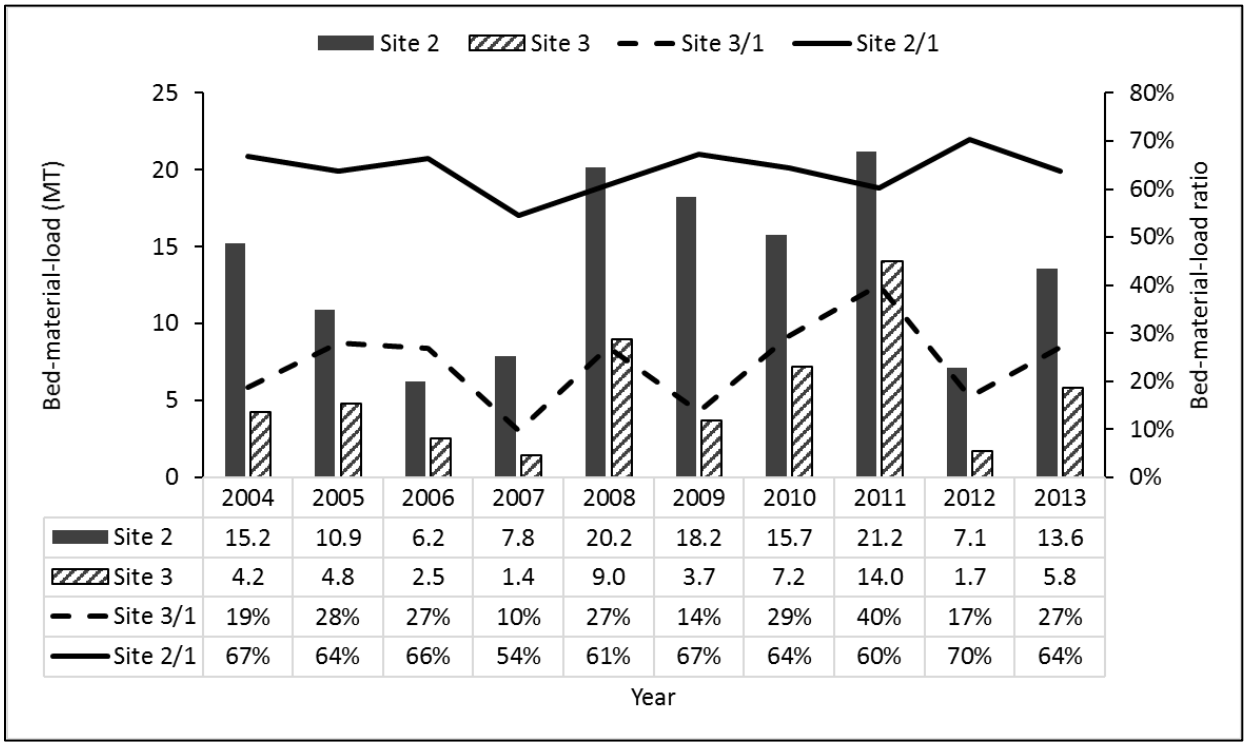

	2004	2005	2006	2007	2008	2009	2010	2011	2012	2013
Site 2	15.2	10.9	6.2	7.8	20.2	18.2	15.7	21.2	7.1	13.6
Site 3	4.2	4.8	2.5	1.4	9.0	3.7	7.2	14.0	1.7	5.8
Site 3/1	19%	28%	27%	10%	27%	14%	29%	40%	17%	27%
Site 2/1	67%	64%	66%	54%	61%	67%	64%	60%	70%	64%

Figure 3.5. Estimated bed material loads in million metric tons (MT) during 2004-2013 downstream of the Mississippi-Atchafalaya River diversion (Site 2) and at the end of the diversion outflow channel (Site 3). The ratio is the BML ratio between outflow channel (Site 3) and upstream of the diversion (Site 1).

3.3.4. Erosion and deposition in the Outflow channel and mainstem channel

Riverbed elevation changes show that the channel bed near the ORCS mainly aggraded during 2004-2013, especially in the Mississippi mainstem (Figure 3.6). Erosion mainly occurred in the outflow channel, especially downstream of the Lowsill structure. In terms of volume changes of riverbed sediment, the largest deposition occurred in the sub-reach of RK 513 (i.e., 3.3×10^6 m^3), while the largest erosion occurred in the sub-reach of out01 (i.e., -4.5×10^6 m^3) (Figure 3.7&Table 3.2). In the mainstem, only two sub-reaches (i.e., RK 504 and 497) were slightly sourced. The six sub-reaches between RK 510 and 502 are located between Site 1 and 2 which

was used later in the estimation of the bed material load budget. Overall, sediment volume changes of channel bed in the mainstem between site 1 and 2 (Δ1) and outflow channel (Δ2) are 3.1×10^6 and -5.0×10^6 m^3, respectively. They are equivalent 4.4×10^6 and -7.0×10^6 metric tons sediment assuming the bulk density of bed sediment is 1.4 metric ton per cubic meter.

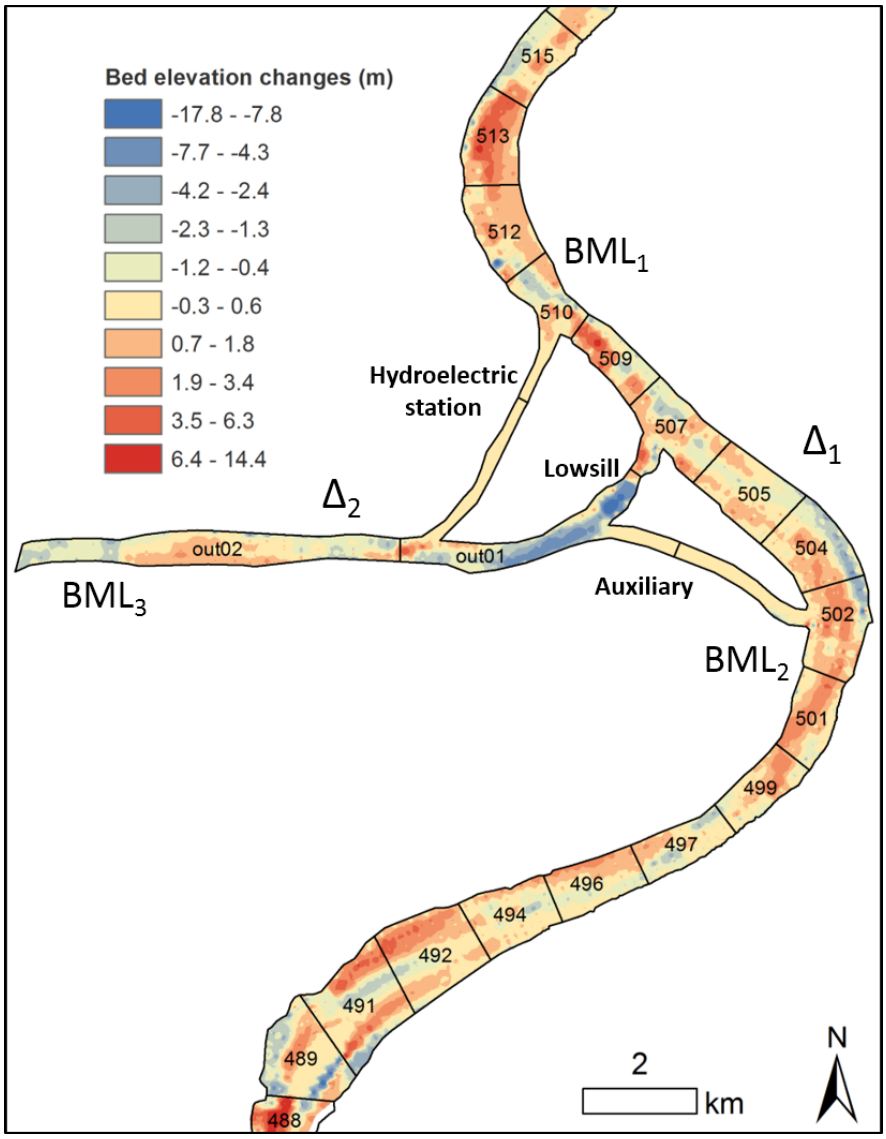

Figure 3.6. Riverbed elevation changes at the Old River Control Structures between 2004 and 2013. Deposition mainly occurred in the Mississippi main channel, while erosion mainly occurred in the outflow channel, especially downstream of the Lowsill structure.

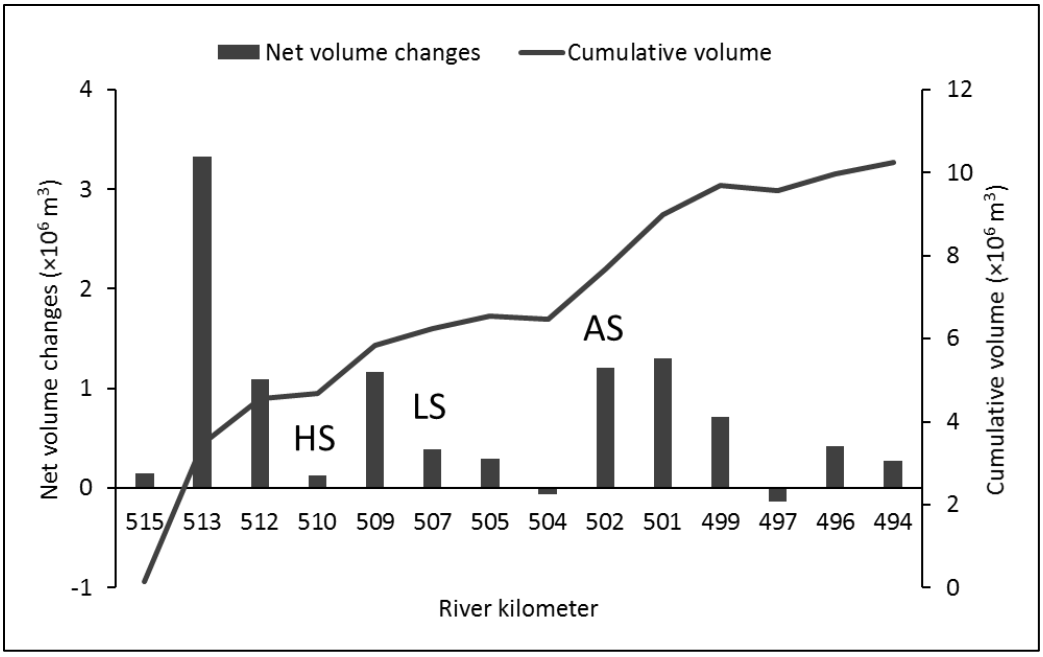

Figure 3.7. Volume changes and cumulative volume of the riverbed materials in the Mississippi mainstem between 2004 and 2013. The mainstem was divided into fourteen sub-reaches based on river mile. HS, LS, and AS indicates, respectively, where the Hydroelectric power station, Lowsill Structure, and Auxiliary Structure.

Table 3.2. Estimated riverbed deformation (deposition and erosion) in the study river reach during 2004-2013. The mass was calculated assuming the bulk density is 1.4 metric ton per cubic meter for the bed material. Sub-reaches RK 510 – 502 are located between Site 1 and 2. The net volume changes in riverbed sediment were set to Δ1 in this reach. Δ2 indicates the net volume changes in riverbed sediment of the outflow channel.

Sub-reach	km	Riverbed volume changes ($\times 10^6$ m^3)			Net mass changes(MT)
		Erosion	Deposition	Net volume changes	
Mainstem	515	0.6	0.7	0.1	0.2
	513	0.2	3.5	3.3	4.0
	512	0.3	1.4	1.1	1.3
	510[1]	0.5	0.6	0.1	0.1
	509	0.3	1.4	1.2	1.4
	507[2]	0.7	1.0	0.4	0.5
	505	0.3	0.6	0.3	0.3
	504	1.0	0.9	-0.1	-0.1
	502[3]	0.6	1.8	1.2	1.5
	501	0.1	1.4	1.3	1.6
	499	0.2	0.9	0.7	0.9
	497	0.5	0.4	-0.1	-0.2
	496	0.3	0.7	0.4	0.5
	494	0.3	0.6	0.3	0.3
Outflow	out01	4.9	0.4	-4.5	-5.4
	out02	1.6	1.1	-0.5	-0.6
	Sum-main (Δ1)	3.3	6.5	3.1	3.7
	Sum-out (Δ2)	6.5	1.5	-5.0	-6.0
	Sum-total	12.2	17.5	5.3	6.3

[1, 2, 3] bifurcation node at the [1]Hydroelectric station; [2]Lowsill Structure; [3]Auxiliary Structure.

3.4. DISCUSSION

3.4.1. Bed material load distribution at the ORCS

With the estimated total bed material load input/output of the reach and the volume changes of the riverbed sediment, we could assess the sediment budget of the reach between 2004 and 2013. A sediment budget equation was developed for the reach.

$$\Delta_1+\Delta_2 = \Delta_{BML} + \Delta_D = (BML_1 - BML_2 - BML_3) + \Delta_D \quad (3.4)$$

where Δ_1 and Δ_2 are volume changes in riverbed sediment in the mainstem (before the diversion structures) and outflow channel during 2004 and 2013 (Table 3.3). Δ_{BML} is the net changes of bed material load of the reach, which is equal to the difference between the BML input from the upstream of the ORCS (BML_1) and output at Site 2 (BML_2) and Site 3(BML_3). Δ_D is the dredging amount in the mainstem before the diversion structures.

The total BML_3 during 2004-2013 was 42 MT (Figure 3.8). In fact, part of the BML_3 came from bed erosion of the Outflow Channel based on the DEM analysis (i.e., 6 MT). Therefore, the BML diverted to the Outflow Channel at the bifurcation node should be 36 MT (i.e., 42 MT – 6 MT), which accounted for 18% of the input BML at Site 1 (i.e., 201 MT). As mentioned before, the average ratio of the diverted water was 24% during 2004-2013. Therefore, the total diverted BML was disproportionately lower than the diverted water amount. It is well known that one of the two flow paths at a bifurcation will enlarge if its sediment transport capacity exceeds the sediment supply to it (Pittaluga et al., 2015). At the Mississippi-Atchafalaya River diversion, 24% diverted discharge only delivered 18% of BML which could cause bed erosion at the Outflow Channel. This is well consistent with the observed bed erosion and channel enlargement in the Outflow Channel (Figure 3.6).

Two factors could cause the occurrence of unproportioned lower bed material transport into the Outflow Channel. Firstly, the bifurcation node of the Hydroelectric Station is in outer bend of the channel (Figure 3.8). Helical flow may direct bedload sediment transporting towards the inner bend. As a result, more water flows into the Outflow Channel instead of bedload sediment. Secondly, although the Auxiliary structure is in the convex bank which is in favor of coarse sediment intake, the diversion angle is about 120° (Figure 3.8). The research from Bulle (1926) found that an increase in diversion angle results in an increase of bedload staying in the main

channel and a diversion angle of 120° has the maximum capacity of keeping bedload. This indicates that the design of the Auxiliary structure diversion angle is not favorable to the bedload intake. Even if bedload is diverted into the Outflow Channel, sediment could be deposited in a separation zone at the inlet of the bifurcated channel. Dutta, Wang, Tassi, and Garcia (2017) reported the width of a flow separation zone in the Outflow Channel increases with an increasing diversion angle. The region below the flow separation zone has relatively low shear stress and sediment entering this zone tends to be deposited. With 120° diversion angle, the separation zone after the Auxiliary structure could be very large and cause severe sediment deposition. Therefore, overall, the configuration of the Auxiliary structure is not beneficial for bedload transport through it. The riverbed DEM in 2013 shows scoured channel downstream of the Hydroelectric station and aggraded channel before the Auxiliary Structure. This is coincident with the theoretical analysis. The Lowsill structure may have the relative maximum efficiency in transporting BML through the Outflow Channel among the three diverted channels based on its location. The field measurements from the USACE do found that more bed load moved through the Outflow Channel when the Lowsill Structure was opened (Heath et al., 2015). However, a near 90° diversion angle is still not an optimal angle for bedload transport (Dutta et al., 2017).

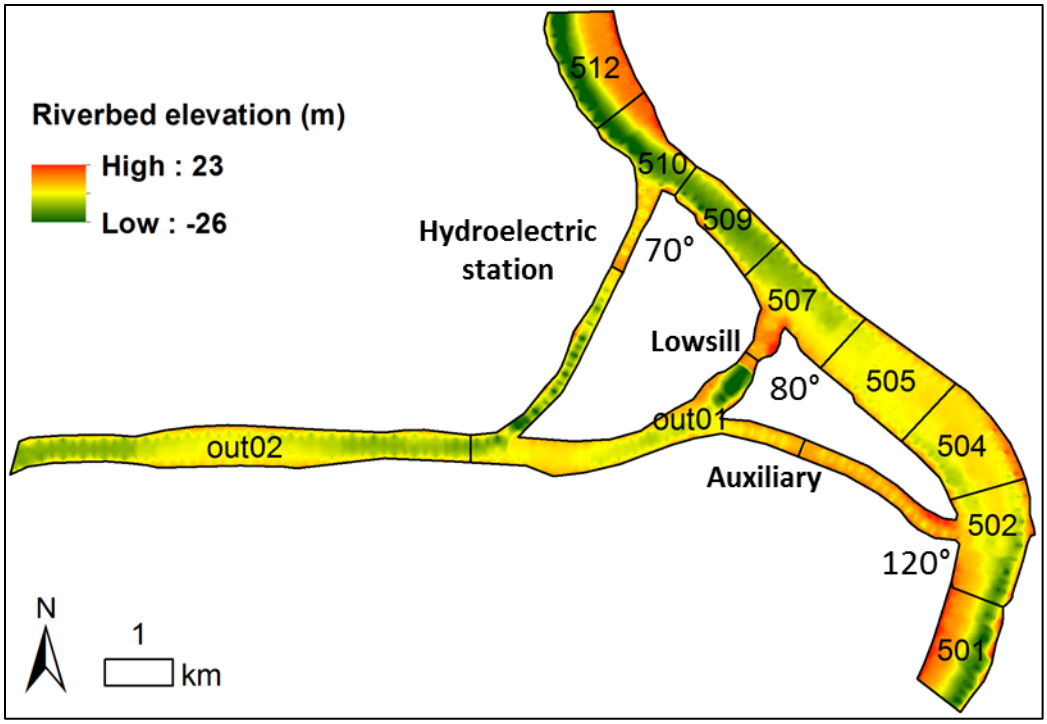

Figure 3.8. Riverbed elevation at the Mississippi-Atchafalaya River diversion in 2013. The reference datum is NAVD 88. The numbers in the Mississippi River main channel indicate river kilometers from the river's mouth at the Gulf of Mexico.

Downstream of the diversion, 165 MT BML should be transported across Site 2 (201 MT – 36 MT) based on our estimation of BML at Sites 1 and 3. However, our calculation based on Yang's formula shows that only 142 MT BML moved across Site 2, suggesting deposition of 23 MT sediment in the reach between RK 510 and 502. Our bathymetric analysis found only 4.4 MT increase in riverbed sediment of the reach. According to the record of the USACE (USACE, 2018), the reach was dredged, and the total amount of dredged was about 2.3 × 106 m3, which is equivalent to 3.2 MT sediment. Considering the amount of deposited and dredged sediment, 15.4 MT (i.e., 23 – 4.4 – 3.2 MT) difference between the estimated BML budget and observed riverbed deformation were unaccounted for. Possible causes for the discrepancy could include unaccounted sediment deposition on the floodplain during high flows, estimation error owing to the

determination of the parameters (i.e., bed slope, grain size), and bed material load formula. This will be further discussed in the below section.

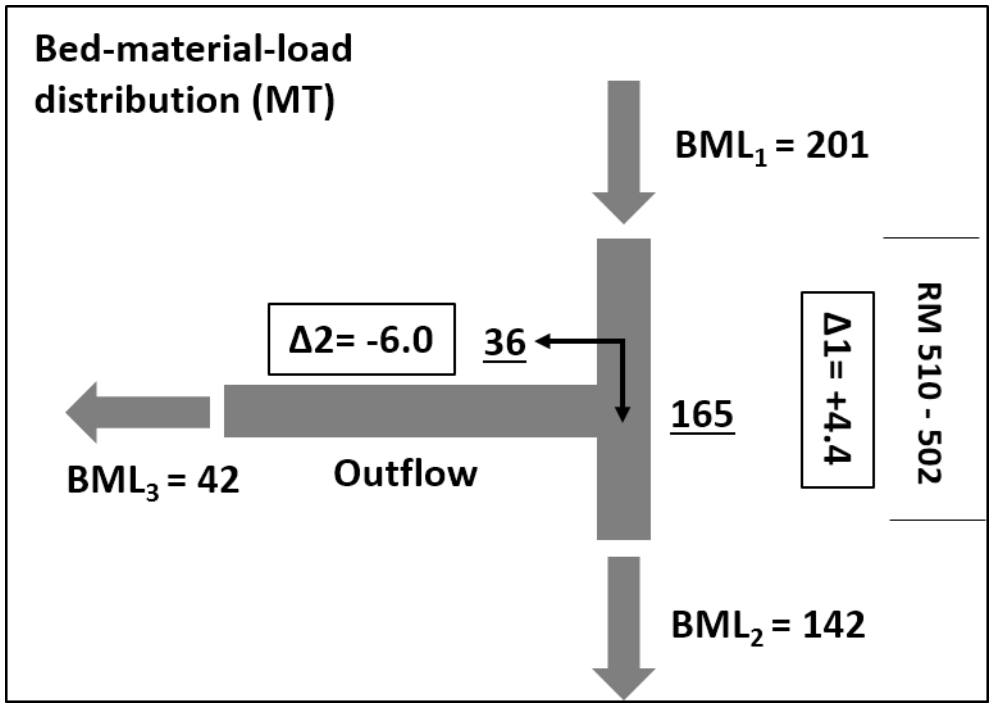

Figure 3.9. Total bed material load fluxes in million tons (MT) at the ORCS for the period from 2004 to 2013. The Lowsill structure was assumed diverting all the BML to the Outflow Channel. The routing number of the BML at the bifurcation (underlined number) was estimated based on estimated BML at Sites 1, 2, and 3 and bathymetric analysis of the riverbed volume changes (boxed number).

3.4.2. Flow effects on bed material load

To determine bed material load during different flow conditions, BML curves were plotted with corresponding water discharge (Figure 3.10). The relations show that the BML at the three sites is well expressed by second-order polynomial equations. The National Oceanic and Atmospheric Administration (NOAA) used the river stage at Red River Landing (Figure 3.1) to forecast river flood for the Lowermost Mississippi River region. The river stage at this station is divided into five ranges: low flow, action flow, intermediate flow, high flow, and peak flow, which

were related by Rosen and Xu (2014) to the discharge at Tarbert Landing , respectively, <13,000 cms, 13,000-18,000 cms, 18,000-25,000 cms, 25,000-32,000 cms, and >32,000 cms. The discharge ranges at Sites 1 and 3 were determined based on the ranges at Site 2. The amount of BML was estimated under each discharge range at the three sites (Table 3.3).

From 2004 to 2013, days with the intermediate flow (i.e., 18,000-25,000 cms) in the Mississippi mainstem made approximately 20% of the entire period, but they transported 33% of the total BML at Sites 1 and 2. Days with low flow stage accounted for about 50% of all time, but they only transported ~20% of the total BML. Unlike in the mainstem, 29% of the total BML was transported during the peak flow time, which accounted for only 5% of the entire study period. The amount of transported sediment was also high during the intermediate (27%) and high flows (15%). indicating the critical role of the diversion control in bed material transport down to the Atchafalaya River.

Previous studies found that the entrance channel to the Auxiliary Structure trapped a significant portion of the diverted sediment, particularly during floods (Heath et al., 2015). The relationship of discharge and bed material transport indicates that diversion gates should be opened as many as possible during peak flow for diverting as much as coarse sediment into the Outflow Channel. However, during intermediate flow, the diversion gates could be optionally closed to maximum the coarse sediment transport in the Mississippi mainstem for reducing sediment deposition.

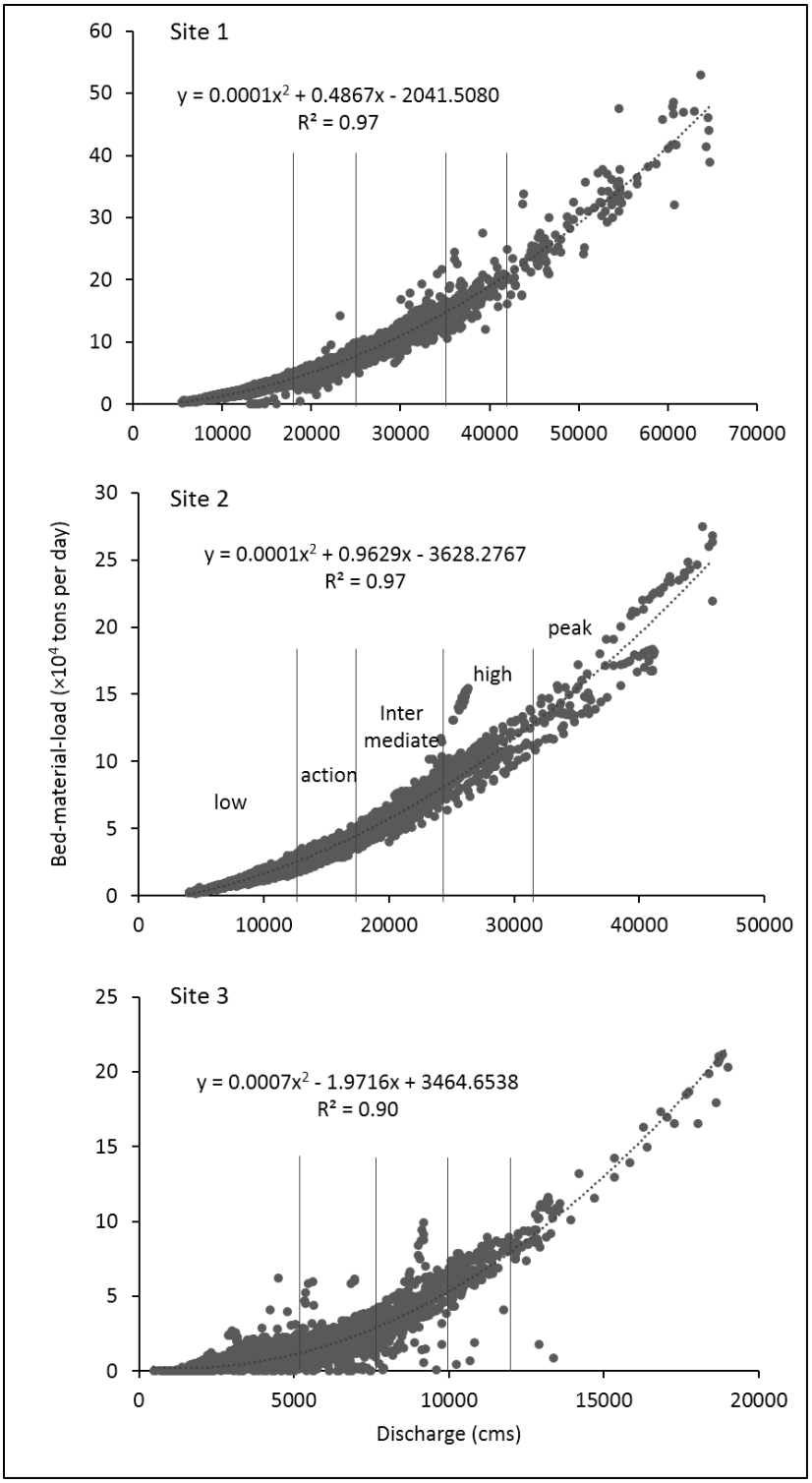

Figure 3.10. The relationship between discharge and bed material load at the three sites near the Mississippi-Atchafalaya River diversion.

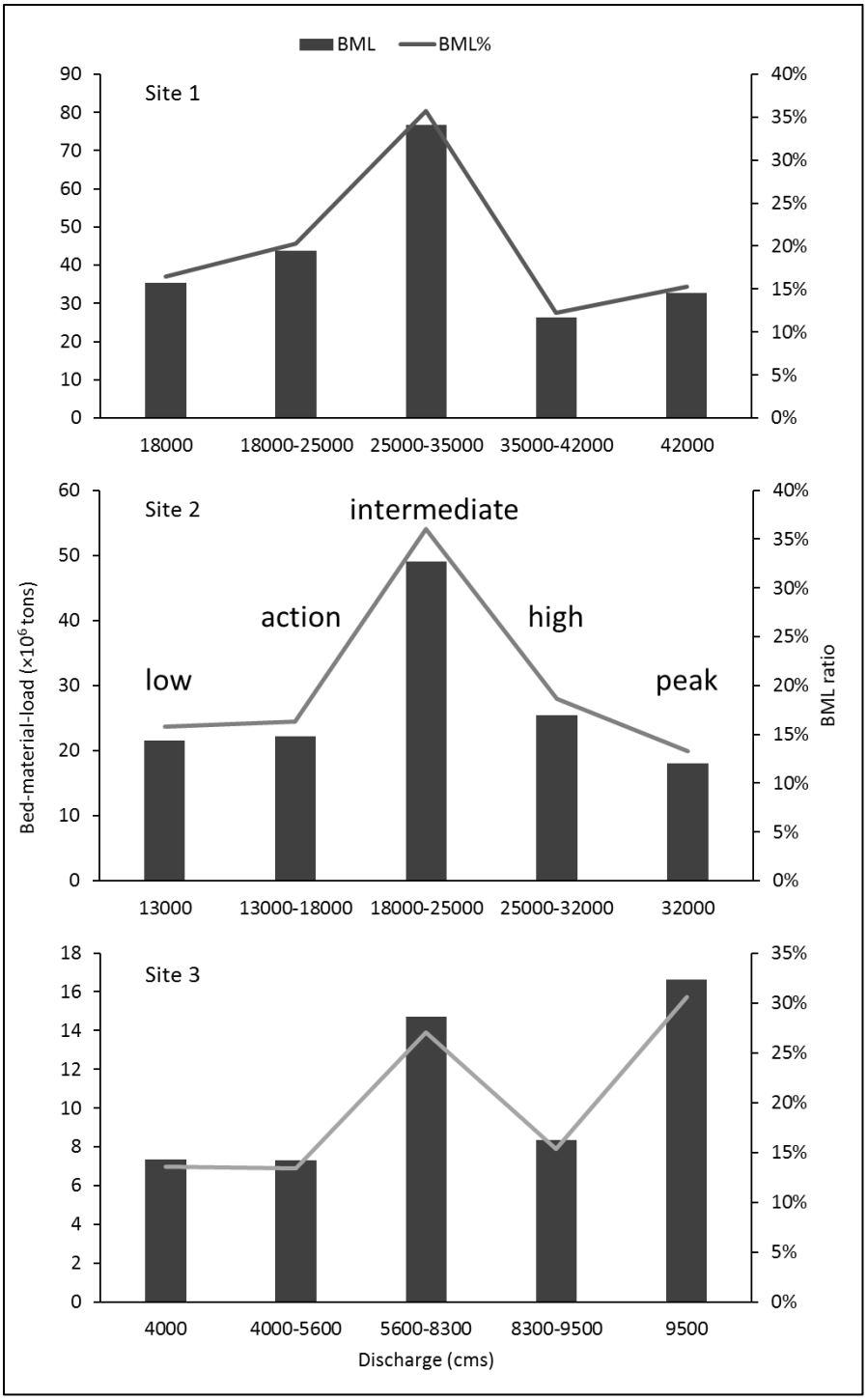

Figure 3.11. The relationship between bed material loads and discharge ranges at the upstream (site 1) and bifurcated downstream sites (sites 2 and 3) near the controlled Mississippi-Atchafalaya River diversion. The discharge ranges were determined based on the U.S. National Oceanic and Atmospheric Administration's (NOAA) flow stages at Red River Landing (i.e., low, action, intermediate, high, and peak).

Table 3.3. The relationship between bed material loads and discharge ranges at the upstream site (site 1) and downstream sites (Sites 2 and 3) near the controlled Mississippi-Atchafalaya River diversion. The discharge ranges were determined based on the U.S. National Oceanic and Atmospheric Administration's (NOAA) flow stages at Red River Landing (i.e., low, action, intermediate, high, and peak).

Site	Discharge ranges (cms)	BML (MT)	BML%	Days	Days%
1	18,000	35.3	16%	1900	52%
	18,000-25,000	43.7	20%	740	20%
	25,000-35,000	76.7	36%	740	20%
	35,000-42,000	26.3	12%	160	4%
	42,000	32.8	15%	108	3%
2	13,000	21.5	16%	1818	50%
	13,000-18,000	22.2	16%	683	19%
	18,000-25,000	49.0	36%	794	22%
	25,000-32,000	25.4	19%	248	7%
	32,000	18.1	13%	110	3%
3	4,000	7.4	14%	1807	49%
	4,000-5,600	7.3	13%	737	20%
	5,600-8,300	14.7	27%	747	20%
	8,300-9,500	8.4	15%	174	5%
	9,500	16.6	31%	188	5%

3.4.3. Comparison of estimated BML with USACE's measurements

As mentioned before, there is a difference of 15.4 MT of riverbed sediment between the two estimates based on hydrodynamic approach and channel morphological approach. To assess possible estimation errors from the two different approaches, we compared the estimated BML using Yang's formula with BML measurements reported by the USACE. Although the measurements were conducted in 2010, 2011, and 2016, the data were rather limited because only ten field trips were made (Heath et al., 2015; Jones et al., 2018). During each trip water and sediment fluxes were determined using acoustic Doppler current profiling (ADCP) and multibeam sounds. Several measured BMLs in 2010 and 2011 were given for Sites 1 and 2 . For the outflow channel, four BML values in 2010, 2011 and 2016 were reported at a location approximately 3700 m upstream of our Site 3 in this study. A t-test was run to decide the difference between means of measured and estimated BML.

Results show that overall, our estimates of BML using Yang's formula is consistent with the measurements by the USACE at Sites 1 and 3 (Figure 3.12). P-values indicate that there is no statistically significant difference between the two groups of data at these two sites. However, at Site 2, our BML estimates were significantly lower than the USACE reported BML when the discharge was greater than 18,000 cms.

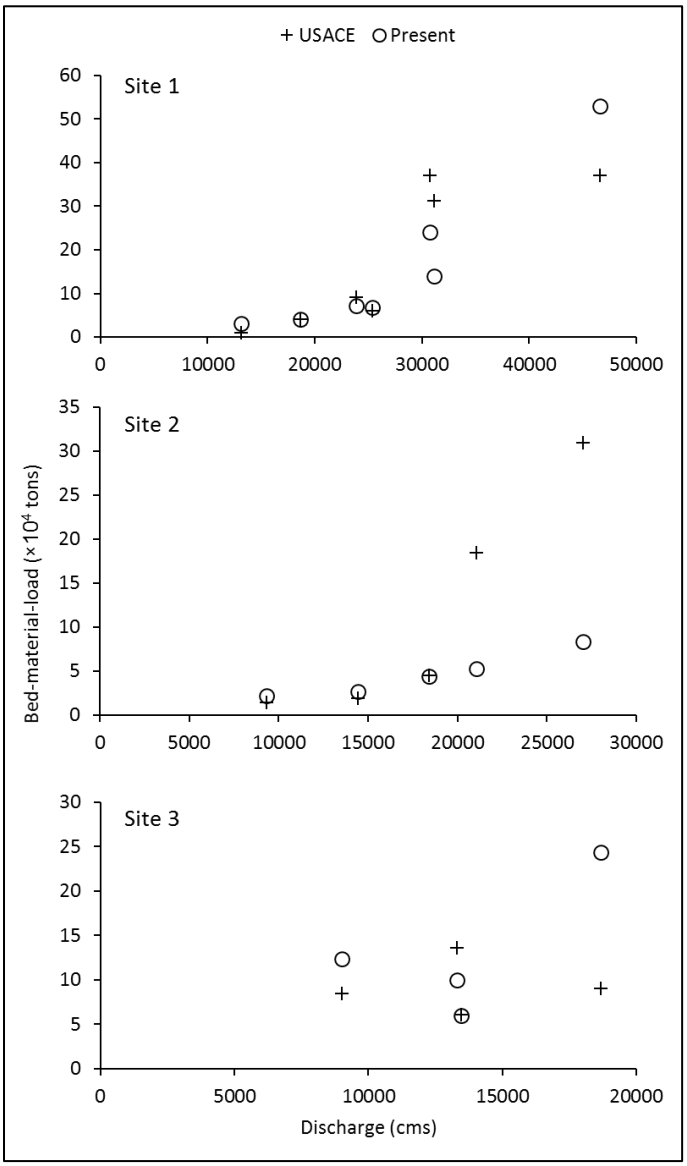

Figure 3.12. Comparison between estimated bed material load using Yang's formula and measured BML by the U.S. Army Corps of Engineers at three sites near the Mississippi-Atchafalaya River diversion.

Table 3.4. A t-test between BML estimates of this study (Present) and the measurements by the U.S. Army Corps of Engineers (USACE).

Site	Group	N	Mean	Std Dev	Min	Max	P-value
1	USACE	7	179,605	163,759	10,746	371,160	0.8414
	Present	7	159,852	178,325	30,685	529,053	
2	USACE	5	114,441	129,192	14,593	309,343	0.0072
	Present	5	45,747	24,598	22,151	83,692	
3	USACE	4	93,057	31,610	61,065	136,550	0.1679
	Present	4	131,982	78,777	60,153	243,308	

Theoretically, such discrepancy between our estimates and the USACE measurements could occur when the water slope was underestimated during the high flow. Because there is no gauging station immediately upstream of the ORCS, it is difficult to estimate water slope changes upstream and downstream of the ORCS during high flow. It is possible that with the higher diversion of water into the Outflow channel during high flow, the water-energy slope can be increased significantly immediately downstream of the diversion at Site 2. The lower BML estimates during high flow at Site 2 may have resulted from a possible underestimation of the total BML across Site 2 during 2004-2013, which might have been the main reason for the 15.4 MT sediment that was uncounted for. Other errors may also exist such as those incurred in morphological estimation as well as in field measurements. Because the comparison is based on a very limited number of field measurements, a solid conclusion cannot be drawn and we suggest conduct further field measurements in the future.

3.4.4. Implications

Although channel aggradation has been widely reported downstream of river diversions (Baker, Bledsoe, Albano, & Poff, 2011; Caskey et al., 2015; Gaeuman, Schmidt, & Wilcock, 2005), studies on bed material transport at diversions are very limited, resulting in scarcity of field

measurements of bed material load transport. In our knowledge, both field measurements and modeling estimations of BML are even rarer for engineering-controlled diversions. The complexity of the flow and sediment distribution and the difficulty of BML measurements are the main reasons for the rare calculations. Our study demonstrates that it is possible to quantitatively estimate BML distribution at an engineering-controlled river diversion using a simple, well-established bed material transport model. The approach of this study can be useful for investigation on bed material load transport and stability of other controlled river diversions in the world.

It has been debated whether the ORCS has been diverting proportional sediment from the Mississippi into the Atchafalaya. Our finding - BML from the Outflow Channel is lower than its diverted water ratio - is further proof that, proportionally, more bed materials are transported downstream from the diversion location in the Mississippi channel, providing the foundation for downstream aggradation. This may have a long-term effect on the stability of the diversion. First, the less input BML would continue to scour the bed of the Outflow Channel, further increasing its gradient to the Mississippi main channel. Second, the excess sediment deposited in the mainstem downstream can further reduce the flow capacity of the channel, creating backwater conditions when the river flow is high. Furthermore, a recent study (Wang & Xu, 2018b) found that there is a large quantity of sands stored immediately upstream of the ORCS, the mobilization of which could make the situation even worse. All these factors together can increase the risk of a sudden river avulsion under a megaflood.

3.5. CONCLUSIONS

This study assessed riverbed material fluxes at an engineering-controlled bifurcation of one of the world's largest alluvial rivers, the Mississippi-Atchafalaya River diversion in south Louisiana, USA. Our study found a total bed material load of 201 million metric tons (MT) that

moved from upstream of the diversion during a 10-year period from 2004 to 2013. Approximately 36 MT (i.e., 18%) of the mobilized bed material was diverted into the Atchafalaya mainly through two bifurcation nodes, leaving 82% of the bed material in the Mississippi mainstem. These findings demonstrate that, proportionally, fewer bed materials moved into the Atchafalaya under the current 24% flow diversion. Severe bed scouring occurred in the controlled Outflow Channel, while aggradation in the Mississippi mainstream was widely present, implying reduced flow capacity and potential risk of high backwater under megafloods.

Furthermore, our study shows that Yang's classic sediment transport equation provides plausible results of bed material fluxes for a highly complicated river diversion, and that integration of the bed material transport equation and channel morphological assessment is a viable approach to investigate sediment dynamics at controlled river bifurcations.

CHAPTER 4. FLOOD EFFECTS ON MORPHOLOGY AND MIGRATION OF THE CONFLUENCE BAR OF TWO ALLUVIAL RIVERS ON THE MISSISSIPPI VALLEY LOESS PLAINS, USA

4.1. INTRODUCTION

River confluences are important locations in alluvial river networks, which can significantly influence channel morphology, migration, and avulsion (Best, 1986; Mosley, 1976). Over the past several decades, flow structure, sediment dynamics, and bed morphology at the river confluences have been extensively studied in laboratory experiments, theoretical analyses, and modeling simulations (Ashmore and Parker, 1983; Best, 1986; Best, 1988; Biron et al., 1993; Booker et al., 2001; Boyer et al., 2006; Bradbrook et al., 2000; Sukhodolov et al., 2017). In addition, morphodynamics of channel and planform around the confluence areas have also been assessed (Benda et al., 2004; de Morais et al., 2016; Gutierrez et al., 2014). However, less attention has been paid to the migration of river confluence bars as affected by floods.

In a recent study on the planform morphodynamics of large river confluences over decadal timescales, Dixon et al. (2018) found that confluence migrations would be much higher and more common than previously assumed. For example, in the Ganges-Brahmaputra-Meghna basin, more than 80% of large confluences were mobile over the past 40 years. Dixon et al. (2018) postulated that high river discharge, large sediment loading, and low cohesive bank strength mostly contributed to the high rates of confluence migration. They also divided confluence into three categories which are fixed, pinned, and upstream adjustment confluence based on confluence migration. Although their study demonstrated that confluence migration is ubiquitous, the remote sensing images they used with the relative coarse temporal solution were unable to explain how the migration proceeded under different flow conditions and especially during floods.

A river confluence is typically composed of a confluence mouth bar, a separation zone bar, a downstream scour zone, and a mid-channel bar in the post-confluence channel (Best, 1986; Mosley, 1976). As a critical element for confluence migration, morphologic changes of the confluence mouth bars have not thoroughly studied in the past. Investigation of the confluence mouth bars can not only improve the scientific understanding of confluence migration under different flow conditions but also can have practical relevance for assessing hazard risk for downstream engineering structures such as bridges and roads. In South Louisiana of the United States, for instance, a 70-m long bridge crosses the Amite River downstream near the confluence of its confluence with the Comite River. The two rivers are both alluvial rivers on the Mississippi Valley Loess Plain, carrying considerably high sand loads during floods. There is a concern over the migration of the confluence bar, which could possess a direct threat to the safety of the bridge. Understanding flood effects on and predicting confluence bar migration can help develop engineering solutions to mitigate potential hazards to the bridge and human lives.

Traditional field measurements, as well as remote sensing assessments of river confluences, often do not offer sufficient time resolution that is needed to quantify flood effects on confluence bar migration. On one hand, field surveys of rivers can be very time-consuming and costly, prohibiting frequent field data collection for morphological assessment. On the other hand, remotely sensed data and/or aerial images often do not capture the timespans of river floods. It is only with recent advances in terrestrial laser scanning, which allows detailed and rapid assessment of river channel morphological changes following flood events.

This study takes advantage of remote sensing and terrestrial laser scanning techniques to investigate longer-term and flood-event effects on river confluence bar migration and morphology. The study was conducted at a confluence of two alluvial rivers on the Mississippi Valley Loess

Plain in south Louisiana, USA. Specifically, the study aimed to accomplish the following objectives: (1) characterize decadal-scale confluence migration by using a series of remote sensing images taken between 2002 and 2017, (2) estimate the correlation between confluence migration rate and flood days during five different periods from 2002 to 2017, (3) conduct field measurements on morphologic changes of the confluence before and after three floods with different magnitudes by using a Terrestrial Laser Scanner, (4) estimate the morphologic changes of the confluence mouth bar, including its projected surface area and volume before and after each flood.

4.2. MATERIALS AND METHODS

4.2.1. Study area

The Amite River is a 188-km long coastal alluvial river in southeastern Louisiana with its headwater in Mississippi and emptying into Lake Maurepas (Fig. 4.1). The drainage basin of the Amite River is approximately 4800 km^2. About 58% of the total area is covered by forests (Wu and Xu, 2007). The Comite River is a right bank tributary of the Amite River, with a confluence near the city of Denham Springs, Louisiana (Fig. 4.1). The width of the two rivers is similar (i.e., about 30 m). The junction angle between the two rivers is about 60°. Upstream of the river confluence, the floodplain of the Amite River had been intensively mined for sand and gravel since the early 1970s (Hood et al., 2007; Mossa and McLean, 1997). There are no gauging stations currently available to monitor sediment concentrations of these two rivers upstream of the confluence. However, long-term average total suspended sediment (TSS) downstream of the confluence near Port Vincent (Fig. 4.1) was 46 mg L^{-1} between 1978 and 2001(Wu and Xu, 2007).

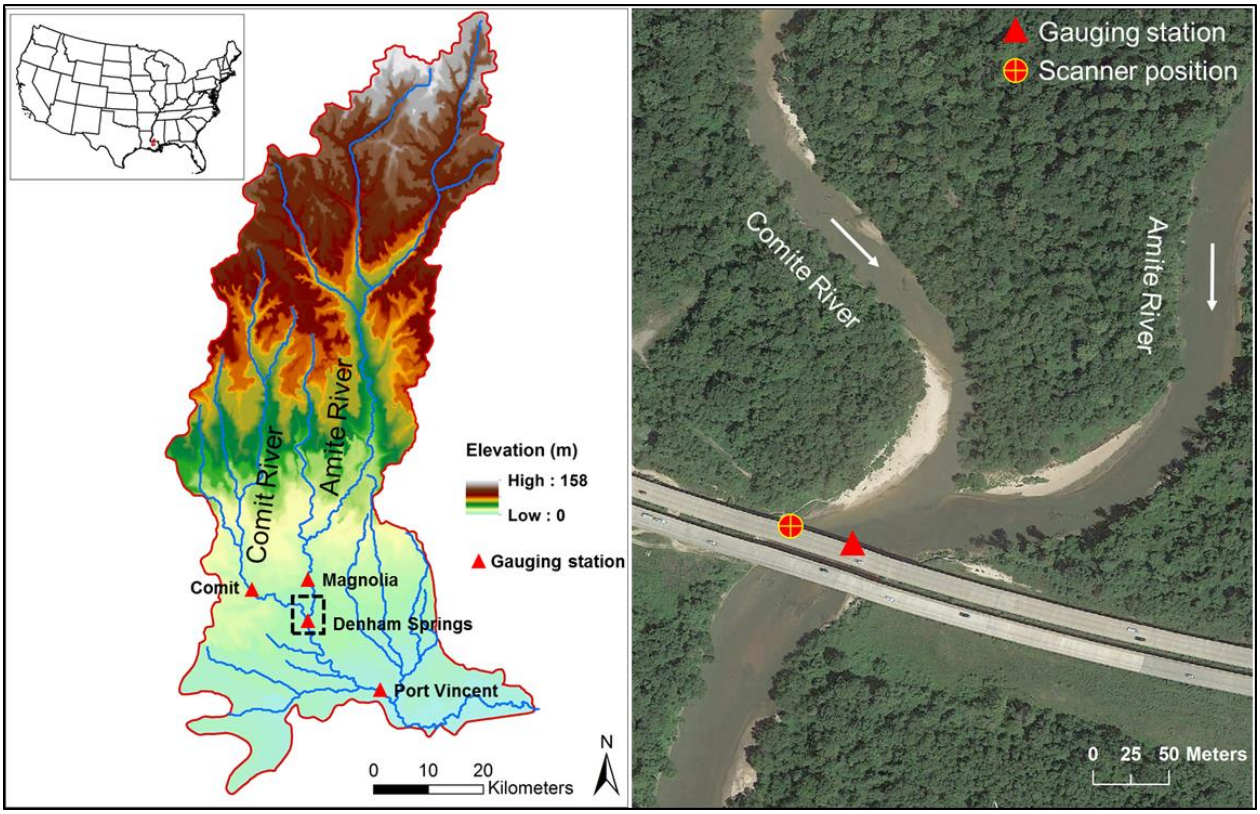

Fig. 4.1. Amite River Basin (Left), the river confluence of the Amite River and Comite River (Right). The background remote sensing image was taken in 2016. Source: Google Earth Pro. Terrestrial Laser Scanner was placed on the river bank underneath the bridge. The USGS gauging station near Denham Springs was located on the edge of the bridge.

Currently, there are four gauging stations operated by the U.S. Geological Survey on these two rivers down- and upstream of the confluence (Fig. 4.1a). These gauging stations supply long-term daily discharge and river stage data except the station at Magnolia only measuring river stage. The long-term daily discharge averaged 59 $m^3 s^{-1}$ at Denham Springs station (Wu and Xu, 2007).

4.2.2. Data and Methods

To characterize long-term morphologic changes of the river confluence, six remote sensing images, taken between Feb 28, 2002, and Nov 13, 2017, were downloaded from Google Earth Pro (Table 4.1 & Fig. 4.2). The time intervals between every two images are from 2 to 5 years. In ArcGIS 10.3 (ESRI, Redlands, California, USA), all downloaded images were firstly

georeferenced using the same control points. Secondly, the river confluence boundary was digitized in each image. In this step, we only traced the boundary of the vegetated area which could minimize the effects of different river stages on bar surface area estimation. Thirdly, the surface area of vegetated mouth bar was estimated during different periods.

Table 4.1. Remote sensing images downloaded from Google Earth Pro to characterize long-term morphologic changes of the Amite River and Comite River confluence.

Image Date	Stage (m)	Image Date	Stage (m)
2/28/2002	3.31	10/28/2010	2.87
6/15/2005	3.25	8/26/2015	3.09
7/22/2007	3.21	11/13/2017	3.28

Fig. 4.2. Remote sensing images show morphologic changes of the Amite River and Comite River confluence between 2002 and 2017. The old highway bridge was removed and a new one was built around 2010.

Daily discharge and river stage data between January 2002 and December 2017 were obtained from the gauging station at Magnolia (ID# 07377300), near Comite (ID# 07378000), and Denham Springs (ID# 07378500). The average river stage at Denham Spring was 3.84 m during 2002-2017. The flood stage and major flood stage at the station are 8.84 m and 11.88 m,

respectively, according to the stage classification by the National Oceanic and Atmospheric Administration (NOAA). The NOAA defines the flood stage as river stage for a specific location at which a rise in water surface level starts to produce a hazard to lives, property, or commerce. At Denham Springs, flooding will begin in the westernmost parts of Denham Springs when the river reaches flood stage. In this study, we define the floods with a stage between NOAA flood stage and major flood stage as moderate floods. Flood days above the flood stage at Denham Springs were counted for five different periods between 2002 and 2017 according to the daily river stage data. The correlation between the surface area change of the confluence mouth bar and the flood days during each period was then estimated.

Weibull exceedance probabilities and return period of the daily river stage were calculated based on the daily stage data at Denham Springs. Discharge ratio between the Comite and Amite river was calculated using the daily discharge data near Comite and Denham Springs.

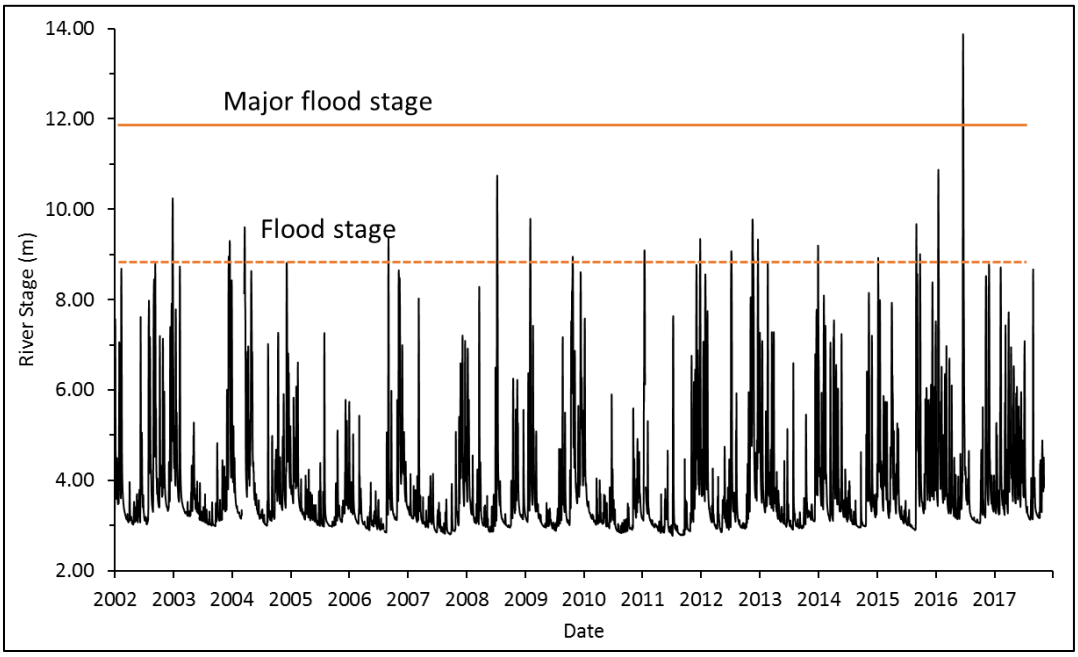

Fig. 4.3. River stage data at Denham Spring gauging station (ID# 07378500) between 2002 and 2017. Flood stage and major flood stage are 8.84 m (dash orange line) and 11.88 m (orange line) at this station according to the National Oceanic and Atmospheric Administration.

To assess rapid morphologic changes of the river confluence, the confluence was scanned four times in 2017 by a Riegl VZ-1000 terrestrial laser scanner (Fig. 4.4). The river had similar low river stages during these scans (i.e., from 3.26 m to 3.30 m). The first two field surveys occurred before and after a small single peak flood in March. The third survey was conducted after a relatively large single peak flood in April. In September, the confluence was measured again after a multi-peak flood occurred between April and September.

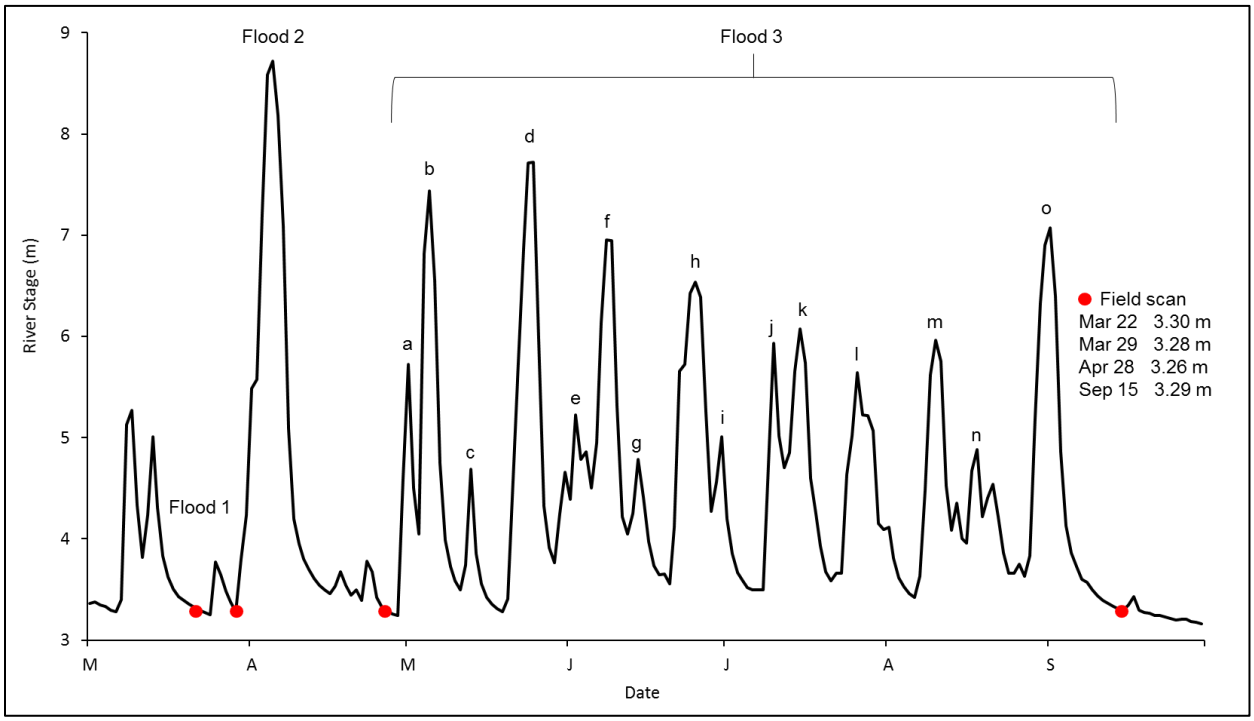

Fig. 4.4. Dates and corresponding river stages of the terrestrial laser scanning at the river confluence between March 2017 and September 2017. Floods 1 and 2 are characterized as single peak floods, while flood 3 is characterized as a multi-peak flood (i.e., peaks a-o).

The scanner was placed in the same place each time, i.e., right bank of the river under the bridge. The position had an excellent view to scan the confluence mouth bar (Fig. 4.1). The scanner provides a measurement range up to 1400 m with 5 mm repeatability and 8 mm accuracy. A camera (Nikon D810) mounted on the scanner was used to take photos for facilitating visualization and

interpretation of the laser data. Five Riegl flat 5-cm reflector were stuck to the bridge piers. They were finely scanned during each field survey and used for data post-processing.

The raw cloud point data from the four field scans were processed in RiSCAN PRO software (RIEGL, Horn, Austria). They were firstly registered using the five reflectors. Registration error was less than 3 mm ensuring the high-accuracy change detection of the confluence morphology. Registered point cloud data was then filtered into a smaller point cloud to most likely represent the bare-earth topography. This process contained three steps. Firstly, a vertical reference plane at 3.30-meter-high water surface was established. This was the highest river stage during the four scans. Secondly, we used the height filter to delete the noise points below the reference plane which are mainly objects reflected from the water (i.e., river bank and trees). The points located higher than 2 m above the reference plane were also filtered because they are mainly trees. Thirdly, only the last return of the remaining point data was kept for removing the impact of other vegetation. The filtered point cloud data were finally gridded to 0.5 m × 0.5 m digital elevation models (DEMs). The holes within the DEMs were closed by setting a larger grid size.

The volume of the mouth bar above the 3.30 m reference plane was estimated for each DEM. Here we used “using existing surface” method to calculate the bar volume. This method calculates the volume between the bar surface and the reference plane (i.e., 3.30 m water surface). In addition, the cumulative volume of the bar between the reference plane and the bar top was calculated at 0.1 m intervals. Instead of comparing specific profiles of the bar surface pre- and post-floods, we estimated bar surface change (i.e., deposition and erosion) on the whole bar surface using “surface comparison” function.

4.3. RESULTS

4.3.1. Long-term morphologic changes of the Amite-Comite confluence

The river confluence showed significantly morphologic changes from 2002 to 2017 (Fig. 4.5). For the confluence channel, deposition occurred on the right bank causing the river channel to narrow to about 28 m. On the contrary, the left bank eroded about 36 m. In addition, the junction angle between two river channels changed from ~90° to ~60° (Fig. 4.2). For the confluence mouth bar, it gradually migrated downstream between 2002 and 2017. In total, its bar front migrated about 55 m in the past 16 years which is equivalent to 3.4 m downstream migration every year. The migration was mainly caused by the growth of its left edge, while the position of its right edge only slightly changed.

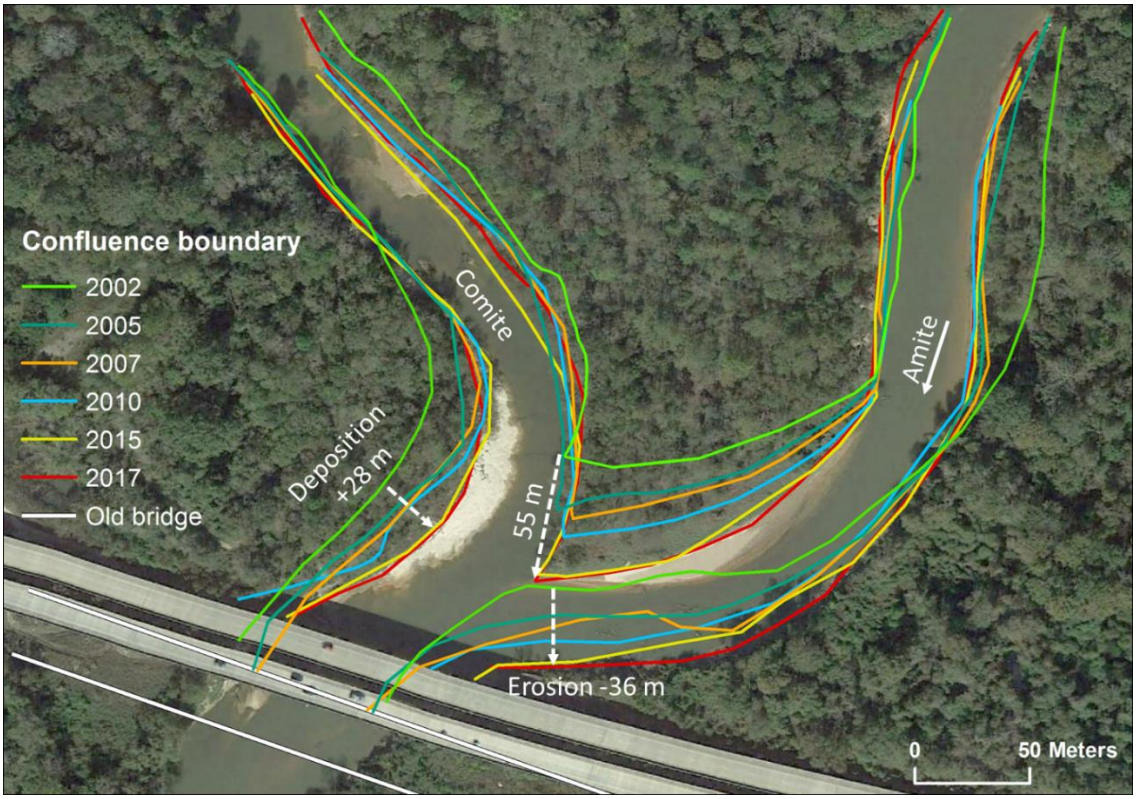

Fig. 4.5. Morphologic changes of the confluence between 2002 and 2017. The lines depict the boundaries of the vegetated area of the river confluence channels. The confluence angle changed from ~90° to ~60° from 2002 to 2017.

The average annual increase in the surface area of the confluence mouth bar shows that the bar migration rate varied largely during different periods from 2002 to 2017 (Fig. 4.6). The rate was close to 600 m^2/year from 2002 to 2004. Then it dropped to 230 m^2/year in 2005. After that, it increased slightly to near 300 m^2/year from 2005 to 2014. However, there was no significant increase in the vegetated surface area of the mouth bar during 2015-2017 (i.e., 77 m^2/year). This is also shown in Fig. 5 where the bar boundaries in 2015 and 2017 nearly overlap.

The regression R-square between the total increased surface area of the confluence mouth bar and the flood days is low during five different periods between 2002 and 2017 (i.e., $r^2 = 0.16$, Fig. 4.7). However, it shows a significant positive correlation if the data during 2015-2017 were excluded (i.e., $r^2 = 0.96$).

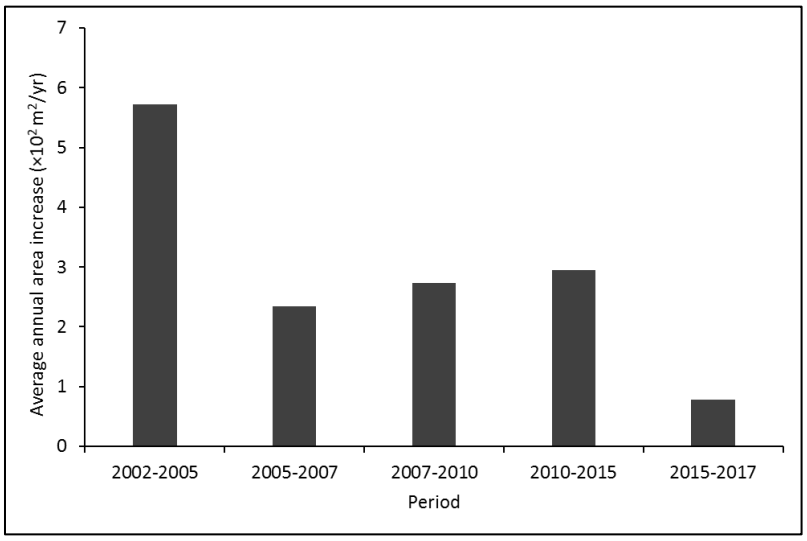

Fig. 4.6. The average annual increase of the vegetated area of the confluence mouth bar between 2002 and 2017.

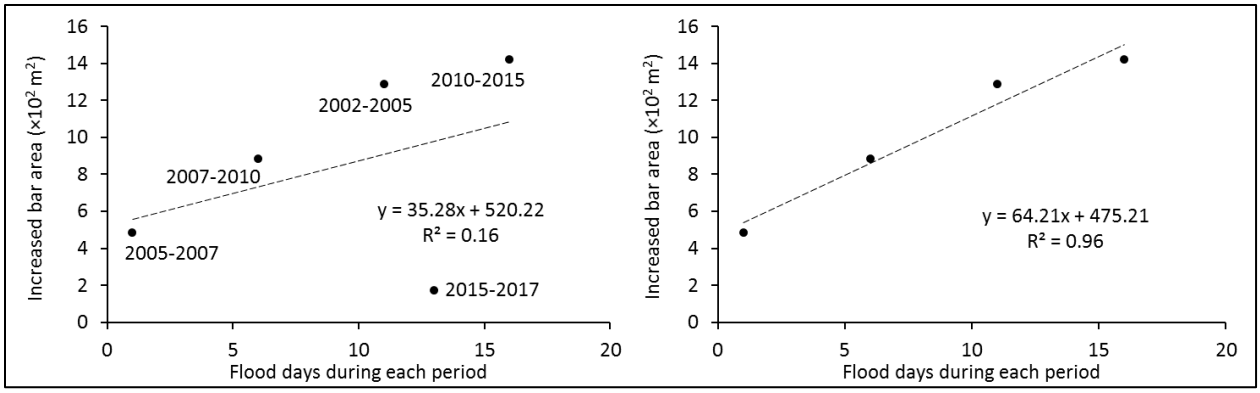

Fig. 4.7. Correlation between the total surface area change of the confluence mouth bar and the flood days (river stage above the flood stage at Denham Springs gauging station) during different periods between 2002 and 2017 (left). The same correlation if the data during 2015-2017 was excluded (right).

4.3.2. Short-term morphologic changes of the river confluence

4.3.2.1. Hydrologic analysis

Long-term daily river stage averaged 3.87 m at the river confluence. Flood 1 occurred on Mar 25 with a similar stage to the average stage of the river (i.e., 3.77 m vs. 3.87 m) (Fig. 4.4). Flood 2 occurred on April 5 with a peak stage at 8.72 m, which was the flood with 0.7-year recurrence interval. Flood 3 occurred between April and September including fifteen small flow pulses (events usually occurs more than one times per year) with the peak stages between 4.69 m (flood c) and 7.72 m (flood d). The relatively larger floods, such as floods b, d, f, and o had one-month to three-month recurrence intervals. Long-term discharge ratio between Comite River and Amite River was 0.29 during 2002-2017. The ratio increased from 0.16 between Mar 22 and Apr 28 to 0.37 between Apr 29 and Sep 15. The bar top is about 2 m higher than the low river stage (i.e., 3.30m). Therefore, the bar is entirely inundated when the stage reaches above 5.30 m.

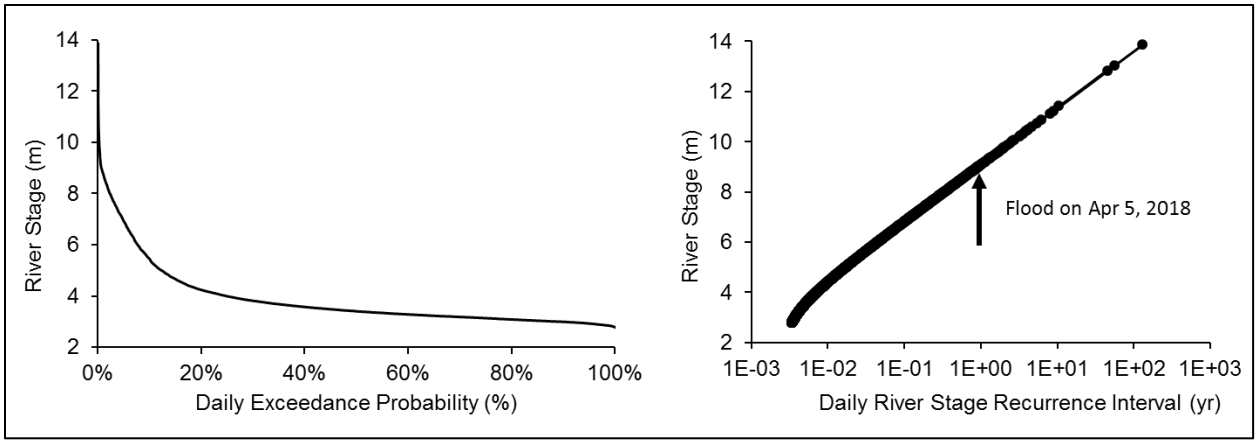

Fig. 4.8. Daily exceedance probability of the river stage (left). Daily river stage recurrence interval (yr) (right).

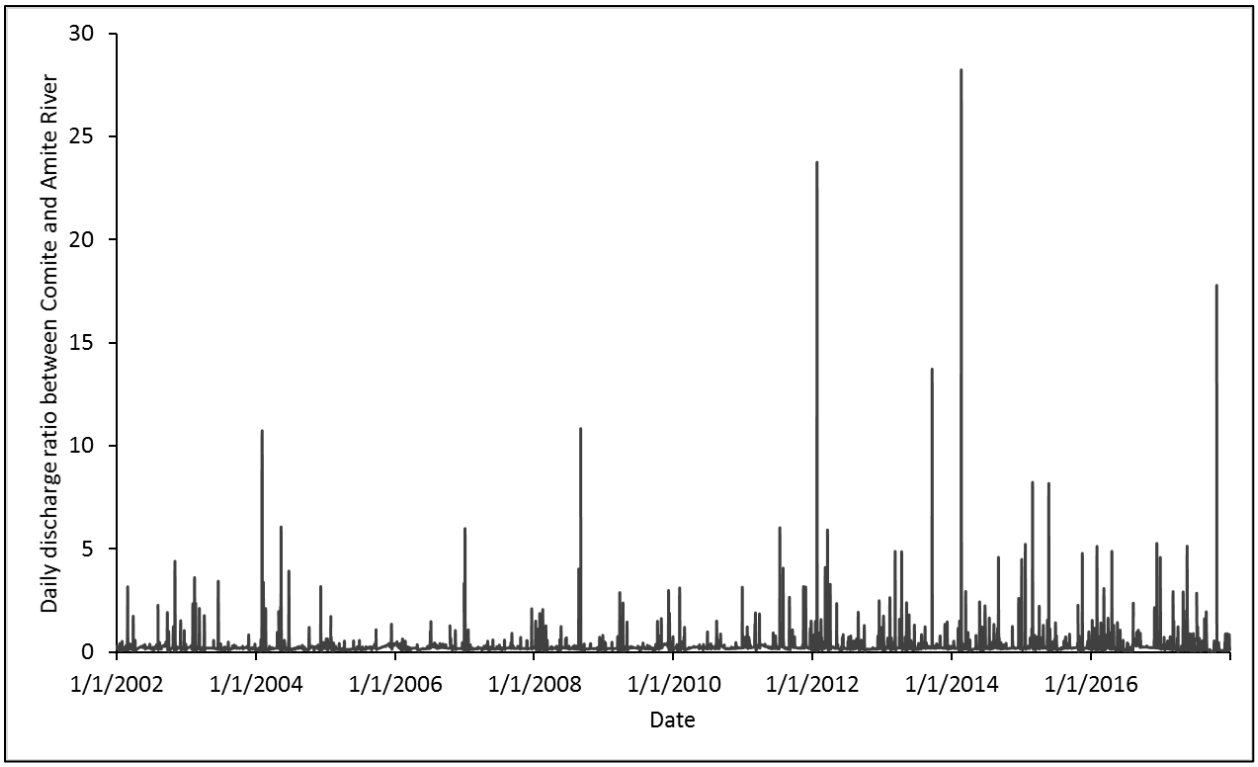

Fig. 4.9. Daily discharge ratio between Comite River and Amite River.

4.3.2.2. Morphologic changes of the river confluence bar from March to September

Generated DEMs data represent the bar head and edge very well, while most of the bar top was filtered owning to the dense vegetation coverage (Fig. 4.10a-d). Overall, the confluence mouth bar is highly dynamic from March to September in 2017. Before and after flood 1, there was little boundary change of the bar (Fig. 4.10e), and its projected surface area had little change (i.e., 1%, Table 4.2). On its left edge, 24 m^3 sediment was deposited (Fig. 4.11b), although 3 m^3 sediment was flushed away on the right edge (Fig. 4.11a&d). The erosion and deposition mainly occurred in the lower part of the bar, i.e., between 5 cm and 20 cm height interval (Fig. 4.11c). The total bar volume increased from 202 m^3 to 223 m^3 or 10% after the first flood (Table 4.2).

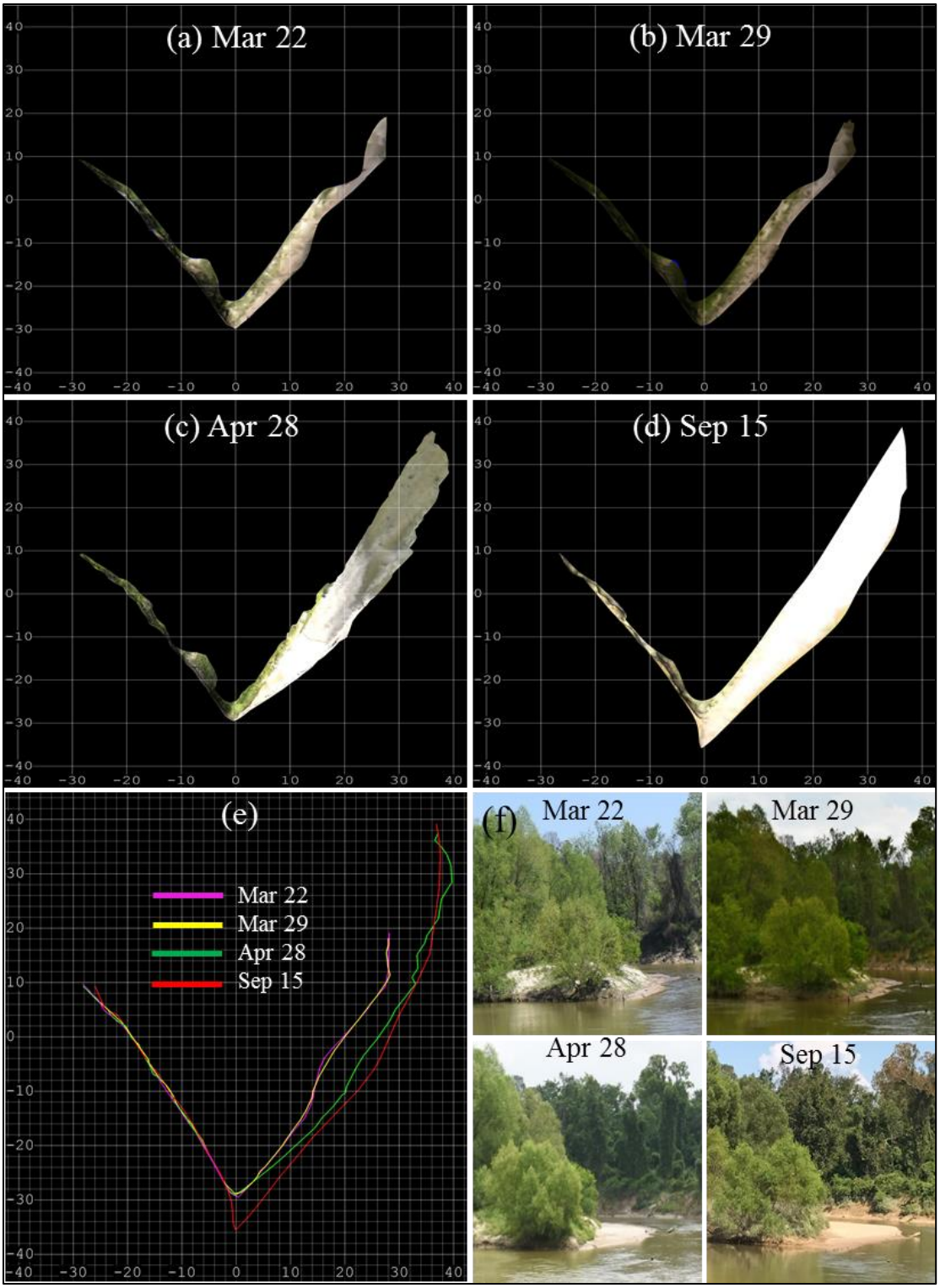

Fig. 4.10. Morphologic changes of the confluence mouth bar from Mar 22 to Sep 15, 2017 (a – d). The DEMs data were shown in orthographic view and natural color. The unit in the images is meter. (e) changes of the bar boundaries. (f) front view of the bar during each field scan, which was taken by the mounted camera.

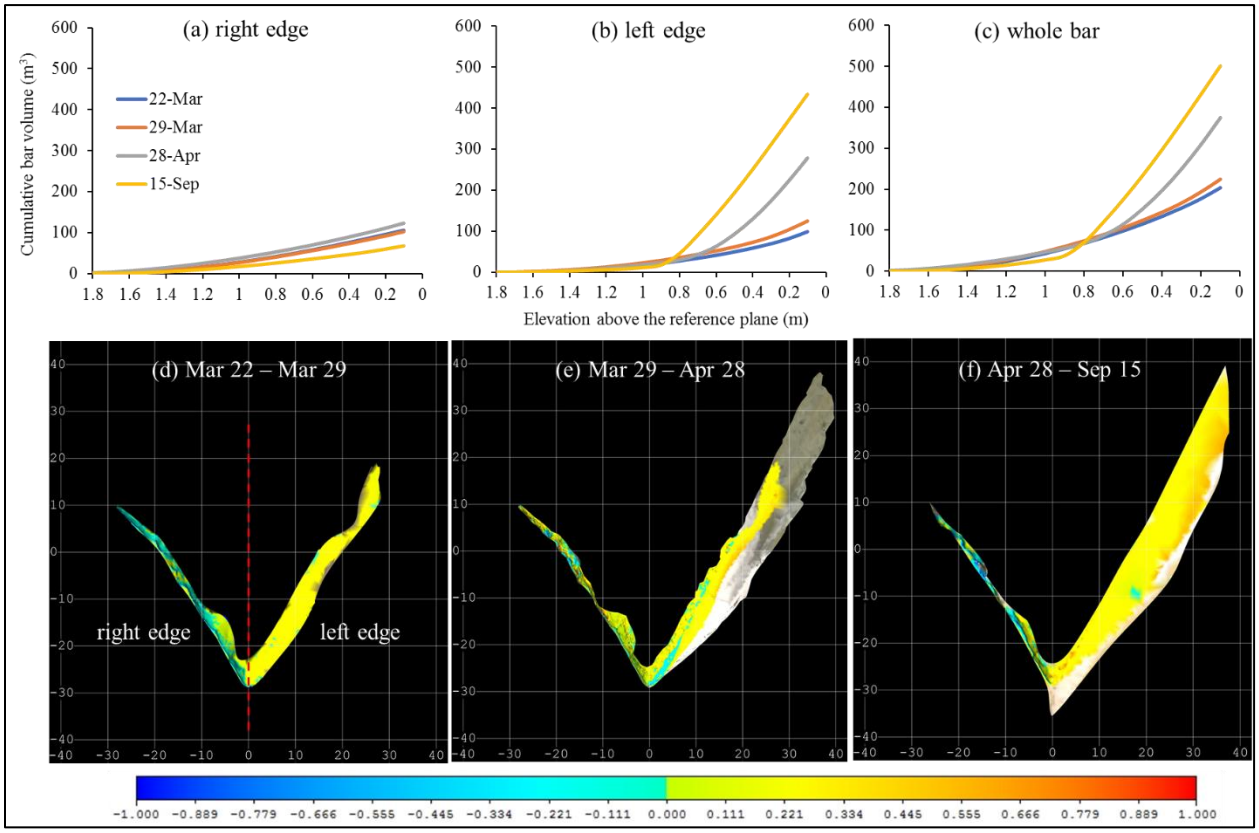

Fig. 4.11. Changes of cumulative bar volume on the right edge, left edge and the whole bar after different intensities of floods (a-c). The bar volume was calculated based on a 0.1 m height interval. The reference plane is the 3.30-m river stage. Morphologic changes of the confluence mouth bar (d-f).

Table 4.2. Surface area and volume changes of the confluence mouth bar between March 22, 2017, and September 15, 2017. The bar volume was the emerged portion between the bar surface and the referenced plane at 3.30 m water surface.

Date	Projected bar surface area (m^2)	Area increase	Cumulative surface area increase	Bar volume (m^3)	Volume increase	Cumulative volume increase
22-Mar	320	-	-	202	-	-
29-Mar	322	1%	1%	223	10%	10%
28-Apr	689	114%	115%	375	68%	86%
15-Sep	701	2%	119%	501	34%	148%

Following the second flood, the most significant change of the confluence bar was the extension of its left edge. It laterally spread about four meters and elongated over 20 meters upstream. As a consequence, the projected surface area of the bar was more than double its previous area (i.e., from 322 m^2 to 689 m^2, Table 4.2, Fig. 4.10e). Erosion was observed in the left-margin area of the bar head. Bar volume increased about 154 m^3 on this side, which was mainly caused by the sediment deposited below the 0.7 m height interval (Fig. 4.11b). Different from the previous observation, the right edge gained sediment at each height interval causing about 20 m^3 volume increase, although its upstream part was partially eroded (Fig. 4.11a). Overall, the volume of the whole bar increased from 223 m^3 to 375 m^3 or 68% (Table 4.2).

During the third flood, sedimentation continued on the left edge causing one to two meters lateral spreading. In addition, bar head elongated about 6 m downstream. However, the projected surface area of the bar increased only 2%, which was mainly induced by the erosion on the left upstream edge. Severe erosion was found on the right edge resulting in about 54 m^3 sediment was removed (i.e., 48%) (Fig. 4.11a). In contrast, 156 m^3 sediment deposited on the left edge. Overall, the total volume of the bar increased from 375 m^3 to 501 m^3 or 34% from Apr 28 to Sep 15.

During the whole study period, the right edge of the bar was eroded about one meter, while the left edge laterally spread four to six meters toward the main channel. The projected surface area of the bar increased from 320 m^2 to 701 m^2 or 119% (Table 4.2). In a total of 299 m^3 sediment was deposited on the bar and the bar volume increased 148% (Table 4.2).

4.4. DISCUSSION

The large morphologic changes of the Amite-Comite River confluence demonstrate that network of alluvial rivers in lowland is highly dynamic. This type of confluence migration is uncommon in natural river systems according to the statistics in the Ganges-Brahmaputra-Meghna

and Amazon basin, which only accounts for 4.8% and 6.7% of all types of confluence migration, respectively (Dixon et al., 2018). Dixon et al. (2018) concluded that this type of migration is caused by lateral migration of a tributary channel. In the present study, remote sensing images during 2002-2017 do show that the migration resulted from the channel meandering process of the main channel where the point bar on the left edge of the confluence mouth bar kept growing and the left bank of the main channel retreated.

Regression analysis shows a significant positive relationship between the total increased vegetated area of the mouth bar and total days of moderate floods during four different periods of 2002-2015. However, when major floods occurred during 2015-2017, the vegetated area of the mouth bar had little change. Thus, we propose that moderate floods are capable of leading bar growth and confluence migration, while major floods may prevent the bar from growth. Bartholdy and Billi (2002) studied the flood effects on channel and bar morphology and they also found that bar development and channel migration take place during moderate floods but are interrupted by large floods with 10 to 20 years return periods.

The Laser scanning measurements in 2017 allow us to detail the morphodynamics of the mouth bar before and after floods with varied intensities. Results support the observations from the analysis of remote sensing images. A single peak flood with a magnitude close to a moderate flood (i.e., flood 2) doubled the size of the projected surface area of left bar edge and produced the largest sediment deposition compared to the lower magnitude floods (i.e., flood 1 and 3). During the flood 2, the bar was fully inundated seven days from April 1 to April 7. According to the findings from previous studies (Kiss and Sipos, 2007; Wintenberger et al., 2015), it is very likely that the deposition on the left bar edge occurred during the falling limb of the flood. At the time, sediment deposited on the top of the bar were reworked causing a lateral spreading towards to bar

margin. The surface area of the left bar edge increased much more than the right edge could be explained by the much gentler slope it has.

Bar margins usually experience significant lateral erosion when water leaves the bar or during low river stage (Kiss and Sipos, 2007; Wintenberger et al., 2015). However, the confluence mouth bar in the present study continuously gained sediment during summer time when the river stage is the lowest during the year (Flood 3). Although Flood 3 contains only small flow pulses, upstream erosion, downstream elongation, and lateral spreading of the left bar edge occurred during the time. This illustrates that the main-channel side of the confluence bar experienced complex adjustments during the multipeak flood event with lower magnitudes. Although the bar surface area had little change from April to September, the bar volume increased 34% indicating that vertical deposition dominated the deposition process instead of lateral spreading of the bar. The could be explained by less sediment supply during the lower intensity flow pulses. Vegetation colonization may also happen during this period due to the much less inundation time. In addition, it should be noted that the bar front elongated about 6 m downstream after flood 3. This region is the stagnation zone of the river confluence. Previous studies found that flow velocity in this zone is a deficit or even reverse (Konsoer and Rhoads, 2014; Rhoads and Sukhodolov, 2008). Our measurement suggests that low magnitude floods favor the sediment deposition in the stagnation zone. The largest erosion occurred on the right edge of the bar during flood 3. The flow discharge ratio between the Comite and the Amite River was 0.16 during flood 1 and 2 but it increased to 0.37 during flood 3. The higher discharge in the Comite River may be the main reason causing the erosion on the right bar edge.

The migration of the river confluence is mainly caused by the sediment deposition on the left edge of the mouth bar. This could be explained by two reasons. Firstly, the left edge of the bar

is the convex bank of the Amite River channel where sediments tend to deposit and form a point bar. Laser scanning results revealed that sediment deposition on the left edge was much more pronounced. The bar volume of the left edge changed from less 100 m^3 to more than 400 m^3 from March to September 2017 (Fig. 4.11b). Especially after flood 2, the nearly 4-meter laterally spread of the left edge is consistent with the average bar migration rate during 2002-2017 (i.e., 3.4 m/yr). Secondly, it clearly shows in Fig. 4.9 that sometimes the discharge in the Comite River is much higher that the Amite River. Backwater may very likely happen at the time on the river confluence, which benefits the sediment deposition on the point bar and the upstream Amite River.

Laser measurements also reveal that the features of sediment deposition and erosion on two edges of the mouth bar could change in response to the flood magnitudes. During low magnitude floods (i.e., flood 1 and 3), sediment was deposited on the left edge but was removed from the right edge. During high magnitude flood (i.e., flood 2), sediment was deposited on the right edge as well as the left edge (Fig. 4.11). This can be explained by the bar is usually fully submerged during large floods when the river stage goes beyond 5.30 m. However, there were little changes in the vegetated bar area during the period of 2015-2017. At the time, an extremely large flood occurred in August 2016 which its peak stage was about 1.5 m higher than the previous record at Denham Springs (Fig. 4.12). It is very likely such unprecedented flood has caused serious erosion on both sides of the confluence mouth bar and resulted in the little growth of the mouth bar. Bartholdy and Billi (2002) pointed out that large floods could cut through the point bars and force the channel back towards a straight planform. Future study is needed to clarify such situation by measuring morphologic changes of the confluence mouth bar before and after a major flood (i.e., river stage is higher than 11.88 m).

Fig. 4.12. Google Earth image (taken on Aug 15, 2016) shows the 2016 large flood in the Amite River. The flood exceeded the previous river stage record (set on May 19, 1953). The image clearly shows that sediment concentration in the Amite River was much higher than the Comite River when a large flood occurred.

The results presented in the current study also indicate that the morphology of a confluence mouth bar is very sensitive to the river stage changes. Even if a minor flow pulse with the stage close to the long-term average stage occurred (i.e., flood 1), it could cause sediment deposition and erosion on different bar edges (Fig. 4.11d). It also indicates that Terrestrial Laser Scanning technology is an ideal tool for the event-based morphologic changes study of river channels.

With the abundant sediment storage in the upstream Amite River, the rapid sediment deposition on the point bar is very likely to continue in the future. This may lead to severe erosion on the left bank. The riverbed scours zone could also migrate downstream due to the change of the junction angle, bend migration, and channel cut-off. These processes may largely threaten the highway bridge safety. The current study also has an implication for the modeling simulation of river confluence migration. Long-term confluence migration could be simulated based on the

flow variations and sediment transport once the mechanisms of the migration are identified. In addition, future studies could also focus on the bar morphology changes during rising and falling limbs which usually contribute very different in bar development (Best et al., 2003).

4.5. CONCLUSIONS

This study investigated morphologic changes of a confluence of two active meandering alluvial rivers in lowland Louisiana. Long-term remote sensing images show that the confluence continuously migrated about 55 m downstream between 2002 and 2017. Sediment deposition on the main channel side of the confluence mouth bar is the major driver for the confluence migration. Regression analysis shows that the increase rate of the vegetated area of the bar is highly related with the days of moderate floods (river stage is between flood stage and major flood stage). However, the extreme floods may interrupt the bar growth and confluence migration.

Short-term Laser scanning measurements were conducted before and after three floods with different intensities in 2017. Results show that a single moderate flood could double the projected surface area of the mouth bar and increased its volume by 68%. The bar growth was mainly from the elongation and spreading of the bar edge at the main channel side. The confluence mouth bar kept gaining sediment even during low flow stage (flood 1 and 3). Sediment tends to deposition on the stagnation zone during low magnitude floods and causes elongation of bar front. Overall, the projected surface area and volume of the bar increased by 119% and 148% during the half-year study from March to September, respectively. Our study highlights the importance of episodic floods on the evolution and migration of confluence mouth bar, which could be the major driver for the confluence migration. The high accuracy Terrestrial Laser Scanner is proved to be a powerful tool to study river confluence morphodynamics.

CHAPTER 5. SUMMARY AND CONCLUSION

This thesis research was completed as a comprehensive assessment of sediment transport and channel morphology in the highly engineered lowermost Mississippi River as well as a natural alluvial river in Southeast Louisiana. The research comprised three studies that (1) assessed patterns and mechanisms of riverbed deformation in the last 500-km channel of the Mississippi River in the last two decades, (2) estimated bed material loads at the Mississippi-Atchafalaya River bifurcation, and (3) analyzed flood effects on the migration of the Amite-Comite river confluence. Results from this research are summarized below.

In the 500-km lowermost Mississippi River, significant sediment deposition occurred in the uppermost 88 kilometers immediately below the Mississippi-Atchafalaya River diversion and the last 37 kilometers where the river starts to breach off into the Gulf of Mexico, causing flow reduction and downstream sedimentation. Continuous bed aggradation downstream of the Mississippi-Atchafalaya diversion may largely increase the risk of avulsion if unprecedented floods occur. The observed trends in the reach between RK 386 and RK 163 suggest that it has substantial potential for trapping sediment. From 1992 to 2013, although marginal sediment deposition was found in the lowermost Mississippi River (i.e., 51×10^6 m^3), the river trapped approximately 337×10^6 m^3 sediment (mainly sand) considering the dredged volume of riverbed sediment. This rejects the initial hypothesis that the lower reach of this highly engineered large alluvial river functions as a conduit for sediment transport. The total volume of trapped sediment over the past 22 years is equivalent in mass to 68% (i.e., 404 MT) of the total suspended sand discharged into the LmMR (i.e., 598 MT), assuming a bulk density of 1.2 metric ton per cubic meter for the riverbed material. On an annual mass budget, only about 9 MT sand is discharged from the river into the Gulf of Mexico.

Overall, the study shows the complexity of sediment transport in the lower reach of a large alluvial river, in that distinctive bed deformation can occur in different reaches because of flow deduction and backwater effects. The findings offer insights into potential bed deformation trends for lower reaches of other large river systems with no or limited bathymetry, discharge, and sediment data. Such information could also be applicable for other rivers to develop sustainable river engineering strategies and plans.

Based on the estimation of bed material loads at the Mississippi-Atchafalaya River diversion, we found that there were ~215 million metric tons (MT) bed material load transported upstream of the diversion during 2004-2013. About 22% of that (i.e., ~47 MT) were diverted into the outflow channel through the Old River Control Structures. The findings reveal that, proportionally, more bed materials were carried downstream in the mainstem channel under the current flow diversion, while severe bed scouring occurred in the controlled outflow channel. The aggradation in the mainstream reduced flow capacity and increased the risk of an avulsion under a megaflood.

Long-term remote sensing images show that the confluence of the Amite- Comite Rivers continuously migrated about 55 m downstream from 2002 to 2017. Sediment deposition on the main channel side of the confluence mouth bar is the major driver for the confluence migration. Regression analysis shows that the increase rate of the vegetated area of the bar is highly related with the days of moderate floods (river stage is between flood stage and major flood stage). However, the extreme floods may interrupt the bar growth and confluence migration. Short-term Laser scanning measurements were conducted before and after three floods with different intensities in 2017. Results show that a single moderate flood could double the projected surface area of the mouth bar, expanding its bar volume by 68%. The bar growth was mainly from the

elongation and spreading of the bar edge at the main channel side. The confluence mouth bar kept gaining sediment even during low flow stage. Sediment tends to deposition on the stagnation zone during low magnitude floods and causes elongation of bar front. Overall, the projected surface area and volume of the bar increased by 119% and 148% during the half-year study from March to September, respectively.

In summary, this thesis research reveals the complexity of sediment transport and river network development in the lower reaches of alluvial rivers. The research demonstrates longer-term study, in that distinctive bed deformation can occur in different reaches because of flow deduction and backwater effects. Our study is the first try of estimating bed material load at a largely controlled bifurcation based on a simple, well-established bed material transport model. The study also highlights the importance of episodic floods on the evolution and migration of a river confluence.

LITERATURE CITED

Ackers, P., White, W.R., 1973. Sediment Transport; New Approach and Analysis. Journal of the Hydraulics Division, 99(HY11), 2041-2060.

Allen, J.R.L., 1965. A REVIEW OF THE ORIGIN AND CHARACTERISTICS OF RECENT ALLUVIAL SEDIMENTS. Sedimentology, 5(2), 89-191.

Allison, M.A., Meselhe, E.A., 2010. The use of large water and sediment diversions in the lower Mississippi River (Louisiana) for coastal restoration. Journal of Hydrology, 387(3–4), 346-360.

ASCE, T.C.o.R.b.M.o.S.S.a.S.Y.o.t.C.o.S.o.t.H.D., 1982. Relationships between morphology of small streams and sediment yield. Journal of the Hydraulics Division, 108(11), 1328-1365.

Ashmore, P., Parker, G., 1983. CONFLUENCE SCOUR IN COARSE BRAIDED STREAMS. Water Resources Research, 19(2), 392-402.

Aslan, A., Autin, W.J., 1999. Evolution of the Holocene Mississippi River floodplain, Ferriday, Louisiana: Insights on the origin of fine-grained floodplains. Journal of Sedimentary Research, 69(4), 800-815.

Aslan, A., Autin, W.J., Blum, M.D., 2006. Causes of river avulsion: Insights from the late Holocene avulsion history of the Mississippi River, USA - Reply. Journal of Sedimentary Research, 76(5-6), 960-960.

Baker, D.W., Bledsoe, B.P., Albano, C.M., Poff, N.L., 2011. Downstream effects of diversion dams on sediment and hydraulic conditions of rocky mountain streams. River Research and Applications, 27(3), 388-401.

Bartholdy, J., Billi, P., 2002. Morphodynamics of a pseudomeandering gravel bar reach. Geomorphology, 42(3), 293-310.

Benda, L., Andras, K., Miller, D., Bigelow, P., 2004. Confluence effects in rivers: Interactions of basin scale, network geometry, and disturbance regimes. Water Resources Research, 40(5), n/a-n/a.

Best, J.L., 1986. THE MORPHOLOGY OF RIVER CHANNEL CONFLUENCES. Progress in Physical Geography, 10(2), 157-174.

Best, J.L., 1988. Sediment transport and bed morphology at river channel confluences. Sedimentology, 35(3), 481-498.

Best, J.L., Ashworth, P.J., Bristow, C.S., Roden, J., 2003. Three-dimensional sedimentary architecture of a large, mid-channel sand braid bar, Jamuna River, Bangladesh. Journal of Sedimentary Research, 73(4), 516-530.

Biron, P., Roy, A.G., Best, J.L., Boyer, C.J., 1993. BED MORPHOLOGY AND SEDIMENTOLOGY AT THE CONFLUENCE OF UNEQUAL DEPTH CHANNELS. Geomorphology, 8(2-3), 115-129.

Blum, M.D., Roberts, H.H., 2009. Drowning of the Mississippi Delta due to insufficient sediment supply and global sea-level rise. Nature Geoscience, 2(7), 488-491.

Booker, D.J., Sear, D.A., Payne, A.J., 2001. Modelling three-dimensional flow structures and patterns of boundary shear stress in a natural pool-riffle sequence. Earth Surface Processes and Landforms, 26(5), 553-576.

Boyer, C., Roy, A.G., Best, J.L., 2006. Dynamics of a river channel confluence with discordant beds: Flow turbulence, bed load sediment transport, and bed morphology. Journal of Geophysical Research: Earth Surface, 111(F4), n/a-n/a.

Bradbrook, K.F., Lane, S.N., Richards, K.S., 2000. Numerical simulation of three-dimensional, time-averaged flow structure at river channel confluences. Water Resources Research, 36(9), 2731-2746.

Bridge, J.S., Leeder, M.R., 1979. A simulation model of alluvial stratigraphy. Sedimentology, 26(5), 617-644.

Bryant, M., Falk, P., Paola, C., 1995. Experimental study of avulsion frequency and rate of deposition. Geology, 23(4), 365-368.

Caskey, S.T., Blaschak, T.S., Wohl, E., Schnackenberg, E., Merritt, D.M., Dwire, K.A., 2015. Downstream effects of stream flow diversion on channel characteristics and riparian vegetation in the Colorado Rocky Mountains, USA. Earth Surface Processes and Landforms, 40(5), 586-598.

Chatanantavet, P., Lamb, M.P., Nittrouer, J.A., 2012. Backwater controls of avulsion location on deltas. Geophysical Research Letters, 39(1), L01402.

Chen, X., Zong, Y., 1998. Coastal erosion along the Changjiang deltaic shoreline, China: History and prospective. Estuarine Coastal and Shelf Science, 46(5), 733-742.

Chow, V.T., 1959. Open-channel hydraulics. McGraw-Hill civil engineering series. New York, McGraw-Hill, 1959.

Church, J.A., White, N.J., 2006. A 20th century acceleration in global sea-level rise. Geophysical Research Letters, 33(1), n/a-n/a.

Church, M., 2006. Bed material transport and the morphology of alluvial river channels, Annual Review of Earth and Planetary Sciences. Annual Review of Earth and Planetary Sciences, pp. 325-354.

Cochrane, T.A., Arias, M.E., Piman, T., 2014. Historical impact of water infrastructure on water levels of the Mekong River and the Tonle Sap system. Hydrology and Earth System Sciences, 18(11), 4529-4541.

Coleman, J.M., Roberts, H.H., Stone, G.W., 1998. Mississippi River delta: an overview. Journal of Coastal Research, 14(3), 698-716.

Couvillion, B.R., Barras, J.A., Steyer, G.D., Sleavin, W., Fischer, M., Beck, H., Trahan, N., Griffin, B., Heckman, D., 2011. Land area change in coastal Louisiana from 1932 to 2010: U.S. Geological Survey Scientific Investigations Map 3164.

CPRA, 2007. Integrated Ecosystem Restoration and Hurricane Protection: Louisiana's Comprehensive Master Plan for a Sustainable Coast, Coastal Protection & Restoration Authority.

CPRA, 2012. Louisiana's Comprehensive Master Plan for a Sustainable Coast, Coastal Protection and Restoration Authority of Louisiana, Baton Rouge, LA.

de Morais, E.S., dos Santos, M.L., Cremon, E.H., Stevaux, J.C., 2016. Floodplain evolution in a confluence zone: Parana and Ivai rivers, Brazil. Geomorphology, 257, 1-9.

Dixon, S.J., Sambrook Smith, G.H., Best, J.L., Nicholas, A.P., Bull, J.M., Vardy, M.E., Sarker, M.H., Goodbred, S., 2018. The planform mobility of river channel confluences: Insights from analysis of remotely sensed imagery. Earth-Science Reviews, 176(Supplement C), 1-18.

Edmonds, D.A., 2012. Stability of backwater-influenced river bifurcations: A study of the Mississippi-Atchafalaya system. Geophysical Research Letters, 39(8), n/a-n/a.

Edmonds, D.A., Slingerland, R.L., 2008. Stability of delta distributary networks and their bifurcations. Water Resources Research, 44(9).

Einstein, H.A., 1950. The bed-load function for sediment transportation in open channel flows. Technical bulletin / United States Department of Agriculture: no. 1026. Washington : U.S. Dept. of Agriculture, 1950.

Engelund, F.A., Hansen, E., 1967. Monograph on sediment transport in alluvial streams. Teknisk forlag, Copenhagen.

Fernandes, A.M., Tornqvist, T.E., Straub, K.M., Mohrig, D., 2016. Connecting the backwater hydraulics of coastal rivers to fluvio-deltaic sedimentology and stratigraphy. Geology, 44(12), 979-982.

Fisk, H.N., 1944. Geological investigation of the alluvial valley of the lower Mississippi River: U.S. Department of the Army, Mississippi River Commission.

Fisk, H.N., 1952. Geological investigation of the Atchafalaya Basin and the problem of Mississippi River diversion, Wterways Experiment Station.

Frazier, D.E., 1967. Recent deltaic deposits of the Mississippi River; their development and chronology. Transactions - Gulf Coast Association of Geological Societies, 17, 287-315.

Gaeuman, D., Schmidt, J.C., Wilcock, P.R., 2005. Complex channel responses to changes in stream flow and sediment supply on the lower Duchesne River, Utah. Geomorphology, 64(3-4), 185-206.

Galler, J.J., Allison, M.A., 2008. Estuarine controls on fine-grained sediment storage in the lower Mississippi and Atchafalaya Rivers. Geological Society of America Bulletin, 120(3-4), 386-398.

Galler, J.J., Bianchi, T.S., Alison, M.A., Wysocki, L.A., Campanella, R., 2003. Biogeochemical implications of levee confinement in the lowermost Mississippi River. Eos, Transactions American Geophysical Union, 84(44), 469-476.

Ganti, V., Chadwick, A.J., Hassenruck-Gudipati, H.J., Fuller, B.M., Lamb, M.P., 2016. Experimental river delta size set by multiple floods and backwater hydrodynamics. Science Advances, 2(5), e1501768.

Gornitz, V., 1995. Sea-level rise; a review of recent past and near-future trends. Earth Surface Processes and Landforms, 20(1), 7-20.

Gutierrez, R.R., Abad, J.D., Choi, M., Montoro, H., 2014. Characterization of confluences in free meandering rivers of the Amazon basin. Geomorphology, 220, 1-14.

Harmar, O.P., Clifford, N.J., Thorne, C.R., Biedenharn, D.S., 2005. Morphological changes of the Lower Mississippi River: geomorphological response to engineering intervention. River Research and Applications, 21(10), 1107-1131.

Heath, R.E., Brown, G.L., Little, C.D., Pratt, T.C., Ratcliff, J.J., Abraham, D.D., Perkey, D., Ganesh, N.B., Martin, K., May, D.P., 2015. Old River Control Complex Sedimentation Investigation.MRG&P Report No. 6.

Higgins, S.A., 2016. Review: Advances in delta-subsidence research using satellite methods. Hydrogeol. J., 24(3), 587-600.

Hood, D.R., Patrick, D.M., Corcoran, M.K., 2007. Fluvial Instability and Channel Degradation of Amite River and its Tributaries, Southwest Mississippi and Southeast Louisiana, US Army Corps of Engineers.

Jones, K.E., Abraham, D.D., McAlpin, T.O., Ganesh, N., 2018. 2016 Old River Control Complex Sedimentation Data - Supplement to Old River Control Complex Sedimentation Investigation (MRG&P Report No. 6).

Joshi, S., Xu, Y., 2015. Assessment of Suspended Sand Availability under Different Flow Conditions of the Lowermost Mississippi River at Tarbert Landing during 1973–2013. Water, 7(12), 6672.

Joshi, S., Xu, Y.J., 2017. Bedload and Suspended Load Transport in the 140-km Reach Downstream of the Mississippi River Avulsion to the Atchafalaya River. Water, 9(9), 716.

Kesel, R.H., 2003. Human modifications to the sediment regime of the Lower Mississippi River flood plain. Geomorphology, 56(3–4), 325-334.

Kiss, T., Sipos, G., 2007. Braid-scale channel geometry changes in a sand-bedded river: Significance of low stages. Geomorphology, 84(3), 209-221.

Kleinhans, M.G., Ferguson, R.I., Lane, S.N., Hardy, R.J., 2013. Splitting rivers at their seams: bifurcations and avulsion. Earth Surface Processes and Landforms, 38(1), 47-61.

Kleinhans, M.G., Jagers, H.R.A., Mosselman, E., Sloff, C.J., 2008. Bifurcation dynamics and avulsion duration in meandering rivers by one-dimensional and three-dimensional models. Water Resources Research, 44(8).

Kleinhans, M.G., Weerts, H.J.T., Cohen, K.M., 2010. Avulsion in action: Reconstruction and modelling sedimentation pace and upstream flood water levels following a Medieval tidal-river diversion catastrophe (Biesbosch, The Netherlands, 1421–1750 AD). Geomorphology, 118(1–2), 65-79.

Knox, R.L., Latrubesse, E.M., 2016. A geomorphic approach to the analysis of bedload and bed morphology of the Lower Mississippi River near the Old River Control Structure. Geomorphology, 268, 35-47.

Konsoer, K.M., Rhoads, B.L., 2014. Spatial-temporal structure of mixing interface turbulence at two large river confluences. Environmental Fluid Mechanics, 14(5), 1043-1070.

Lamb, M.P., Nittrouer, J.A., Mohrig, D., Shaw, J., 2012. Backwater and river plume controls on scour upstream of river mouths: Implications for fluvio-deltaic morphodynamics. Journal of Geophysical Research-Earth Surface, 117, 15.

Lane, E.W., 1955. The importance of fluvial morphology in hydraulic engineering. Proceedings of the American Society of Civil Engineers, 81(82).

Lane, E.W., 1957. A study of the shape of channels formed by natural streams flowing in erodible material. U.S. Army Engineer Division, Missouri River, Corps of Engineers.

Little, C.D., Biedenharn, D.S., 2014. Mississippi River Hydrodynamic and Delta Management Study (MRHDM)–Geomorphic Assessment, U.S. Army Corps of Engineers.

Meade, R.H., Moody, J.A., 2010. Causes for the decline of suspended-sediment discharge in the Mississippi River system, 1940-2007. Hydrological Processes, 24(1), 35-49.

Miori, S., Repetto, R., Tubino, M., 2006. A one-dimensional model of bifurcations in gravel bed channels with erodible banks. Water Resources Research, 42(11), n/a-n/a.

Mohrig, D., Heller, P.L., Paola, C., Lyons, W.J., 2000. Interpreting avulsion process from ancient alluvial sequences: Guadalope-Matarranya system (northern Spain) and Wasatch Formation (western Colorado). Geological Society of America Bulletin, 112(12), 1787.

Mosley, M.P., 1976. An Experimental Study of Channel Confluences. The Journal of Geology, 84(5), 535-562.

Mossa, J., 2013. Historical changes of a major juncture: Lower Old River, Louisiana. Physical Geography, 34(4-5), 315-334.

Mossa, J., 2016. The changing geomorphology of the Atchafalaya River, Louisiana: A historical perspective. Geomorphology, 252, 112-127.

Mossa, J., McLean, M., 1997. Channel planform and land cover changes on a mined river floodplain - Amite River, Louisiana, USA. Applied Geography, 17(1), 43-54.

Nittrouer, J.A., Allison, M.A., Campanella, R., 2008. Bedform transport rates for the lowermost Mississippi River. Journal of Geophysical Research: Earth Surface, 113(F3), n/a-n/a.

Nittrouer, J.A., Mohrig, D., Allison, M.A., Peyret, A.P.B., 2011. The lowermost Mississippi River: a mixed bedrock-alluvial channel. Sedimentology, 58(7), 1914-1934.

Nittrouer, J.A., Shaw, J., Lamb, M.P., Mohrig, D., 2012. Spatial and temporal trends for water-flow velocity and bed-material sediment transport in the lower Mississippi River. Geological Society of America Bulletin, 124(3-4), 400-414.

Nittrouer, J.A., Viparelli, E., 2014. Sand as a stable and sustainable resource for nourishing the Mississippi River delta. Nature Geoscience, 7(5), 350-354.

Nordin, C.F., Queen, B.S., 1992. Particle Size Distributions of Bed Sediments Along the thalweg of the Mississippi River, Cairo, IL to Head of Passes.

Penland, S., Ramsey, K.E., 1990. RELATIVE SEA-LEVEL RISE IN LOUISIANA AND THE GULF OF MEXICO - 1908-1988. Journal of Coastal Research, 6(2), 323-342.

Pittaluga, M.B., Coco, G., Kleinhans, M.G., 2015. A unified framework for stability of channel bifurcations in gravel and sand fluvial systems. Geophysical Research Letters, 42(18), 7521-7536.

Pittaluga, M.B., Repetto, R., Tubino, M., 2003. Channel bifurcation in braided rivers: Equilibrium configurations and stability. Water Resources Research, 39(3), n/a-n/a.

Pranzini, E., Wetzel, L., Williams, A.T., 2015. Aspects of coastal erosion and protection in Europe. Journal of Coastal Conservation, 19(4), 445-459.

Qian, N., 1990. Fluvial processes in the lower Yellow River after levee breaching at Tongwaxiang in 1855. International Journal of Sediment Research, 5(2), 1-13.

Redolfi, M., Guidorizzi, L., Tubino, M., Bertoldi, W., 2017. Capturing the spatiotemporal variability of bedload transport: A time-lapse imagery technique. Earth Surface Processes and Landforms, 42(7), 1140-1147.

Rhoads, B.L., Sukhodolov, A.N., 2008. Lateral momentum flux and the spatial evolution of flow within a confluence mixing interface. Water Resources Research, 44(8).

Roberts, H.H., Coleman, J.M., Bentley, S.J., Walker, N., 2003. An embryonic major delta lobe; a new generation of delta studies in the Atchafalaya-Wax Lake delta system. Transactions - Gulf Coast Association of Geological Societies, 53, 690-703.

Rosen, T., Xu, Y.J., 2013. Recent decadal growth of the Atchafalaya River Delta complex: Effects of variable riverine sediment input and vegetation succession. Geomorphology, 194, 108-120.

Rosen, T., Xu, Y.J., 2014. A Hydrograph-Based Sediment Availability Assessment: Implications for Mississippi River Sediment Diversion. Water (20734441), 6(3), 564-583.

Saucier, R.T., 1994. Geomorphology and Quaternary Geologic History of the Lower Mississippi Valley, U. S. Army Engineer Waterways Experiment Station,Vicksburg, Mississippi.

Schumm, S.A., 1963. A tentative classification of alluvial river channels; an examination of similarities and differences among some Great Plains rivers. Geological Survey (U.S.). Circular: 477. Washington, 1963.

Schumm, S.A., 1985. PATTERNS OF ALLUVIAL RIVERS. Annual Review of Earth and Planetary Sciences, 13, 5-27.

Silva, R., Luisa Martinez, M., Hesp, P.A., Catalan, P.A., Osorio, A.F., Martell, R., Fossati, M., da Silva, G.M., Marino-Tapia, I., Pereira, P., Cienguegos, R., Klein, A., Govaere, G., 2014. Present and Future Challenges of Coastal Erosion in Latin America. Journal of Coastal Research, 1-16.

Slingerland, R., Smith, N.D., 1998. Necessary conditions for a meandering-river avulsion. Geology, 26(5), 435-438.

Stouthamer, E., Cohen, K.M., Gouw, M.J.P., 2011. Avulsion and its implications for fluvial-deltaic architecture; insights from the Holocene Rhine-Meuse Delta. Special Publication - Society for Sedimentary Geology, 97, 215-231.

Sukhodolov, A.N., Krick, J., Sukhodolova, T.A., Cheng, Z., Rhoads, B.L., Constantinescu, G.S., 2017. Turbulent flow structure at a discordant river confluence: Asymmetric jet dynamics with implications for channel morphology. Journal of Geophysical Research-Earth Surface, 122(6), 1278-1293.

Syvitski, J.P.M., Kettner, A.J., Overeem, I., Hutton, E.W.H., Hannon, M.T., Brakenridge, G.R., Day, J., Vorosmarty, C., Saito, Y., Giosan, L., Nicholls, R.J., 2009. Sinking deltas due to human activities. Nature Geoscience, 2(10), 681-686.

Toffaleti, F.B., 1977. A procedure for computation of the total river sand discharge and detailed distribution bed to surface.

Tornqvist, T.E., 1994. MIDDLE AND LATE HOLOCENE AVULSION HISTORY OF THE RIVER RHINE (RHINE-MEUSE DELTA, NETHERLANDS). Geology, 22(8), 711-714.

Viparelli, E., Nittrouer, J.A., Parker, G., 2015. Modeling flow and sediment transport dynamics in the lowermost Mississippi River, Louisiana, USA, with an upstream alluvial-bedrock transition and a downstream bedrock-alluvial transition: Implications for land building using engineered diversions. Journal of Geophysical Research. Earth Surface, 120(3), 534.

Vorosmarty, C.J., Meybeck, M., Fekete, B., Sharma, K., Green, P., Syvitski, J.P.M., 2003. Anthropogenic sediment retention: major global impact from registered river impoundments. Global and Planetary Change, 39(1-2), 169-190.

Walling, D.E., 2006. Human impact on land-ocean sediment transfer by the world's rivers. Geomorphology, 79(3-4), 192-216.

Walling, D.E., Fang, D., 2003. Recent trends in the suspended sediment loads of the world's rivers. Global and Planetary Change, 39(1-2), 111-126.

Wang, B., Xu, Y.J., 2016. Long-term geomorphic response to flow regulation in a 10-km reach downstream of the Mississippi–Atchafalaya River diversion. Journal of Hydrology: Regional Studies, 8, 10-25.

Wang, B., Xu, Y.J., 2018a. Decadal-Scale Riverbed Deformation and Sand Budget of the Last 500 km of the Mississippi River: Insights Into Natural and River Engineering Effects on a Large Alluvial River. Journal of Geophysical Research: Earth Surface, 123(5), 874-890.

Wang, B., Xu, Y.J., 2018b. Dynamics of 30 large channel bars in the Lower Mississippi River in response to river engineering from 1985 to 2015. Geomorphology, 300, 31-44.

Wang, H., Wu, X., Bi, N., Li, S., Yuan, P., Wang, A., Syvitski, J.P.M., Saito, Y., Yang, Z., Liu, S., Nittrouer, J., 2017. Impacts of the dam-orientated water-sediment regulation scheme on the lower reaches and delta of the Yellow River (Huanghe): A review. Global and Planetary Change, 157(Supplement C), 93-113.

Wang, Z.B., Fokkink, R.J., DeVries, M., Langerak, A., 1995. Stability of river bifurcations in 1D morphodynamic models. Journal of Hydraulic Research, 33(6), 739-750.

Wheaton, J.M., Brasington, J., Darby, S.E., Kasprak, A., Sear, D., Vericat, D., 2013. Morphodynamic signatures of braiding mechanisms as expressed through change in sediment storage in a gravel-bed river. Journal of Geophysical Research: Earth Surface, 118(2), 759-779.

Williams, R.D., Rennie, C.D., Brasington, J., Hicks, D.M., Vericat, D., 2015. Linking the spatial distribution of bed load transport to morphological change during high-flow events in a shallow braided river. Journal of Geophysical Research-Earth Surface, 120(3), 604-622.

Wintenberger, C.L., Rodrigues, S., Claude, N., Jugé, P., Bréhéret, J.-G., Villar, M., 2015. Dynamics of nonmigrating mid-channel bar and superimposed dunes in a sandy-gravelly river (Loire River, France). Geomorphology, 248, 185-204.

Wu, K., Xu, Y.J., 2007. Long-term freshwater inflow and sediment discharge into Lake Pontchartrain in Louisiana, USA. Hydrological Sciences Journal-Journal Des Sciences Hydrologiques, 52(1), 166-180.

Xue, C.T., 1993. HISTORICAL CHANGES IN THE YELLOW-RIVER DELTA, CHINA. Marine Geology, 113(3-4), 321-330.

Yang, C.T., 1973. Incipient Motion and Sediment Transport. Journal of the Hydraulics Division, 99(HY10), 1679-1704.

Yang, C.T., 1979. UNIT STREAM POWER EQUATIONS FOR TOTAL LOAD. Journal of Hydrology, 40(1-2), 123-138.

Yang, C.T., Huang, C., 2001. Applicability of sediment transport formulas. International Journal of Sediment Research, 16(3), 335-353.

Yang, S.L., Milliman, J.D., Li, P., Xu, K., 2011. 50,000 dams later: Erosion of the Yangtze River and its delta. Global and Planetary Change, 75(1-2), 14-20.

Yang, S.L., Zhang, J., Xu, X.J., 2007. Influence of the Three Gorges Dam on downstream delivery of sediment and its environmental implications, Yangtze River. Geophysical Research Letters, 34(10).

Zhang, K., Douglas, B.C., Leatherman, S.P., 2004. Global warming and coastal erosion. Climatic Change, 64(1-2), 41-58.

APPENDIX A. PERMISSION TO REPRINT CHAPTER 2

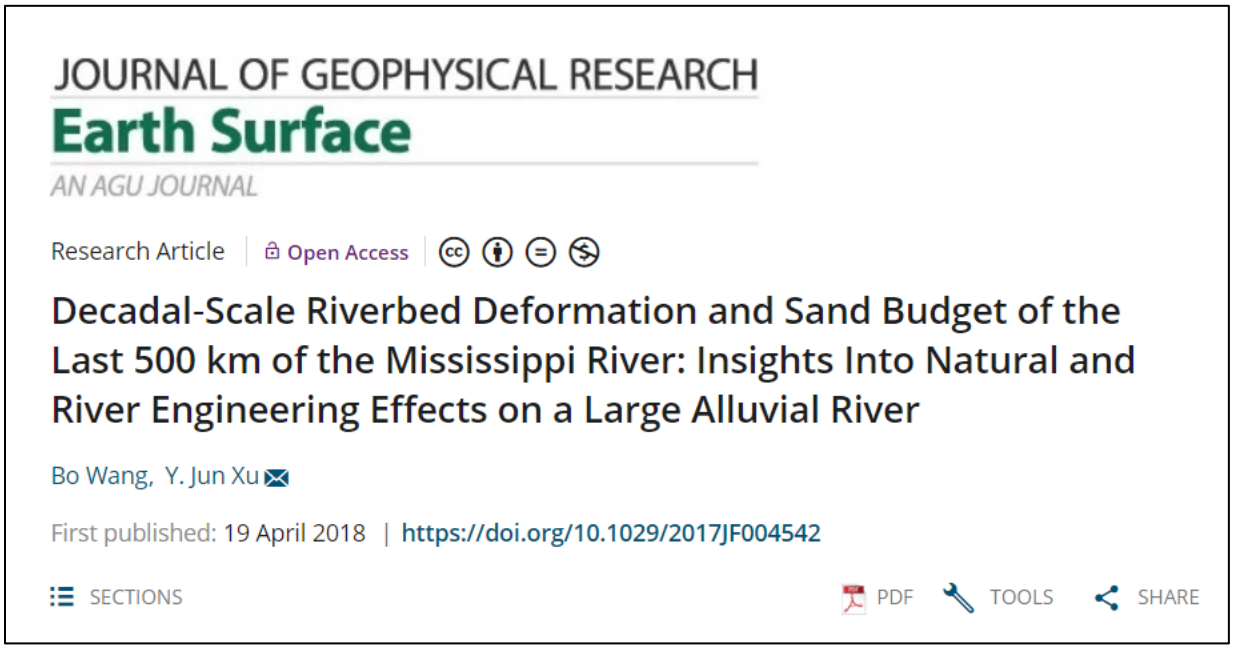

JOURNAL OF GEOPHYSICAL RESEARCH
Earth Surface
AN AGU JOURNAL

Research Article | Open Access

Decadal-Scale Riverbed Deformation and Sand Budget of the Last 500 km of the Mississippi River: Insights Into Natural and River Engineering Effects on a Large Alluvial River

Bo Wang, Y. Jun Xu

First published: 19 April 2018 | https://doi.org/10.1029/2017JF004542

SECTIONS PDF TOOLS SHARE

Copyright Clearance Center RightsLink®

Home | Create Account | Help

Title: Decadal-Scale Riverbed Deformation and Sand Budget of the Last 500 km of the Mississippi River: Insights Into Natural and River Engineering Effects on a Large Alluvial River

Author: Bo Wang, Y. Jun Xu

Publication: Journal of Geophysical Research: Earth Surface

Publisher: John Wiley and Sons

Date: May 2, 2018

Copyright © 2018, John Wiley and Sons

LOGIN

If you're a copyright.com user, you can login to RightsLink using your copyright.com credentials.

Already a RightsLink user or want to learn more?

Open Access Article

This article is available under the terms of the Creative Commons Attribution Non-Commercial No Derivatives License CC BY-NC-ND (which may be updated from time to time) and permits **non-commercial** use, distribution, and reproduction in any medium, without alteration, provided the original work is properly cited and it is reproduced verbatim.

For an understanding of what is meant by the terms of the Creative Commons License, please refer to Wiley's Open Access Terms and Conditions.

Permission is not required for **non-commercial** reuse. For **commercial** reuse, please hit the "back" button and select the most appropriate **commercial** requestor type before completing your order.

If you wish to adapt, alter, translate or create any other derivative work from this article, permission must be sought from the Publisher. Please email your requirements to RightsLink@wiley.com.

BACK | CLOSE WINDOW

Copyright © 2018 Copyright Clearance Center, Inc. All Rights Reserved. Privacy statement. Terms and Conditions.
Comments? We would like to hear from you. E-mail us at customercare@copyright.com

VITA

Bo Wang was born in Tongliao, Inner Mongolia, China, in 1985, the son of Xijun Wang, and Yuqin Liu. He graduated from China University of Geosciences in June 2008, earning his Bachelor of Science in Land Resource Management. In June 2011, he earned his Master of Science in Earth Exploration and Information Technology from the China University of Geosciences. After working for half of a year as an engineer at the Guangxi Institute of Surveying and Mapping of Land Resources, he moved to Baton Rouge, Louisiana in January 2012 to pursue his doctoral degree in Geography at the Louisiana State University. He earned his doctoral degree in December 2017. In June 2015, Bo started to pursue a master's degree in Watershed Hydrology in the School of Renewable Natural Resources, Louisiana State University. After graduation, he will continue working as a postdoctoral researcher on river hydrodynamics and fluvial geomorphology.